IDENTIFICATION OF VERY LOW DENSITY LIPOPROTEIN RECEPTOR (*VLDLR*) MUTATIONS IN CEREBELLAR HYPOPLASIA AND QUADRUPEDAL LOCOMOTION (UNERTAN SYNDROME) IN HUMANS

A THESIS SUBMITTED TO
THE DEPARTMENT OF MOLECULAR BIOLOGY AND GENETICS
AND THE INSTITUTE OF ENGINEERING AND SCIENCE OF
BILKENT UNIVERSITY
IN PARTIAL FULFILLMENT OF THE REQUIREMENTS FOR
THE DEGREE OF MASTER OF SCIENCE

BY ŞAFAK ÇAĞLAYAN
JULY 2008

I certify that I have read this thesis and that in my opinion it is fully adequate, in scope and in quality, as a thesis for the degree of Master of Science.

Prof. Tayfun Özçelik

I certify that I have read this thesis and that in my opinion it is fully adequate, in scope and in quality, as a thesis for the degree of Master of Science.

Prof. Nurten Akarsu

I certify that I have read this thesis and that in my opinion it is fully adequate, in scope and in quality, as a thesis for the degree of Master of Science.

Assoc. Prof. Işık Yuluğ

Approved for the Institute of Engineering and Science

Director of Institute of Engineering and Science

Prof. Mehmet Baray

ABSTRACT

IDENTIFICATION OF VERY LOW DENSITY LIPOPROTEIN RECEPTOR (*VLDLR*) MUTATIONS IN CEREBELLAR HYPOPLASIA AND QUADRUPEDAL LOCOMOTION (UNERTAN SYNDROME) IN HUMANS

Şafak Çağlayan
M.S in Molecular Biology and Genetics
Supervisor: Prof. Tayfun Özçelik
July 2008, 134 Pages

Cerebellar hypoplasia and quadrupedal locomotion in humans, also known as Unertan syndrome, is a severe neurodevelopmental condition accompanied by dysarthria and impaired cognitive skills. The molecular underpinnings of development of the brain structures required for bipedal gait in humans can be established through identification of the gene(s) associated with this disorder. Four consanguineous families from Turkey exhibiting this autosomal recessive trait were studied. In two families (A and D), affected individuals shared homozygosity in a critical 1.032-Mb region in chromosome 9p24. Sequence analysis linked the disease to two distinct mutations in the very low density lipoprotein receptor (*VLDLR*) gene; the nonsense change R257X in family A and the single nucleotide deletion leading to frameshift I780TfsX3 in family D. *VLDL* receptor is a co-receptor of reelin molecule. Reelin signaling pathway is involved in neuronal migration and lamination to form brain cortices during embryonic development. Mutant *VLDL* receptors are truncated proteins that cannot be inserted into the membrane. Homozygosity mapping linked the disease locus in family B to chromosome 17p13. Family C does not share homozygosity in neither of the loci.

ÖZET

İNSANDA SEREBELLAR HİPOPLAZİ VE QUADRUPEDAL YÜRÜMEDE (ÜNERTAN SENDROMU) DÜŞÜK YOĞUNLUKLU LİPOPROTEİN RESEPTÖRÜ (*VLDLR*) MUTASYONLARININ TESPİT EDİLMESİ

Şafak Çağlayan
Moleküler Biyoloji ve Genetik Yüksek Lisans
Danışman: Prof. Tayfun Özçelik
Temmuz 2008, 134 Sayfa

Serebellar hipoplazi ve quadrupedal yürüme şiddetli bir nörogelişimsel hastalıktır. Unertan sendromu olarak da bilinen bu duruma disartirik konuşma ve zeka geriliği eşlik etmektedir. İnsanda bipedal yürüme için gerekli beyin yapılarının gelişmesinin moleküler temelleri, bu bozukluğa yol açan gen(ler)in bulunması ile kurulabilir. Çalışmada, otozomal resesif hastalığı taşıyan Türkiye'deki dört akraba aile incelenmiştir. Ailelerin ikisinde (A ve D), hasta bireyler 9p24 kromozomunda 1.032-Mb büyüklüğündeki bir kritik bölgede homozigosite göstermektedirler. Dizi analizi, hastalığı düşük yoğunluklu lipoprotein reseptörü (*VLDLR*) genindeki iki farklı mutasyona bağlamıştır; A ailesindeki R257X anlamsız değişim ve D ailesindeki I780TfsX3 çerçeve kaymasına yol açan tek nükleotidlik delesyon. *VLDL* reseptörü reelin molekülünün reseptörlerinden birisidir. Reelin sinyal yolağı embriyonik gelişim sürecinde beyin korteksinin oluşması için nöronların taşınmasında ve tabakalanmasında rol oynamaktadır. Mutant *VLDL* reseptörleri hücre zarına eklenemeyecek kesik proteinler olarak oluşmaktadırlar. Homozigosite haritalaması B ailesindeki hastalık bölgesini 17p13 kromozomuna bağlamıştır. C ailesi iki bölgenin hiçbirisi ile homozigosite paylaşmamaktadır.

TO MY PARENTS,
ZEHRA AND AZİZ ÇAĞLAYAN
FOR THEIR LOVE AND SUPPORT

ACKNOWLEDGEMENTS

It would not be easy to thank enough all people with whom I did this study. Yet, I will try…

Foremost, I would like to thank and express my sincerest gratitude to my supervisor Prof. Tayfun Özçelik for his guidance, encouragement, and support throughout my thesis work. I have learned a lot from his scientific and personal advices. Without his vision and commitment, the project would have never reached the great result it did.

I am indebted to Prof. Nurten Akarsu since she did a great part of this study with performing genomic mapping studies. More than that, her cheerful ambiance always motivated me during our studies.

I am really very lucky for meeting Elif Uz who was my second advisor. I learnt a lot about life from her and I wish she would continue to be one of my best fellows with her immense compassion.

I would like to thank Chigdem Mustafa Aydın, Melda Kantar, Emre Onat and Süleyman Gülsüner. We shared several things that I cannot write down all along with benches and desks.

I have been very happy to be a member of Bilkent MBG family. It would be very difficult to find such a lovely people in such a peaceful environment.

I am very grateful to all my friends for whom I need a chapter to mention all. Nevertheless, my special "big thanks" go to Hande Koçak, Ceren Sucularlı, Tolga Acun, Bala-Gur Dedeoglu and Zeynep Keskin-Tokcaer for their sincere friendship.

It is impossible to express my endless love and thanks to my family. I will forever grateful to them…

TABLE OF CONTENTS

LIST OF TABLES

LIST OF FIGURES

ABBREVIATIONS

ApoER2	apolipoprotein E receptor 2
bp	base pair
ddH2O	deionized water
del	deletion
DNA	deoxyribonucleic acid
dNTP	deoxynucleotide triphosphates
E	embryonic-day
MgCl2	magnesium chloride
mM	milimolar
µl	microliter
mRNA	messenger RNA
PCR	polymerase chain reaction
Q-PCR	Quantitative real-time PCR
RNA	ribonucleic acid
RT-PCR	reverse transcriptase PCR
SCA	spinocerebellar ataxia
SNP	single nucleotide polymorphism
TAE	tric-acetic acid-EDTA
VLDLR	very low density lipoprotein receptor

PART I: INTRODUCTION

1.1 Quadrupedal Locomotion in Humans: Unertan Syndrome

This unique phenotype was first described by Prof. Uner Tan in a consanguineous family living in southern Turkey. Non-progressive cerebellar hypoplasia, quadrupedal locomotion, dysarthric speech and mental retardation are the hallmarks of this condition, which is named as Unertan syndrome based on the name of discoverer (Tan, 2005).

1.1.1 Families described in Turkey

Initially we studied family A, a consanguineous kindred living in southeast region of Turkey (Figure 1.1). There are seven affected individuals in this family. All affected individuals walk quadrupedally. There is one girl who can walk bipedally, but she prefers quadrupedal locomotion. Other main features of the affected individuals are cerebellar hypoplasia, impaired cognitive skills, and primitive language (Tan *et al*., 2008a; Ozcelik *et al*., 2008a).

Family B is the first identified family (Figure 1.2). Five of 19 children walk in a quadrupedal fashion. Two children using bipedal locomotion have a neurological phenotype similar to that of their quadruped siblings (Tan, 2005; Turkmen *et al*., 2006).

Another family exhibiting Unertan syndrome is family C residing in southern Turkey (Figure 1.3). There are four affected individuals and two of them ambulate quadrupedally. One of the remaining two is a biped ataxic man who was a quadruped during childhood, and the other patient, who was also a quadruped, is no longer able to ambulate now (Tan, 2006b).

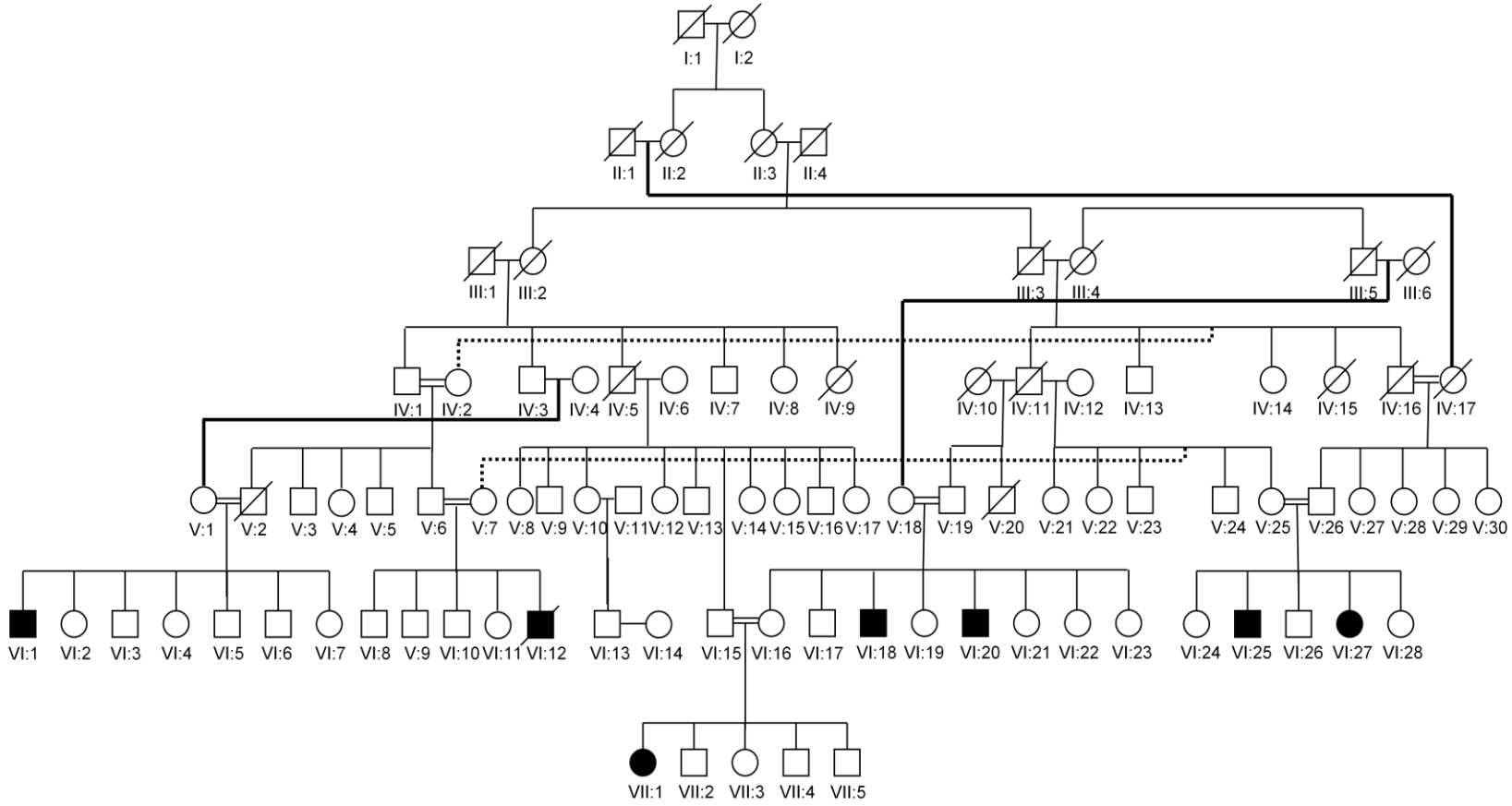

Figure 1.1 Pedigree of family A residing in southeastern Turkey. Filled symbols represent the affected individuals. Squares indicate males, and circles indicate females. All affected individuals are resulting from consanguineous marriages.

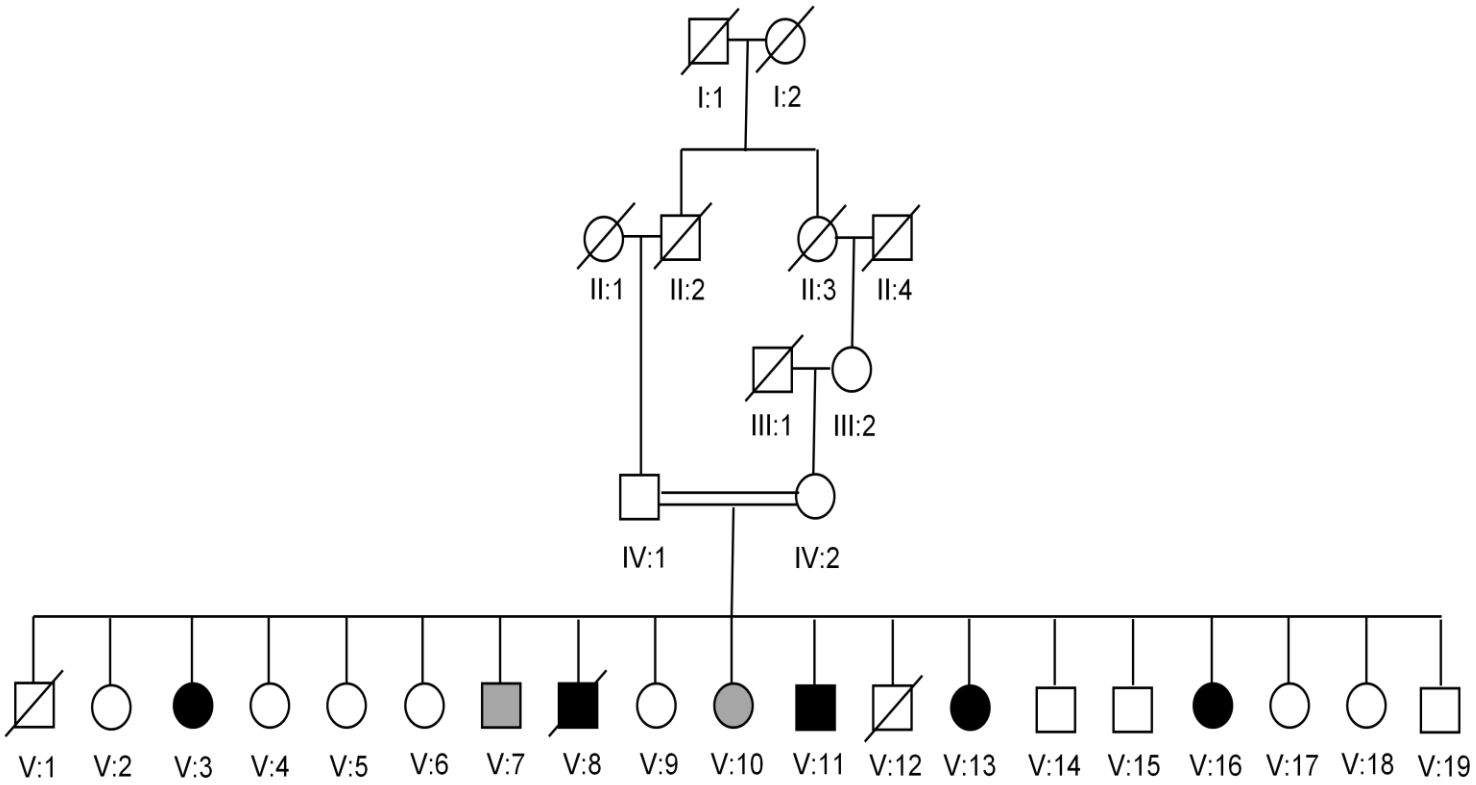

Figure 1.2 Pedigree of family B. Parents of the affected children are second cousins. Two children, who use bipedal locomotion, but have a neurological phenotype similar to that of their quadruped siblings are shown with gray symbols.

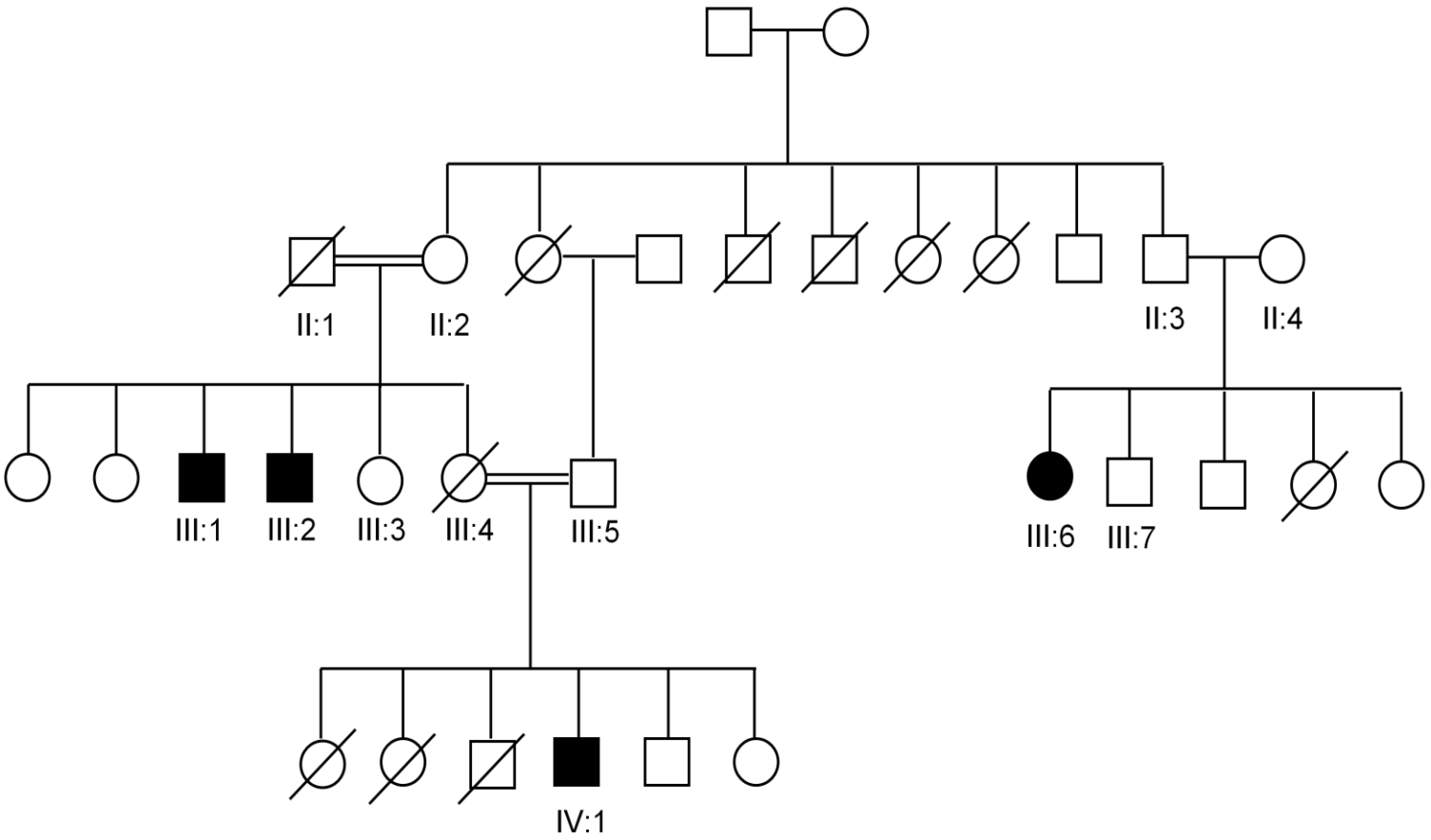

Figure 1.3 Pedigree of family C. Pedigree analysis show consanguineous matings in the family.

Family D was encountered during the course of our studies (Figure 1.4). This consanguineous family is from western Turkey and all of the three affected individuals are quadrupeds (Tan, 2008b; Ozcelik *et al*., 2008a).

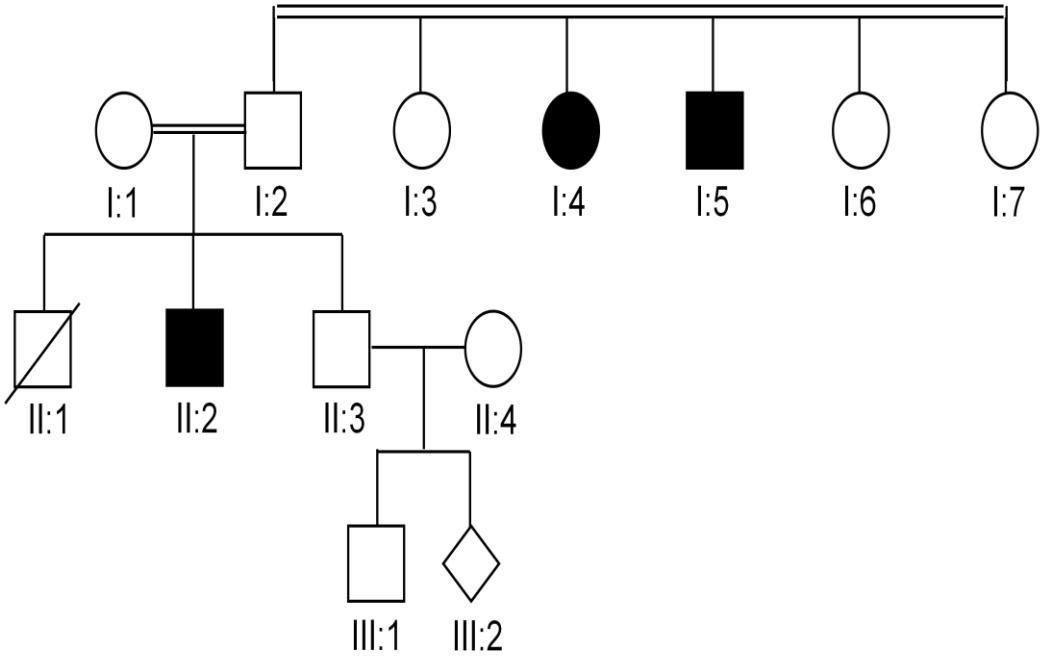

Figure 1.4 Pedigree of family D.

1.2 Ataxia

The word ataxia means “absence or loss of order” and the term ataxia is generally used to describe uncoordinated walking. Actually, ataxia is neither a specific disease nor a disorder. It is a set of symptoms affecting coordination of gait, speech (dysarthria), hands, arms, and eye movements (nystagmus).

Atrophy of cells in the cerebellum or its connections, diseases causing cerebellar or spinocerebellar degeneration, or damages to cerebellar/spinal structures are the most common causes of ataxia.

There are several medical and neurological conditions that can lead to ataxia. According to the National Ataxia Foundation of the USA, ataxia can appear in people suddenly as a result of one or more of these conditions: head trauma, stroke, brain hemorrhage, brain tumor, congenital abnormality, severe viral infection, exposure to certain drugs or toxins (i.e. alcohol, anti-convulsive medicines), cardiac or respiratory arrest. Additionally there are several conditions that may result in ataxia over time. These are hypothyroidism, deficiencies of certain vitamins (E, B12), exposure to certain drugs or toxins (heavy metals, anti-convulsive medicines, chronic alcohol exposure, and certain cancer drugs), congenital abnormality, multiple sclerosis, syphilis (locomotor ataxia), hereditary disorders, idiopathic (unknown cause) cerebellar degeneration disorders (Official website of the National Ataxia Foundation of the USA; http://www.ataxia.org/).

Cerebellar/spinocerebellar syndromes are a heterogenous group of neurological disorders causing ataxia. Patients with spinocerebellar syndromes exhibit classical ataxia features like disequilibrium, progressive incoordination of gait and limbs, and speech and eye movement disturbances. Other neurological symptoms including pyramidal or extrapyramidal signs, spasticity, ophthalmoplegia, and dementia can be also found in patients (Mariotti & Di Donato, 2001).

Ataxic individuals can display different symptoms and severity of the disease can be variable among patients. Because of this variability in phenotypes and neuropathological findings, making a proper clinical classification and differential diagnosis is very difficult. Nevertheless, certain types of ataxias can be differentiated with the help of additional specific symptoms. Also other affected family members can be useful in diagnosis in the case of hereditary ataxias. Hence, spinocerebellar syndromes can be distinguished into two forms: 1) sporadic ataxias of unknown cause or that are acquired due to associated illness and 2) inherited spinocerebellar ataxias (Mariotti & Di Donato, 2001).

It is a challenging task for clinicians to diagnose sporadic ataxia since they should rule out every possibility of hereditary ataxia before making a final diagnosis. Phenotypes with multiple system atrophy are the major group in the set of sporadic spinocerebellar syndromes of unknown cause. Acquired or non-hereditary spinocerebellar syndromes can be due to certain environmental factors including alcoholism or vitamin deficiencies. Multiple sclerosis, vascular diseases, and tumors or paraneoplastic syndromes can also cause cerebellar ataxias (Table 1.1) (Mariotti & Di Donato, 2001). Conditions resulting in sporadic ataxia can affect only the cerebellum ("pure cerebellar" form) or they can cause additional symptoms such as neuropathy (dysfunction of the peripheral nerves), dementia (impaired intellectual function), weakness, rigidity, or spasticity of the muscles ("cerebellar plus" form) (Official website of the National Ataxia Foundation of the USA; http://www.ataxia.org/).

Table 1.1 Sporadic spinocerebellar syndromes. (Mariotti & Di Donato, 2001)

Unknown causes
Multiple system atrophy Olivopontocerebellar atrophy Striatonigral degeneration Shy-Drager syndrome
Immune
Multiple sclerosis Glutamic acid decarboxylase antibody Paraneoplastic syndromes
Systemic diseases
Celiac diseases Vitamin E malaabsorption

Hereditary ataxias are neurological disorders caused by a defect in a certain gene that is inherited through families. This group of diseases is characterized by progressive degeneration of the cerebellum and spinocerebellar tracts of the spinal cord accompanied by various pathologies in central and peripheral nervous systems (Di Donato *et al.*, 2001).

Since clinical phenotypes of different genotypes of inherited ataxias show significant overlap, it is difficult to make a classification based on clinical or histopathological findings (Banfi & Zoghbi, 1994). So, it is more useful to divide hereditary cerebellar/spinocerebellar syndromes according to the inheritance mode as autosomal dominant, autosomal recessive, X-linked and mitochondrial disorders (Mariotti & Di Donato, 2001).

There is no specific treatment for directly curing diseases that cause ataxia. Aims of therapies are generally to diminish the severity of symptoms. For example if ataxia is due to a stroke, vitamin deficiency, or exposure to a toxic drugs or chemicals, then treatment would target specific ailment. Physical therapy is a widely used option for people with impaired gait. Furthermore, ataxic individuals can use adaptive devices (i.e. a cane, crutches, walker, or wheelchair to help for walking; devices to assist feeding, and self cares for patients having difficulties in hand and arm coordination; and communication devices if speech is impaired) to be able to live independently.

1.2.1 Autosomal dominant ataxias

Autosomal dominant cerebellar/spinocerebellar ataxias are a complex group of neurodegenerative diseases. These disorders are clinically heterogeneous since affected individuals exhibit several overlapping neurological symptoms. These symptoms include loss of balance and motor coordination, dysarthric speech, ophthalmoplegia, pyramidal and extrapyramidal signs, dementia, pigmentary neuropathy, peripheral neuropathy, oculomotor disturbances of cerebellar and supranuclear genesis, retinopathy, optic atrophy, spasticity, sphincter disturbances, cognitive impairment, and epilepsy (Duenas *et al.*, 2006; Zoghbi, 2000; Schols *et al.*, 2004).

The prevalence of the autosomal dominant ataxias is assumed as three cases per 100,000 individuals, although real number can be higher. Different ethnic and continental populations show diverse prevalence rates for specific types because of heterogeneity of the disorders (Schols *et al.*, 2004). Onset of ataxia symptoms is generally between 30 and 50 years of age. However, there are individuals with disease onset in childhood or at later decades after 60 years (Duenas *et al.*, 2006).

Disease onset in adulthood, occurrence of anticipation (disease onset becomes at earlier ages and disease become more severe in successive generations) and atrophy of cerebellum are common clinical features of autosomal dominant ataxias. Nonetheless, variable and unpredictable association of signs of central nervous system and peripheral nervous system can accompany common symptoms. Because of this, clinical classification is complicated. Yet, autosomal dominant ataxias have been divided into three groups based on clinical findings: ADCA (Autosomal dominant cerebellar ataxia) I, ADCA II and ADCA III (Harding, 1993; Duenas *et al.*, 2006). This type of classification and diagnosis is especially useful for patient management.

On the other hand identification of genetic basis of most of these disorders have had a significant impact on nosology, diagnostic procedures and the management of patients. It led to the development of a new classification system based on molecular genetic data, and improvements in diagnosis and patient management (Di Donato, 1998). In this systematic, autosomal dominant ataxias are distinguished into 29 defined subtypes, of which the causative genes and pathogenic mutations are known in 15 (Table 1.2) (Duenas *et al.*, 2006, Schols *et al*., 2004). Molecular genetics approaches have revealed that the main pathogenic mechanisms of these disorders include abnormal proteins or RNAs, which "gain a toxic function", and lead to neuronal and systemic dysfunction (Gatchel & Zoghbi, 2005; Orr & Zoghbi, 2007).

Table 1.2 Summary of the molecular features of spinocerebellar ataxias.

(Duenas *et al*., 2006)

SCA subtype	Genomic location	Gene/locus	Protein	Mutation
SCA1	6p23	ATXN1	Ataxin 1	CAG repeat
SCA2	12q24	ATXN2	Ataxin 2	CAG repeat
SCA3	14q24.3-q31	ATXN3	Ataxin 3	CAG repeat
SCA4	16q24-qter	SCA4	U	U
SCA5	11q13	SPTBN2	Beta-III spectrin	D, MM
SCA6	19p13	CACNAIA	CACNAIA	CAG repeat
SCA7	3p21.1-p12	ATXN7	Ataxin 7	CAG repeat
SCA8	13q21	KLHLIAS	Kelch-like I	CTG repeat
SCA9	Reserved	U	U	U
SCA10	22q13	ATXN10	Ataxin 10	ATTCT repeat
SCA11	15q15.2	TTBK2	TTBK2	D, I
SCA12	5q31-q33	PPP2R2B	PPP2R2B	CAG repeat
SCA13	19q13.3-q13.4	KCNC3	KCNC3	MM
SCA14	19q13.4	PRKCG	PRKCG	MM
SCA15	3p24.2-pter	U	U	U
SCA16	8q23-q24.1	U	U	U
SCA17	6q27	TBP	TBP	CAG repeat
SCA18	7q22-q32	U	U	U
SCA19*	1p21-q21	U	U	U
SCA20	11p13-q11	U	U	U
SCA21	7p21.3-p15.1	U	U	U
SCA22*	1p21-q23	U	U	U
SCA23	20p13-p12.3	U	U	U
SCA24	1p36	U	U	U
SCA25	2p21-p13	U	U	U
SCA26	19p13.3	U	U	U
SCA27	13q34	FGF14	FGF14	MM
SCA28	18p11.22-q11.2	U	U	U
SCA29	3p26	U	U	U
DRPLA	12p13.31	ATN1	Atrophin 1	CAG repeat
Undefined**	16q22.1	PLEKHG4	Puratrophin 1	5’SNS

* SCAs 19 and 21 are likely allelic forms of the same gene.

** The gene encoding Puratrophin 1 lies on the same chromosomal region where the SCA4 gene localizes.

Genes in genomic location are noted according to Ensembl. D, deletions; I, insertions; MM, missense mutations; SCA, spinocerebellar ataxia; SNS, single-nucleotide substitutions; U, unknown.

1.2.2 Autosomal recessive ataxias

Autosomal recessive ataxias are a group of rare and clinically heterogeneous neurological diseases. The most important symptom of these disorders is spinocerebellar ataxia, involving the cerebellum, brainstem, or spinocerebellar long tracts. Patients exhibit poor balance with falls, imprecise hand coordination, postural or kinetic tremor of the extremities or trunk, dysarthria, dysphagia, vertigo, and diplopia (Perlman, 2004). Various neurologic, ophthalmologic and systemic pathologies affecting both central and peripheral nervous system, and in some cases other systems and organs can accompany ataxia (Palau & Espinos, 2006).

These phenotypic features can be so rare. Yet, they are important to make a differential diagnosis and to decide on further therapies. Moreover, since these disorders are clinically heterogeneous, detailed assessments and additional diagnostic studies (i.e. neuroimaging or electrophysiological examinations) are required to make a proper differentiation. For example atrophy of cerebellum is a useful distinguishing feature and neuroimaging can be particularly useful to confirm clinical findings. Performing genetic tests/mutation analysis in diagnosis is also possible for the diseases for which causative genes were identified (Di Donato *et al.*, 2001; Fogel & Perlman, 2007). Ataxia associated with deficiency of coenzyme Q10 and abetalipoproteinemia are the only types of recessive ataxias that have specific treatments (Espinos-Armero *et al*., 2005).

Until recent years characterization of autosomal recessive ataxias remained poor when compared to dominant ataxias. Several conditions have been genetically described in the last few years. It has been found that most of the recessive ataxias are associated with a "loss of function" of specific cellular proteins involved in metabolic homeostasis, cell cycle, and DNA repair/protection processing (Di Donato *et al.*, 2001). Generally each disease of this group is caused by defect(s) in a specific gene. Nonetheless, some recessive ataxias are genetically heterogeneous and can be caused by mutation(s) in more than one gene (Palau & Espinos, 2006).

The prevalence of autosomal recessive cerebellar ataxias has been estimated to be 7 in 100,000 individuals (Espinos-Armero *et al*., 2005). Among a large number of rare recessive disorders, Freidriech ataxia is the most common type in Caucasian populations (estimated prevalence is 2-4 cases in 100,000). Other frequent types include ataxia telangiectasia (1-2.5/100,000) and early onset cerebellar ataxia with retained tendon reflexes (1/100,000) (Palau & Espinos, 2006). Remaining types are much rare and prevalence of some can be variable among different regions (Di Donato *et al.*, 2001). For most of the autosomal recessive ataxias disease onset is before age 20 years (Fogel & Perlman 2007).

Based on pathogenic mechanisms five main types of autosomal recessive ataxias can be distinguished: 1) congenital (developmental disorder); 2) ataxias associated with metabolic disorders including ataxias caused by enzymatic defects; 3) ataxias due to DNA repair defects; 4) degenerative and progressive ataxias that include ataxias with known cause and pathogenesis (such as Friedrich ataxia), and ataxias of unknown etiology; 5) ataxias associated with other/additional features (Table 1.3) (Espinos-Armero *et al*., 2005; Palau & Espinos, 2006).

Table1.3 Summary of the molecular features of autosomal recessive ataxias (Palau & Espinos, 2006)

	Protein (Gene or Locus)	Location
Congenital ataxias		
Joubert syndrome		
JBTS 1 (cerebelloparenchymal disorder IV, CPD IV)	U	9q34.3
JBTS 2 (CORS2)	U	11p12-q13.3
JBTS 3	AHI1	6q23.3
JBTS 4 (nephronophthisis 1)	NPHP1	2q13
JBTS 5	CEP290 or NPHP6	12q21.3
JBTS 6	TMEM67	8q21.13-q22.1
JBTS 7	RPGRIP1L	16q12.2
Cayman ataxia	Cayataxin (ATCAY)	19p13.3
Metabolic ataxias		
Ataxia with isolated vitamin E deficiency (AVED)	α-TTP (TTPA)	8q13.1-q13.3
Abetalipoproteinemia	MTP	4q22-q24
Cerebrotendinous xanthomatosis	CYP27A1	2q33-qter
Refsum disease	PAHX or PHYH	10pter-p11.2
	PEX7	6q22-q24
DNA repair defects		
Ataxia telangiectasia	ATM	11q22.3
Ataxia with oculomotor apraxia 1 (AOA 1)	Aprataxin (APTX)	9p13.3
Ataxia with oculomotor apraxia 2 (AOA 2) or SCAR1	Senataxin (SETX)	9q34
Ataxia telangiectasia-like disorder (ATLD)	MRE11A	11q21
Spinocerebellar ataxia with axonal neuropathy (SCAN1)	TDP1	14q31-q32
Xeroderma pigmentosum (XP)	NPHP6	12q21.32
XP of complementation group A	XPA	9q22.3
XP of complementation group B	XPB/ERCC3	2q21
XP of complementation group C	XPC	3p25
XP of complementation group D	XPD/ERCC2	19q13.2-q13.3
XP of complementation group E	XPE (DDB2)	11p12-p11
XP of complementation group F	XPF/ERCC4	16p13.3-p13.13
XP of complementation group G	XPG/ERCC5	13q33
XP variant (XPV) or XP with normal DNA repair rates	POLH	6p21.1-p12
Degenerative ataxias		
Friedrich ataxia	Frataxin (FRDA)	9q13
Mitochondrial recessive ataxic syndrome (MIRAS)	Polymerase γ (POLG)	15q25
Charlevoix-Saguenay spastic ataxia	Sacsin (SACS)	13q12
Early onset cerebellar ataxia with retained tendon reflexes (EOCARR)		13q11-q12
Infantile onset spinocerebellar ataxia (IOSCA)	Twinkle (C10ORF2)	10q24
Marinesco-Sjögren syndrome(MSS)		
Classical MSS	SIL1	5q31
MSS with myoglobinuria	CTDP1	18qter
Coenzyme Q_{10} deficiency with cerebellar ataxia	?	
Posterior column ataxia and retinis pigmentosa (PCARP)	AXPC1	1q31

1.2.3 X-linked ataxias

X-linked ataxias are a group of rare and poorly characterized disorders. Relatively well described diseases in this group include fragile X tremor/ataxia syndrome, which is caused by an RNA gain-of-function-based mechanism (Orr & Zoghbi, 2007), and sideroblastic anemia with spinocerebellar ataxia (Table 1.4).

Table 1.4 Summary of the molecular features of X-linked ataxias

Disease	Genomic location	Gene/locus	Protein	Mutation
SCAX1	Xp11.21-q21.3	U	U	U
SCAX2	U	U	U	U
SCAX3	U	U	U	U
SCAX4	U	U	U	U
SCAX5	Xq25-q27.1	U	U	U
FXTAS	Xq27.3	FMR1	FMRP	CGG repeat
XLSA/A	Xq13.1-q13.3	ABC7	ABC7	MM

FXTAS, Fragile X tremor/ataxia syndrome; MM, missense mutations; SCAX, X-linked spinocerebellar ataxia; U, unknown; XLSA/A, X-linked sideroblastic anemia and ataxia

1.3 Nervous System Development

1.3.1 Neuronal migration and brain development

There are several distinct structures, like cerebellum, neocortex and thalamus, in the brain, which constitutes the central nervous system along with the spinal cord. These specific brain regions are assembled through connections between morphologically and functionally different neurons. Migration of similar neurons into discrete layers and their positioning in these layers during embryonic development is a key step in construction of unique neuronal structures.

1.3.1.1 Formation of the cerebral cortices

During embryogenesis, six-layered structure of the mammalian cortical plate is established through the serial migration of neurons from their proliferative regions to a final position within the cortex. This corticogenesis process is comprised of three stages (Figure 1.5; Gleeson & Walsh, 2000). The first step of the neocortical development is formation of the preplate or primordial plexiform layer. Preplate is established above the ventricular zone and below the pial surface around embryonic-day (E) 10-12 in mice and weeks 8-9 in humans. Ventricular zone contains proliferative cells which give rise to cortical neurons. Second step is construction of the cortical layers. This step begins with migration of first group of cortical neurons to divide the preplate into a deeper sub-plate and a superficial marginal zone, forming cortical plate between these two layers (Marin-Padilla, 1998). During cortical plate stage which takes place in E 10-17 in mice and weeks 10-18 in humans, cortical neurons exit ventricular zone, penetrate through the sub-plate and form sequential cortical layers. This lamination step occurs in an inside-out fashion. Newly-generated neurons pass the sub-plate and older cortical plate neurons, and settle below Cajal-Retzius cells of the marginal zone. So, early-born cells of cortical plate remain in deeper layers and younger cells populate

more superficial layers (Angevine & Sidman, 1961). Degeneration of the sub-plate and lamination of the cortical plate into six-layered neocortex is the last step of corticogenesis (Gleeson & Walsh, 2000). Cells migrate radially and tangentially during development of these neuronal layers (O'Rourke *et al*., 1992). Cortical neurons most often migrate radially along glial cells spanning cerebral wall to reach their final layers (Hatten, 1999). Meanwhile, a fraction of cells turn within the intermediate zone and migrate orthogonal to the radial fibers (O'Rourke *et al*., 1992).

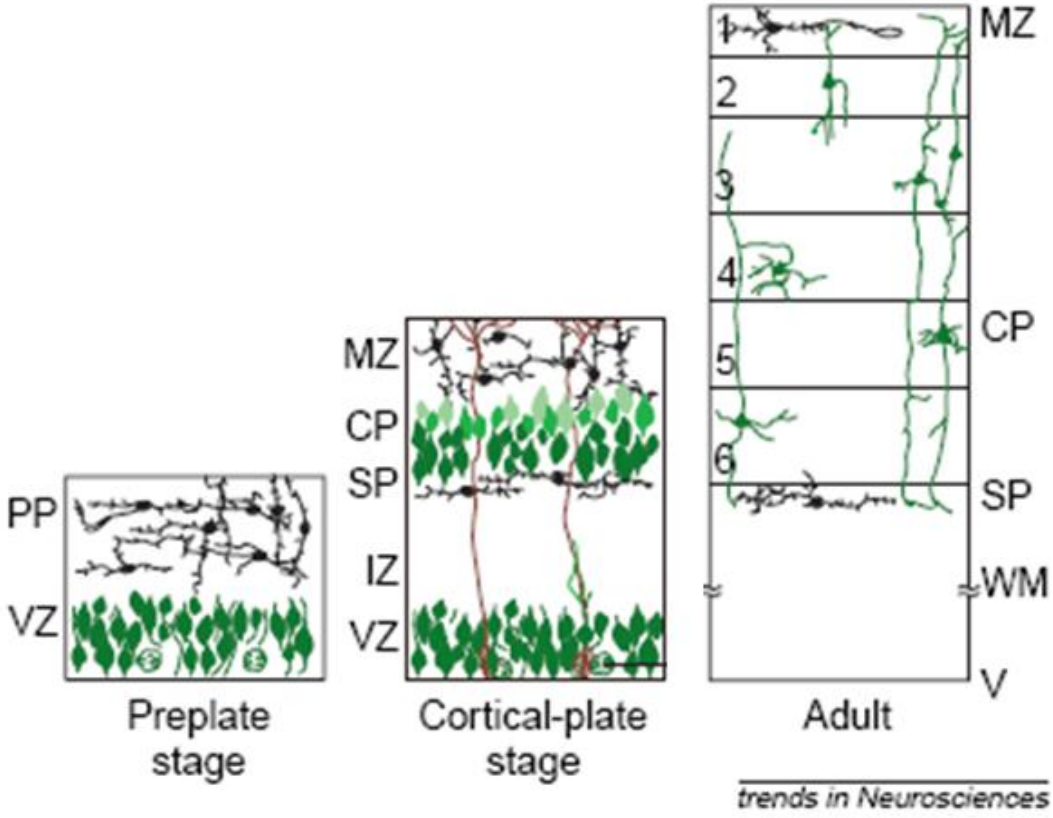

Figure 1.5 Development of the cerebral cortex. Neurons are deposited into cortical plate in an "inside-out" fashion (indicated by the progressive lighter shades of green in more superficial cortical plate neurons). Note radial alignment of the cortical neurons and the relatively cell-free marginal zone. CP, cortical plate; IZ, intermediate zone; MZ, marginal zone; PP, preplate; SP, subplate; VZ, ventricular zone; WM, white matter (Gleeson & Walsh, 2000)

1.3.1.2 Laminating the cerebellum

Cerebellum development is also carried through distinct steps. There are two different germinative zones where the cerebellar neurons are generated. Ventricular zone (also known as the ventricular germinative matrix) gives rise to precursor cells of the deep cerebellar nuclei and the Purkinje cells of the cerebellar cortex. Neurons of deep nuclei are the first generated cells at about E 10-12 in mice (Goldowitz & Hamre, 1998) and week 8 in human embryogenesis (Wang & Zoghbi, 2001). Afterwards, precursors of the Purkinje cells are produced between E 11-13 in mice (Goldowitz & Hamre, 1998) and in week 9 in humans (Hatten, 1999; Wang & Zoghbi, 2001). These precursor cells evolve to mature Purkinje cells. Maturation process continues until postnatal period. Projection of the Purkinje cells to the deep nuclei cells and refinement of input they receive from the inferior olivary complex also take place during this maturation. Purkinje cell precursors start to migrate towards the surface of cerebellum through the wall of cerebellar anlage. In the meantime precursors of the cerebellar granule neurons arise from the rhombic lip. Starting from week 11 in humans, the rhombic cells sweep across the cerebellar anlage, migrate over surface of the cerebellum and establish the external granular layer on the periphery of roof (Wang & Zoghbi, 2001). Beneath the external granular layer, the Purkinje cells establish the Purkinje cell plate and wait for inward migration of the granule cells (Miyata *et al*., 1996, Hatten, 1999). External granular layer above the Purkinje cell plate is the second germinative region of the cerebellum and gives rise to the granule cells. These cells migrate deeper into the cortex along the radially oriented Bergmann glial cells through the field of differentiating Purkinje cells (Wang & Zoghbi, 2001). Granule cells are arrested at their final destination deeper to the Purkinje cells. Three layers are formed at the end of these orchestrated migrations; an outer molecular layer of the granule cell axons and Purkinje cell dendrites, a layer of the Purkinje cells and an inner layer of the granule cells (Figure 1.6). During the course, Purkinje cell plate overlying the germinative zone functions as

a scaffold for proper lamination of the cerebellar cortex (Hatten, 1999). Inward migration of the granule cells continues after birth and the external granular layer disappears within the first year of life in humans (Wang & Zoghbi, 2001). The cerebellar nuclei, which are likely comprised of cells moved through nuclear transitory zone, take their position beneath the Purkinje cell plate. Remarkably, the Purkinje cells are also important in regulating cell proliferation in the external granular layer. Sonic hedhehog, a mitogenic factor, is produced and released by the Purkinje cells and act on precursors of the granule neurons to control proliferation (Wechsler-Reya & Scott, 1999).

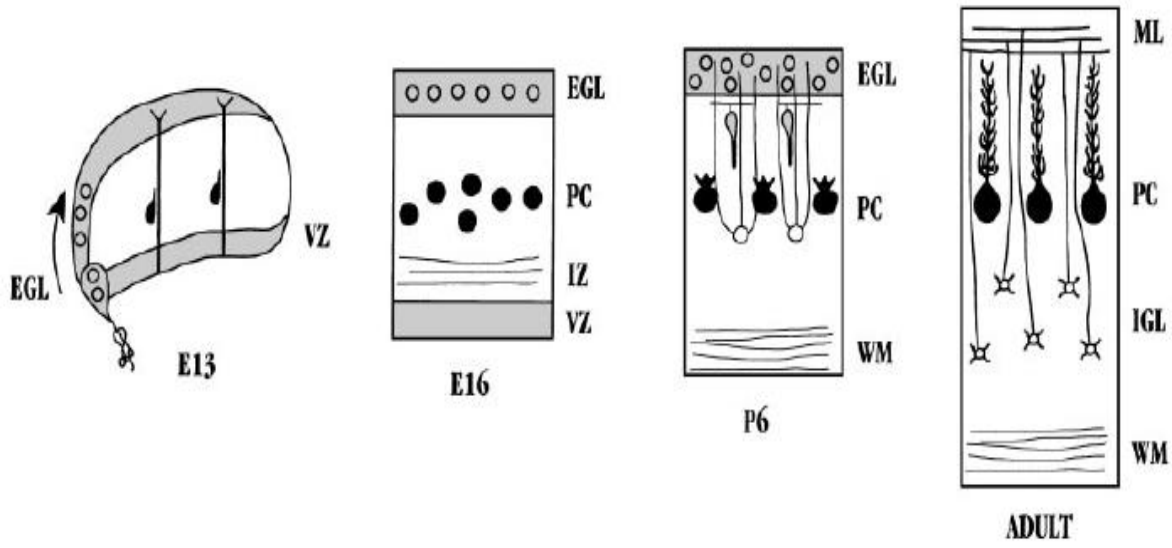

Figure 1.6 Neuronal migrations during development of the cerebellum. At embryonic period, while Purkinje cell precursors (filled circles) are migrating through the wall of the cerebellar anlage, precursors of the granule cells (unfilled circles) sweep across the roof. Afterwards, in the perinatal period, inward migration of the granule cells takes place. Connections between laminated neurons are established during adulthood. EGL, external granular layer; IGL, internal granular layer; PC, Purkinje cells (Hatten, 1999)

1.3.2 Mouse models with neurodevelopmental defects

Reeler and *trembler* mice are the classic examples of mouse models with congenital defects in the nervous system. These mice arose spontaneously, and were described more than 50 years ago (Falconer, 1951). They have been widely used to investigate role of neuronal migration in brain development, and to dissect molecular pathways regulating the choreographed migrations of neurons.

1.3.2.1 *Reeler* mouse

Reeler mouse was recognized with its "reeling" gait (Falconer, 1951). Incoordination of motor skills and ataxic condition of *reeler* mouse was due to its disrupted cortical assembly. The principal defect is neuronal malpositioning resulting from abnormal migration (Rakic & Caviness, 1995; D'Arcangelo *et al*., 1995). Inside-out cell positioning during neurogenesis fails, and layers in the cerebral cortex, cerebellum, hippocampus and other laminated brain regions develop abnormally (Rakic & Caviness 1995; Rice & Curran, 1999).

Neurons of *reeler* mice arise from their birthplace (ventricular zone, subventricular zone and rhombic lip) without any problem. Also cells start their migration on their normal program. However, they cannot establish normal architectural structures because they cannot find their proper location at the end of migration and fail to align into appropriate cell layers (Caviness, 1982; Rice & Curran, 1999). Yet, the rest of their differentiation program is unaffected. Neurons can differentiate to their destined classes, normal dendritic and axonal branching can be achieved, cells can establish successful connections with their targets, and gliogenesis and myelination are not directly affected. On the other hand since neurons do not stay at their normal location, the dendritic trees and axonal pathways are often formed abnormally. The cerebral cortex, the cerebellum, and the hippocampus are the most affected organs of *reeler* mice. Additionally,

abnormal development is observed in several other structures involving the spinal cord, brain stem, thalamus, midbrain, olivary complex, olfactory bulb, cochlear nuclei, facial nerve nucleus, retina, and tectum (Goffinet *et al*., 1984; Goffinet, 1984; Frost *et al*., 1986; Rakic & Caviness, 1995; Yip *et al*., 1998; Rice & Curran, 1999; Rice *et al*., 2001; Tissir & Goffinet, 2003).

Abnormal development of the *reeler* cerebrum can be obviously seen from beginning of cortical plate formation at E 16. In the *reeler* cortex, all major neuron classes are generated on time in the ventricular zone and neuronal cohorts follow their normal migration schedule (Rice & Curran, 2001). Preplate of *reeler* mouse develops as in wild type mouse. Afterwards, however, the inside to outside neurogenesis in the cortical plate stage does not take place (Figure 1.7). Preplate cannot be divided into the marginal zone and the subplate due to failure in invasion of the preplate by the first cohort of migrating cortical neurons (Hoffarth *et al*., 1995; Ogawa *et al*., 1995; Sheppard & Pearlman, 1997; Rice & Curran, 1999). Subsequent waves of cortical neurons can start to migrate along radial glial cells in the intermediate zone. But, they cannot bypass their predecessors, possibly because they do not penetrate the subplate or because they do not dissociate from radial cells properly (Pinto-Lord et al., 1982; Gleeson & Walsh, 2000). Instead, they populate the region beneath the subplate leading to an inversely laminated cortex (Ogawa *et al*., 1995). At the end of serial migrations in a wild type mouse cortex, the marginal zone remains relatively cell-free except for Cajal-Retzius and several other neurons. The six-layered cortical plate contains tightly packed cells which are aligned radially and the subplate assumes the position beneath the cortical plate (Rice & Curran 1999; 2001). On the other hand, in the *reeler* mouse the cortical plate is inverted and its radial alignment is lost (Hunter-Schaedle, 1997). Although neurons seem morphologically normal, their axons run obliquely in the cerebral wall and their dendrites follow tortuous paths (Goffinet, 1979). The Cajal-Retzius cells and subplate cells remain superficial to this disorganized cortical plate in a cell-dense region known as the superplate (Figure 1.8) (Derer, 1985; Rice & Curran 1999; 2001).

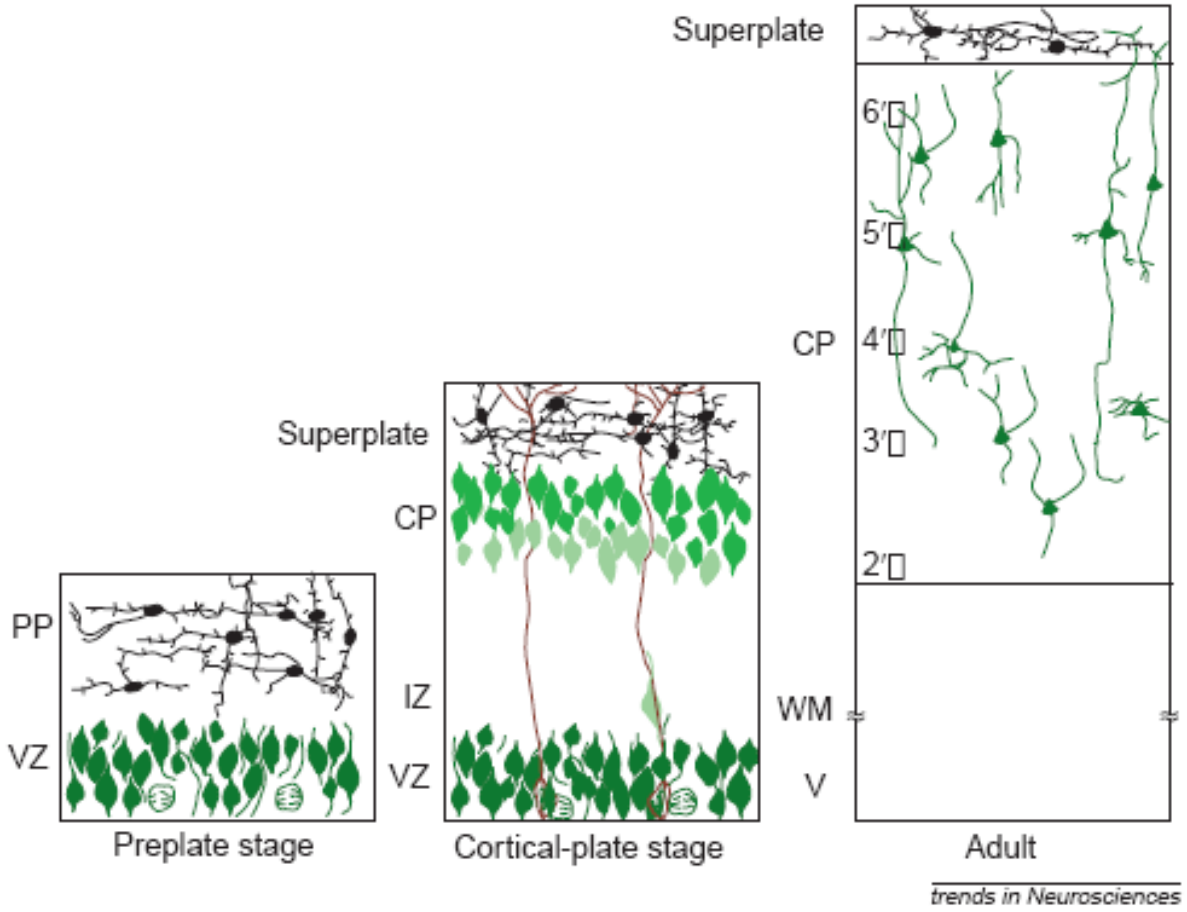

Figure 1.7 Malpositioning of neurons in the *reeler* neocortex. Development of the *reeler* cerebral cortex is characterized with inability of neurons in penetrating through the subplate. Instead, cortical cells remain underneath the preplate and late generated cells do not migrate past their predecessors (indicated by progressive lighter shades of green in deeper cortical plate neurons). Superficial layer of the cortical plate is invaded by several neurons forming superplate structure. 6'-2' numbers represent inverted layers of the cortical plate. Note neuronal projections developing at random directions. (Gleeson & Walsh, 2000)

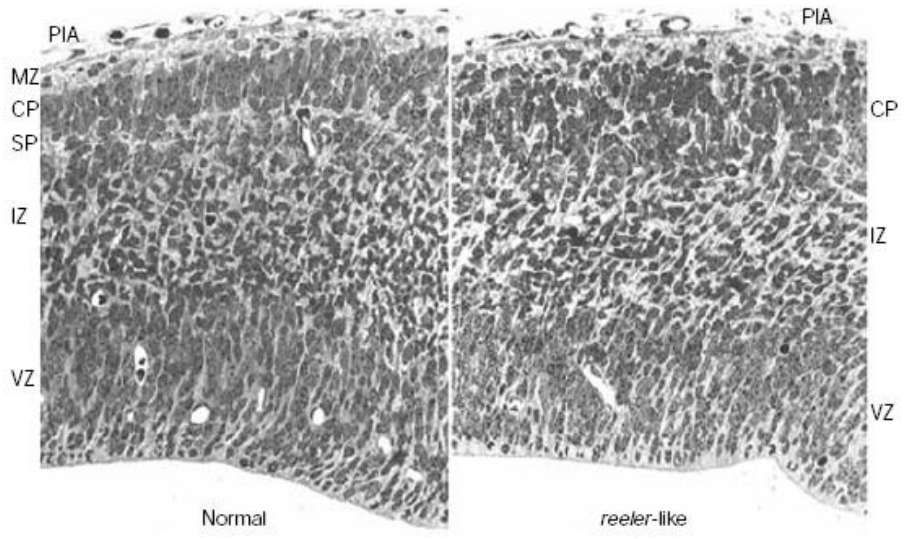

Figure 1.8 Histological appearance of the normal and *reeler* telencephalon. Disorganized cortical plate at embryonic day 14.5 is populated with cells in an oblique direction. (Tissir & Goffinet, 2003)

Most obvious phenotypic feature of *reeler* mouse is impaired gait coordination. This is probably due to severe developmental defect in its cerebellum. Number of the Purkinje cells in the *reeler* cerebellum is decreased when compared to the wild type. Radially migrating Purkinje cells stop prematurely on their migration path. They cannot establish the Purkinje cell plate and instead, reside in ectopic clusters deep in the cerebellum (Figure 1.9) (Goldowitz *et al*., 1997; Gallagher *et al*., 1998, Rice & Curran, 2001). Since Purkinje cells cannot migrate close enough to the granule cells, granule cells do not receive proliferation signals from the Purkinje cells and suffer a secondary degeneration. Moreover, the Purkinje cells cannot function as a structural scaffold for construction of other regions. Disruption of foliation of the cerebellar structures leads to functional deficits in the cerebellum (Rice & Curran 1999; Tissir & Goffinet, 2003).

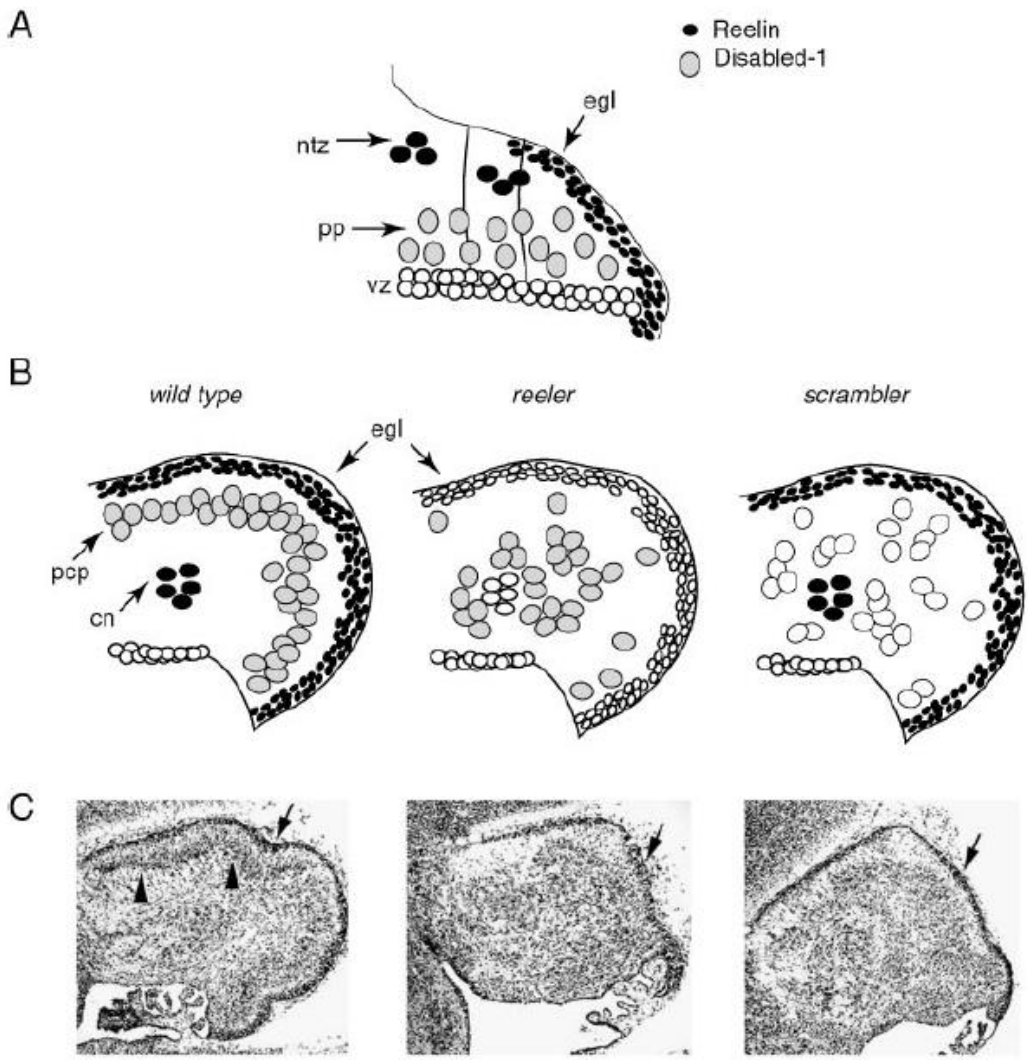

Figure 1.9 Schematic and histological appearance of the normal, *reeler* and *scrambler* cerebellum. A) Cells in the external granular layer (egl) and in the nuclear transitory zone (ntz) are reelin secreting cells (black circles) at early phases of development. Purkinje cell precursors (pp) express reelin receptors and Dab1, and migrate towards reelin secreting cells. B-C) Several days later, Purkinje cell plate (pcp) is established underneath the egl as can be seen in the micrographs (*arrowheads* show pcp and *arrows* indicate egl). In the *reeler* and *scrambler* cerebellum, Purkinje cells are unable to form the Purkinje cell plate. (Rice & Curran, 2001)

Development of the *reeler* hippocampus is also characterized by abnormal migration and malpositioning of neurons. Hippocampus remains poorly laminated; pyramidal cell layer cannot be established and granule cells reside in a disorganized dentate gyrus (Sweet et al., 1996; Tissir & Goffinet, 2003).

1.3.2.2 *Scrambler* and *yotari* mice

More than 10 years ago two new mutant mice with neurodevelopmental defects were discovered. The one arose spontaneously was described at the Jackson Laboratory (Ben Harbor, ME) and named as *scrambler* (Sweet *et al*., 1996). *Yotari* that appeared during generation of knock-out mice is the second mutant mouse exhibiting a *reeler*-like phenotype (Sheldon *et al*., 1997; Yoneshima *et al*., 1997).

Scrambler and *yotari* mice were phenotypically indistinguishable from *reeler* mice. They exhibit ataxia at 2 weeks after birth: trembling, walking with a wide gait, dragging hind limbs and flipping onto backs are certain signs (Howell *et al*., 1997). Impaired gait of these mice is because of defects in their cerebellum which develop smaller than normal and without foliation. Purkinje cells aggregate into a disorganized group at ectopic positions and their dendrites run at random directions. They fail to form a distinct layer. Granule cell population is smaller than normal and inward migration can be achieved by only few of them. Most of the granule cells reside in a superficial position to the Purkinje cells (Figure 1.9) (Howell *et al*., 1997; Goldowitz *et al*., 1997).

Like in *reeler* mice, neurons arise and start their migration on time in *scrambler*. However, they fail to form the inside-out pattern during neurogenesis of laminated structures (Gonzalez *et al*., 1997). Abnormal migration and malpositioning of neurons affect a wide range region involving the cerebral cortex and the hippocampus. The cortical plate is inversely laminated and the marginal zone is invaded by neurons. Vestiges of the normal structures are present in the *scrambler* hippocampus. Nevertheless, the large pyramidal neurons are dispersed (Howell *et al*., 1997).

1.3.2.3 Identification of reelin and Dab1 Genes

The *reeler* phenotype was found to be caused by deletion in reelin gene. Identification of reelin gene was achieved through a transgene insertion into the *reeler* locus (D'Arcangelo *et al*., 1995). Shortly after this discovery, it was found that disruption of the *mouse disabled1* (*Dab1*) gene causes the *scrambler* and *yotari* phenotypes (Howell *et al*., 1997; Sheldon *et al*., 1997; Ware *et al*., 1997). In the meantime, mutations in Cdk5 (cyclin dependent kinase 5) gene or its neuronal specific activator p35 were linked to similar neurodevelopmental disorders in mice (Ohshima *et al*., 1996; Chae *et al*., 1997).

1.3.2.4 *VLDLR* and *ApoER2* knockout mice

Disrupted *VLDLR* and *ApoER2* genes, two members of the LDL receptor family, cause a phenotype characterized by similar behavioral and neuroanatomical defects observed in the *reeler* mouse (Trommsdorff *et al*., 1999).

ApoER2 and *VLDLR* knock-out mice are smaller than normal and are ataxic at 2 weeks age. Cerebellum is smaller than normal and lacks foliation. Purkinje cells remain in ectopic clusters deep in the cerebellum. Pyramidal cells of the hippocampus are dispersed into multiple layers. Granule cells do not establish histotypical layers of dentate gyrus. Although corticogenesis begins normally, neurons migrate abnormally during construction of the cerebral wall. Observation of similar defects in reelin or *Dab1* knock-out mice led to the conclusion that these proteins function on the same signaling pathway (Trommsdorff *et al*., 1999).

On the other hand if only *VLDLR* or only *ApoER2* gene is targeted, mouse has less severe defects than double knock-out mouse. For instance, the marginal zone can be observed as a distinct layer in the cerebral cortex of *ApoER2*$^{-/-}$ or *VLDLR*$^{-/-}$ mice although the inner layer of the cortex is still disorganized. In contrast, similar to *reeler* and *scrambler* mice, in *ApoER2*$^{-/-}$;*VLDLR*$^{-/-}$ mice there is no visible marginal zone since it is invaded by ectopically positioned neurons (Sweet *et al*., 1996; Goldowitz *et al*., 1997; Gonzalez *et al*., 1997; Howell *et al*., 1997; Sheldon *et al*., 1997; Ware *et al*., 1997; Trommsdorff *et al*., 1999).

When neuroanatomical deficits of *ApoER2*$^{-/-}$, *VLDLR*$^{-/-}$ and *ApoER2*$^{-/-}$;*VLDLR*$^{-/-}$ mice are compared, it would be observed that the cerebellum is the most affected organ in *VLDLR*$^{-/-}$ mice and the cerebral cortex is the most affected structure in ApoER2$^{-/-}$ mice. Only mice lacking both receptors exhibit an identical phenotype of *reeler* or *scrambler* mice which have extensive disruptions in both the cerebellum and cerebral cortex (Trommsdorff *et al*., 1999).

In the cerebellum of *VLDLR*$^{-/-}$ mouse, the Purkinje cells do not appropriately receive Reelin signal sent from the granule cells in the external granular layer. So the Purkinje cells do not complete their migration and fail to form the Purkinje cell plate. Nevertheless, Purkinje cells of *ApoER2*$^{-/-}$ mouse can establish a distinct layer in the cerebellum although they are smaller than normal cells and their projections are randomly organized (Trommsdorff *et al*., 1999).

During development of the cerebral cortex of *ApoER2* deficient mouse, cortical layers are formed inversely since most of the neurons fail to reach their normal positions and are horizontally aligned. Yet, in *VLDLR*$^{-/-}$ mouse, cortical neurons can migrate in a radial alignment and find their normal layer. But *VLDLR* deficiency prevents them to distribute properly in their determined layer (Trommsdorff *et al*., 1999).

Moreover, in a recent study it was shown that *ApoER2* and *VLDLR* are involved in different steps of neuronal migration during cortical development; whereas proper migration of late generated neurons depends on functional *ApoER2* protein, *VLDLR* is required to prevent migrating neurons from invading the marginal zone (Hack *et al*., 2007).

All these findings demonstrate that *ApoER2* and *VLDLR* have similar functions and one receptor can partially compensate for the loss of other receptor. Yet, since they can have divergent functions at some points, both of them are important and required for proper development of the laminated brain regions (Rice & Curran, 1999; 2001).

1.3.3 Reelin signaling pathway

After identification and characterization of reelin, several studies were performed to constitute a linear signaling pathway guiding neurons on their way during development of nervous system.

These studies revealed that Reelin is a large glycoprotein (D'Arcangelo *et al*., 1997) secreted by Cajal-Retzius cells in the marginal zone of the cerebral cortex (D'Arcangelo *et al*., 1995; Hirotsune *et al*., 1995; Ogawa *et al*., 1995), and by the external granular layer and deep cerebellar nuclei neurons in the cerebellum (D'Arcangelo *et al*., 1995, Miyata *et al*., 1996). Reelin binds to *VLDLR* and *ApoER2* and is internalized subsequently (D'Arcangelo *et al*., 1999, Hiesberger *et al*., 1999). Binding of Reelin to these lipoprotein receptors induces a tyrosine signaling cascade that phosphorylates *Dab1* (Howell *et al*., 1999). *Dab1* is an adaptor protein and interacts with NPxY motifs in the cytoplasmic tails of *VLDLR* and *ApoER2* (Howell *et al*., 1999; Rice & Curran, 2001). Hence, *VLDL* receptor and *ApoER2* are necessary to transmit Reelin signal to intracellular molecules for proper positioning of cells in brain development.

Cadherin-related neuronal receptors (Senzaki *et al*., 1999) and α3β1 integrin (Dulabon *et al*., 2000) are other transmembrane proteins that Reelin can bind.

Dab1 is phosphorylated by Src family tyrosine kinases (Arnaud *et al*., 2003; Bock & Herz, 2003). Activation of *Dab1* promotes two different signaling pathways. One of them is a kinase cascade modulating activity of *tau* protein, a microtubule stabilizing protein (Hiesberger *et al*., 1999). The other pathway regulates actin cytoskeleton through Crkl/C3G/Rap1 cascade (Ballif *et al*., 2004). Lis1, which is an important regulator of cell positioning during cortical lamination is another intracellular partner of Reelin pathway and binds to phosphorylated *Dab1* upon Reelin stimulation (Assadi *et al*., 2003). Pafah1b complex formed by Lis1 and two other subunits was also found to be interacting with *VLDL* receptor and was recently integrated into Reelin pathway (Zhang *et al*., 2007).

Reelin may dictate different and comparable signals on migrating neurons. It can be a stop signal arresting migration of neurons (Dulabon *et al*., 2000), a chemoattractant for migrating neurons (Gilmore & Herrup, 2000), or it can be necessary for the timely detachment of migrating neurons (Hack *et al*., 2002; Sanada *et al*., 2004).

1.4. Aim and Strategy

The aim of this study is to identify the gene(s) that are associated with quadrupedal locomotion (Unertan syndrome) in humans. Linkage genome scan using high-density microarray platform, homozygosity mapping and candidate gene analysis strategies were employed to achieve this goal.

PART II: MATERIALS AND METHODS

2.1 Recruitment of Families

Four consanguineous families, family A, family B, family C and family D, all from Turkey and exhibiting Unertan syndrome, were studied. Healthy and affected members of these families were referred to Bilkent University, Faculty of Science, Molecular Biology and Genetics Department (Ankara, Turkey) by collaborating physicians at Cukurova University, Faculty of Science (Adana, Turkey). Patients and other unaffected individuals were enrolled after obtaining informed consent according to the protocols approved by the Ethics Committees of Baskent and Cukurova Universities with the decision numbers KA07/47, 02.04.2007 and 21/3, 08.11.2005, respectively.

2.2 DNA and RNA Samples

2.2.1 Sample collection

Peripheral blood was obtained from available patient and healthy members of the families. Samples were collected in tubes containing EDTA. They were divided into 1 ml aliquots in 1.5 ml eppendorf tubes. The samples have been stored at -80°C.

2.2.2 DNA isolation from blood samples

200 µl blood was used for each DNA isolation reaction. To prepare DNA from blood, Nucleospin™ Blood kit (Macherey-Nagel Inc., PA, USA) (#740 951.250) was used according to the manufacturer's instructions. Concentration of the DNA was determined by using NanoDrop™ ND-1000 UV-Vis Spectrophotometer.

2.2.3 Amplification of purified genomic DNA

2.5 µl purified genomic DNA was amplified with REPLI-g™ Midi kit (Qiagen Inc.) (#150043) according to the manufacturer's guidelines. Concentration of amplified DNA was checked by using NanoDrop™ ND-1000 UV-Vis Spectrophotometer.

2.2.4 RNA isolation from blood samples

For extraction of RNA from blood, QlAamp™ RNA Blood Mini kit (Qiagen Inc.) (#52304) was used with 1.5 ml blood. After performing isolations according to the manufacturer's instructions, NanoDrop™ ND-1000 UV-Vis Spectrophotometer was used to quantify concentration of RNA.

2.2.5 cDNA synthesis

cDNA was prepared from 11 µl RNA with RevertAid™ First Strand cDNA Synthesis kit (MBI Fermentas, Amh, NY, USA) (#K1622) according to the guidelines of the manufacturer.

2.3 Genetic Mapping

Determining mode of inheritance is the first and one of the critical steps in genetic modeling of human disorders. Hereditary human disorders have chromosomal, Mendelian (single gene disorders) or complex inheritance patterns. Conditions of the complex inheritance include reduced penetrance, imprinting effect, mitochondrial inheritance, dynamic mutations, epistasis, and gene-environment interaction. On the other hand, diseases obeying Mendelian rules can be inherited over autosomes or sex chromosomes. Autosomal characters can be dominant or recessive, and sex linked characters are basically divided into X-linked dominant, X-linked recessive and Y-linked (Strachan & Read, 2004).

Pedigree analysis of the families diagnosed with Unertan syndrome revealed that the disorder has not been observed over generations. Instead, disease arises in one generation implying vertical transmission, and affected children are resulting from consanguineous marriages. Because of these reasons the mode of inheritance was decided as autosomal recessive.

Second step of genetic modeling studies is to determine how to approach mapping the disease. One approach is candidate gene analysis which was not used initially in our studies since there was no obvious candidate. So, the other method, whole genome genotyping, was performed.

2.3.1 Genome-wide linkage analysis

Whole-genome SNP genotyping was performed with the commercial release of the GeneChip® 250K (*Nsp*I digest) or GeneChip® 10K Affymetrix arrays as described (Matsuzaki *et al*., 2004). Guidelines in GeneChip® mapping assay manuals provided by Affymetrix were followed to carry out experiments (Figure 2.1).

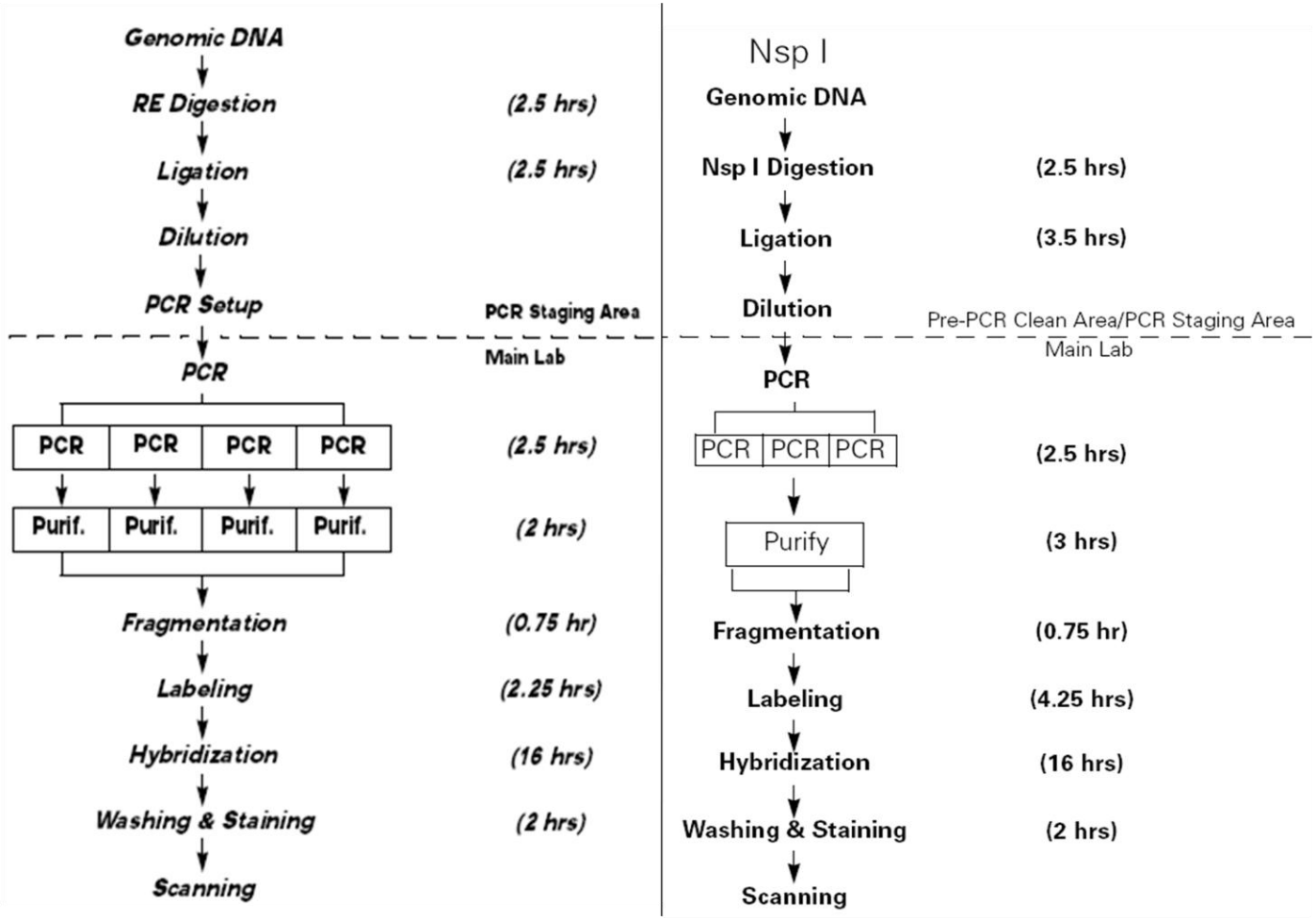

Figure 2.1 Workflow of GeneChip® mapping 10K (*left*) and 500K (*Nsp*I digest; *right*) assays (Affymetrix 10K and 500K manuals).

The third step of genetic mapping is to decide statistical analysis strategy. According to presence or absence of an inheritance mode, parametric or non-parametric statistics method is used to analyze genome wide data obtained from the SNP chips. Parametric analysis is used in linkage studies, and need a pre-determined inheritance mode and large families exhibiting the phenotype. There is no need to know inheritance mode while using non-parametric statistic method and because of this it is used in association studies in disorders demonstrating complex inheritance. Since our pedigrees perfectly fit autosomal recessive inheritance with full penetrance, we used parametric, linkage, approach to analyze the data generated from SNP chips.

To analyze SNP chip data computer based statistical analysis programs are used. These programs include LINKAGE, GENE HUNTER, ALLEGRO and MERLIN programs. MERLIN program was used in our analysis since it allows the user to handle very large numbers of markers rapidly and efficiently (Abecasis *et al*., 2002). It also facilitates fast multipoint analysis which contains number of markers in an interval, i.e relevant markers in 1 cM interval. Hence, multipoint linkage analysis was done with the parametric component of the MERLIN Package v1.01 (Abecasis *et al*., 2002; Abecasis & Wigginton, 2005).

Next step is preparing the input files which describe the pedigree, analytic parameters, map information and marker list included in the analysis. There are four files used by the MERLIN program. These are *pedigree*, *data*, *map*, and *model* files. *Pedigree* file, i.e UTS.ped, describes relationships between individuals and their disease status (Table 2.1). *Data* file, i.e UTS.dat, contains the list of markers and describe the affection status, i.e rare disorders with a model estimation (Table 2.2). Map file, i.e UTS.map, contains the order and genetic positions of the SNP markers (Table 2.3). Disease model is described in the *model* file, i.e UTS.model, in which we specified the disorder as very rare disease (Table 2.4).

Table 2.1 Part of *pedigree* file for family A. Family A was divided into two parts for convenience as shown with numbers 1 and 2 in the family column. In sex column, numbers 1 and 2 indicates male and female respectively. Data for SNP markers of each individual are given in genotypes column. In status column, numbers 1 and 2 indicates unaffected and affected individuals respectively. F, family; FID, father identification number; MID, mother identification number; PID, personal identification number; S, sex

F	PID	FID	MID	S	Genotypes						Status
1	1	0	0	2	1/1	2/2	1/1	1/1	0/0	1/1	1
1	2	0	0	1	1/1	0/0	1/1	1/1	1/1	1/1	1
1	3	2	1	2	1/1	1/2	1/1	1/1	0/0	1/1	1
1	4	2	1	1	1/1	2/2	1/1	1/1	1/1	1/1	2
1	5	2	1	1	1/1	0/0	1/1	1/1	0/0	1/1	1
1	6	2	1	2	1/1	2/2	1/1	1/1	1/2	1/1	2
1	7	2	1	2	1/1	2/2	1/1	1/1	1/1	1/1	1
2	1	0	0	2	1/1	2/2	1/1	1/1	1/1	1/1	1
2	2	0	0	1	1/1	2/2	2/2	1/1	1/2	1/2	1
2	3	2	1	1	1/1	2/2	1/1	1/1	1/2	1/2	2
2	4	2	1	2	1/1	2/2	0/0	1/1	1/2	1/2	1
2	5	2	1	1	1/1	2/2	1/2	1/1	1/1	1/2	1
2	6	2	1	2	1/1	2/2	1/2	1/1	1/1	1/2	1
2	7	2	1	1	1/1	2/2	0/0	1/1	1/2	1/1	2
2	8	2	1	2	1/1	2/2	1/1	1/1	1/1	1/2	1
2	9	0	0	1	1/1	2/2	2/2	1/1	1/1	1/1	1
2	10	2	1	2	1/1	2/2	2/2	1/1	1/2	1/2	1
2	11	9	10	2	1/1	1/2	2/2	1/1	1/2	1/1	2
2	13	9	10	2	1/1	2/2	2/2	1/1	1/1	0/0	1
2	14	9	10	1	1/1	2/2	2/2	1/1	1/1	1/2	1
2	15	9	10	1	1/1	2/2	2/2	1/1	1/2	0/0	1

Table 2.2 Part of *data* file for family A. Second column are the list of the markers. Very rare disease describes the disease and refers to the *model* file where penetrance values of the disease are given. A, affection status; M, marker

M	SNP_A-1513154
M	SNP_A-1511366
M	SNP_A-1509154
M	SNP_A-1514257
M	SNP_A-1518033
M	SNP_A-1516287
M	SNP_A-1516246
M	SNP_A-1514307
M	SNP_A-1509247
M	SNP_A-1515558
M	SNP_A-1511470
M	SNP_A-1507812
M	SNP_A-1509562
M	SNP_A-1518487
M	SNP_A-1509919
M	SNP_A-1512266
M	SNP_A-1510062
M	SNP_A-1512471
M	SNP_A-1511505
M	SNP_A-1510562
M	SNP_A-1519343
M	SNP_A-1515796
M	SNP_A-1516100
M	SNP_A-1515465
M	SNP_A-1515289
M	SNP_A-1519085
M	SNP_A-1509293
M	SNP_A-1518948
M	SNP_A-1508116
.	.
.	.
.	.
.	.
A	VERY_RARE_DISEASE
E	END-OF-DATA

Table 2.3 Part of *map* file showing a sample of SNP markers from chromosome 1, for family A. SNP names and their genetic positions are given in the second and third columns respectively. CHR, chromosome number

CHR	MARKER	LOCATION
1	SNP_A-1509443	3.859.407
1	SNP_A-1518557	5.848.183
1	SNP_A-1517286	8.655.963
1	SNP_A-1516024	8.853.158
1	SNP_A-1514538	9.387.403
1	SNP_A-1516403	9.510.903
1	SNP_A-1518687	12.351.566
1	SNP_A-1509959	12.353.228
1	SNP_A-1515791	13.890.000
1	SNP_A-1513560	13.891.000
1	SNP_A-1512212	13.892.000
1	SNP_A-1519671	14.865.946
1	SNP_A-1515942	15.275.197
1	SNP_A-1512107	20.442.669
1	SNP_A-1514390	21.496.830
1	SNP_A-1518041	24.577.258
1	SNP_A-1508673	28.395.543
1	SNP_A-1519660	28.663.799
1	SNP_A-1511922	28.677.756
1	SNP_A-1510413	28.678.445
1	SNP_A-1509189	29.025.883
1	SNP_A-1518353	29.446.071
1	SNP_A-1509509	29.753.222
1	SNP_A-1516958	30.998.694
1	SNP_A-1515835	31.231.667
1	SNP_A-1516239	31.907.546
.	.	.
.	.	.
.	.	.
.	.	.

Table 2.4 Part of *model* file for family A. We specified the disorder as very rare disease, and determined penetrance as 0.0001, 0.0001 and 0.9999 for individuals carrying, respectively, 0, 1 and 2 copies of the disease allele

VERY_RARE_DISEASE	0.0001	0.0001, 0.0001, 0.9999	Rare_recessive

After description of the input files, the analysis was carried out along a grid of locations equally spaced at 1 cM, which allows multipoint analysis in 1 cM interval. And the graphic was plotted as a pdf output which is given at results part. The syntax used in the analysis is:

Prompt> merlin –d UTS.dat –p UTS.ped –m UTS.map -- model UTS.model -- grid1 -- markerNames -- pdf

2.3.2 Homozygosity mapping and haplotype analysis

Haplotypes were constructed and homozygosity regions were determined through visual inspection of the genotype data. Haplotype analysis was performed on chromosomal regions with positive lod scores. Lod score is logarithm of the odds ratio which is ratio of probability of linkage of a trait and a marker over probability of no-linkage between the disease and the marker. Lod scores are calculated for several estimates of recombination frequency values and a lod score greater than 3.0 is considered as evidence for linkage. In addition to MERLIN analysis, MLINK component of the LINKAGE program (FASTLINK, version 3) was used for pairwise linkage analysis (Lathrop & Lalouel, 1984; Cottingham *et al*., 1993; Schaffer *et al*., 1994).

Polymorphic markers from the critical intervals of chromosomes 9p24 (D9S1779 [0.4 Mb] and D9S1871 [3.7 Mb]) and 17p13 (D17S1298 [3.51 Mb]) were used to test for homozygosity to the respective chromosomal loci.

2.4 Candidate Gene Analysis

2.4.1 Polymerase Chain Reaction (PCR)

2.4.1.1 Primers

Primers covering exons of *VLDLR* gene in NC_000009 sequence were designed by using Primer3 (http://frodo.wi.mit.edu/) and BLAST (http://www.ncbi.nlm.nih.gov/blast/Blast.cgi) websites (Table 2.5). Primers were purchased from Iontek Inc. (Istanbul, Turkey).

2.4.1.2 PCR conditions

4 µl DNA (100-150 ng) was used as a template with 2.5 µl PCR buffer (10X), 1.5 µL $MgCl_2$ (25 mM), 0.3 µl dNTPs (10mM), 1 µl (10pmol/µl) from each primer and 0.2 µl *Taq* DNA Polymerase (5u/µl) (MBI Fermentas, Amh, NY, USA) (#EP0402). Volume of the sample was adjusted to 25 µl with ddH_2O.

Reactions were performed in the Techne™ TC-512 and Techgene thermal cyclers. Reaction conditions were 5 min initial denaturation at 94°C, followed by 35 cycles of 94°C for 30 sec, 58°C – 62°C (A.T.) for 30 sec and 72°C for 30 sec or 40 sec and 5 min final extension at 72°C. A.T. is the annealing temperature at which the primer pair binds to its specific target sequence.

Table 2.5 Primers that were used for sequencing of *VLDLR* gene.

Primer Name	Forward Primer (5' to 3')	Reverse Primer (5' to 3')	Amplified Region	Product Size (bp)
Primer Pair 1	ACTCACGCACGCTCACACT	TCCGAAAGGAGGAAGAAGGT	Exon 1	495
Primer Pair 2	GGAGGAGACTGTGCAAGTTGT	GTGGGCAAACGGAGACCTAC	Exon 1	366
Primer Pair 3	TCCCCATCCATGGGTATTAG	TGATAACCCCACGTCAAACA	Exon 2	365
Primer Pair 4	TGAGCCCTCATGTGAAGCTA	TGTTGGACCAGGGAGAACAT	Exon 3	388
Primer Pair 5	GCAGCAGCTTTGCATTGAT	AGAAACACCAAGCGATGGTC	Exon 4	328
Primer Pair 6	TGAACGGACCAATCTTGATG	GTCGCATACCCAGCTGATG	Exon 5	243
Primer Pair 7	CCCATGAGTTCCAGTGCAG	CTTTCAGGGGCTCATCACTC	Exons 5-6-7	659
Primer Pair 8	CCGATGAAGTCAACTGCAAA	CCTACCTGGGCTTTTAAGTCA	Exon 7	396
Primer Pair 9	GGTAACTTGCCGAGGAGTTAGA	CAGAATTAGTCTTGCTGCTCCT	Exon 8	398
Primer Pair 10	GCAGGTGATGGGAAAGGATA	CAACAGCCATACCAGTCCAA	Exon 9	231
Primer Pair 11	TGGGAGGAGGTGGTTTAGAA	CGATGCTAGATGGGGCTAGA	Exon 10	355
Primer Pair 12	TGAGCTGTGGTGTTAACTGGA	TCCTGACCTACACAGATACCATTC	Exon 11	400
Primer Pair 13	TGCCTTGAGTTTTCTGCTCA	AGTTGAGTGGGTGGTCGAGA	Exon 12	258
Primer Pair 14	GCTTCGCAAGGTTTATGGTG	AAGCCATGTTCAGCTGCTCT	Exon 13	389
Primer Pair 15	TGTCCCAGTTCAGCATTCAG	GGGTACAGGAGGGCAAAAGT	Exon 14	389
Primer Pair 16	GGCAAGGACTCAGGTCTTCA	CCCGGCATACAATAGCAGAT	Exon 15	378
Primer Pair 17	ACAGCTAGCCATGCTGGAAC	CCAGGAACAACTCTGGCTTA	Exon 16	391
Primer Pair 18	GCCAGAGTTGTTCCTGGTGT	ACAGCATAAAGGCCCATGAA	Exon 17	325
Primer Pair 19	GGCCCATGTGTATTCCAACT	CACCCAGGTCTCCTTTCTGA	Exon 18	392
Primer Pair 20	CAACTCAAAAGCAAGGTCCA	GGTAACCACATCCAAAGCTGA	Exon 19	338
Primer Pair 21	CTCTCGGCTGGAAGAACATC	CCTATTGCCATTGTCCCAAC	Exon 19	360
Primer Pair 22	CTTCAGCTTTGGATGTGGTT	CCAGCCCAATTACAGGCTTA	Exon 19	540
Primer Pair 23	AGGACTGGTAACTTGTCGTGCGGAG	GCAGCCAGAGCGCCCAGAGCG	Repeats in 5' UTR	106

2.4.1.3 Agarose gel electrophoresis

1X TAE electrophoresis buffer was used to dissolve agarose (Basica LE, EU) with final percentage of 1.5 % and ethidium bromide with final concentration of 30 ng/µl.

PCR product was mixed with 1/5 volume of 6X loading dye solution before loading onto agarose gel. 1X TAE was used as running buffer for gel with different voltage and time parameters depending on size of the fragment. pUC Mix Marker 8 (0.1 µg/µl) (MBI Fermentas, Amh, NY, USA) (#SM0303) was used as DNA marker. GelDoc imaging system (Bio-Rad, CA, USA) with MultiAnalyst software version 1.1 (Bio-Rad, CA, USA) was used to visualize gel and take photographs.

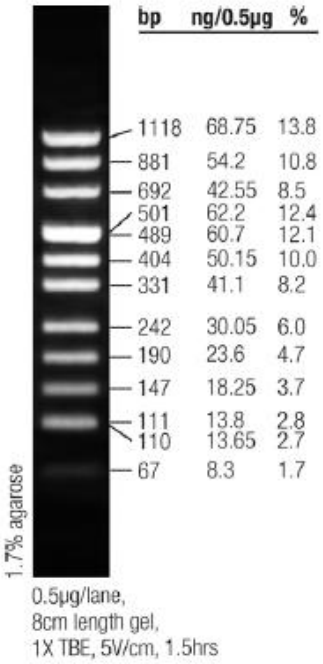

Figure 2.2 Sizes of the fragments of pUC Mix Marker 8 and appearance on agarose gel electrophoresis.

2.4.2 Mutation search

2.4.2.1 Sequencing reactions

PCR products with 20 µl volume and varying concentrations were used for sequencing reactions. They were purified and sequenced by Iontek Corp. (Istanbul, Turkey) by using forward and reverse primers for sense and antisense strand sequencing.

2.4.2.2 Data analysis

Sequencing data were analyzed using Chromas Lite 2.01 (Technelysium Pty Ltd) software.

ClustalW website (http://www.ebi.ac.uk/Tools/clustalw2/index.html) was used for sequence alignment.

2.4.3 Restriction digestion assay

Families and other control individuals were genotyped with
(*i*) F-5'-CCCATGAGTTCCAGTGCAG-3' and
R-5'-CTTTCAGGGGCTCATCACTC-3' primer pair, and
(*ii*) F-5'-GCCAGAGTTGTTCCTGGTGT-3' and
R-5'-ACAGCATAAAGGCCCATGAA -3' primer pair
to screen, respectively, c769C->T and c2339delT mutations.

PCR conditions were 94^{o}C for 5 min as initial denaturation followed by 35 cycles of 94^{o}C for 30 sec, 62^{o}C (primer pair (*i*)) / 58^{o}C (primer pair (*ii*)) for 30 sec and 72^{o}C for 40 sec and 72^{o}C for 5 min as final extension.

Restriction enzyme digestion was carried out from 5 µl PCR product. PCR products were obtained by using primer pair 7 or primer pair 18 and were digested with 0.10 µl *Hph*I (10 u/µl) (MBI Fermentas, Amh, NY, USA) or 0.20 µl *Mbo*I (10 u/µl) (MBI Fermentas, Amh, NY, USA) enzymes respectively, 2 µl restriction buffer and 12.80 µl ddH_2O. Restriction site for *Hph*I enzyme is (5'-GGTGA $(N)_8$↓-3') and for *Mbo*I enzyme is (5'-G↓ATC -3'). Restriction digestion reactions were incubated at 37°C water-bath for 3-4 hours. Digestion products were run on 1.5 % agarose gel after mixed with 4 µl 6X loading dye solution. pUC Mix Marker 8 (0.1 µg/µl) was used as DNA marker. GelDoc imaging system with MultiAnalyst software was used to visualize gel.

2.4.4 Quantitative real-time reverse transcriptase PCR (Q-PCR)

The sequences of the primers targeting *VLDLR* cDNA were:
F-5'-CGAGACTGTCAAAGTACTGCAACTA-3' and
R-5'-CACTAAGAGCAAGAGAGGAAGAATG-3'.

GAPDH (glyceraldehyde-3-phosphate dehydrogenase), and *KDR* (kinase insert domain receptor) were used as reference genes and primers for their cDNAs were:
(*i*) *KDR* (F-5'-CTCAGCAGGATGGCAAAGAC-3' and
R-5'-CAGATACTGACTGATTCCTGCTGT-3'),
(*ii*) *GAPDH* (F-5'-GGCTGAGAACGGGAAGCTTGTCAT-3' and
R-5'-CAGCCTTCTCCATGGTGGTGAAGA-3').

Reactions were performed with cDNA-specific primers according to the SYBR Green I protocol in iCycler (Bio-Rad, CA, USA). 1 µl of cDNA was used in 25 µl PCR reaction mixture containing 12.5 µl SYBR Green mix (Bio-Rad, CA, USA), 0.5 µl of each primer (10 pmol/µl) and 10.5 µl ddH_2O. To cover top of the mixture, 25 µl mineral oil was added to each tube.

All reactions were performed in duplicate with the following cycling protocol: 10 min heat start at 94^{o}C and 50 cycles of denaturation at 94^{o}C for 30 s, annealing at 60^{o}C for 30 s and extension at 72^{o}C for 30 s. Melting curve analysis was performed following amplification step by raising temperature from 55°C to 94°C with 0.5°C increments at each 15 seconds. Relative expression ratios were calculated from duplicate samples using comparative C_t method (Pfaffi, 2004) and normalized according to the housekeeping gene *GAPDH* and the endothelial marker *KDR*.

Real-time PCR products were run on 1.5% agarose gel after mixed with 5 µl 6X loading dye solution. pUC Mix Marker 8 (0.1 µg/µl) was used as DNA marker. GelDoc imaging system with MultiAnalyst software was used to visualize gel.

2.5 Solutions and Buffers

- 1X TAE (Tris-acetic acid-EDTA): 40mM Tris acetate, 2 Nm EDTA, pH 8.0

- Ethidium bromide: 10 mg/ml in water for stock solution

- Agarose gel loading buffer (6X): 15% ficoll, 0.05% bromophenol, 0.05% xylene cyanol

PART III: RESULTS

3.1 Clinical Assessment

Habitual and efficient quadrupedal locomotion is the cardinal and distinctive feature of the affected individuals (Figure 3.1). Quadruped individuals began to crawl on hands and knees or feet and they could never walk upright. They are well balanced without any ataxic movements while walking on their hands and feet. They can stand up for a short period of time, but they do not gain a fully erect position. While standing up, their bodies with their legs remain in a flexed position. They use both diagonal and lateral sequence gaits while walking quadrupedally. Their hands make contact with the ground at the ulnar palm with the weight taken on the wrists and lower ulnar area of the palm. Fingers make little or no contact with the ground preventing wearing of fingers. They can even hold objects with their fingers that are raised off the ground while walking (Tan, 2005; 2006a; Humphrey *et al*., 2005, Turkmen *et al*., 2006).

One of the affected individuals in family A (VII:1 in figure 1.1) and one in family C (IV:1 in figure 1.3) can use bipedal gait although these patients are severely ataxic. Also, aunt of the proband in family D (I:4 in figure 1.4) can walk bipedally, but she prefers to walk in a quadrupedal fashion despite her advanced age (Tan, 2006b; Ozcelik *et al.*, 2008a).

Figure 3.1 Quadrupedal palmigrate walking of Unertan syndrome patients. Locomotion on all four extremities is exemplified by affected brothers VI:20 and VI:18 and cousin VI:25 in family A (*Upper*), and the proband II:2 in family D (*Lower*). The ulnar palm area is heavily callused like in the case of VI:20 since hands make contact with the ground at that area while walking. Strabismus was observed in all affected individuals. (Ozcelik *et al*., 2008a)

Another important characteristic of the phenotype is dysarthria. Affected individuals can use little or no language and have limited vocabulary. Their mother and father can rather easily communicate with them, but not the other people. Mini Mental State Examination Test (standardized for the uneducated Turkish people) was used to determine cognitive abilities and consciousness of the affected individuals. Patients do not know time, place, and date implying that they are mentally retarded and have no conscious experience. Nevertheless, they exhibit no autistic features; they all have good interpersonal skills, are friendly and curious to visitors. They can understand and follow very simple questions and commands (Tan, 2006a; Ozcelik *et al.*, 2008a).

Upon neurological assessment, mild thoracal scoliosis is found in patients and this prevents them from holding their heads upright. Affected individuals do not exhibit any extrapyramidal signs and have no muscle weakness, sensory loss or deformities. All patients had hyperactive lower leg and vivid upper extremity reflexes. Moreover their cranial nerves are intact. Yet, their muscle tonus and tendon reflexes are mildly decreased and they had bilateral dysmetria and dysdiadochokinesis (Tan, 2006a). Additional clinical information on affected individuals in families A and D is provided in Table 3.1 (Ozcelik *et al.*, 2008a).

Table 3.1* Physical and neurological findings of the patients in families A and D (Ozcelik *et al*., 2008a).

	Family A						Family D		
Traits	VI:1	VI:18	VI:20	VI:25	VI:27	VII:1	II:2	I:4	I:5
Gender	Male	Male	Male	Male	Female	Female	Male	Female	Male
Age	35	46	37	17	12	17	38	65	63
Height (cm)	158	152	145	150	135	142	148	150	147
Speech	Dysarthric	Dysarthric	Dysarthric	Dysarthric	Dysarthric	Dysarthric	Dysarthric	Dysarthric	Dysarthric
Mental retardation	Profound	Profound	Profound	Profound	Profound	Severe	Profound	Profound	Profound
Gait	Quadrupedal	Quadrupedal	Quadrupedal	Quadrupedal	Quadrupedal	Ataxic	Quadrupedal	Quadrupedal/ataxic	Quadrupedal
Truncal ataxia	Severe	Severe	Severe	Severe	Severe	Moderate	Severe	Moderate to severe	Severe
Romberg	Absent	Absent	Absent	Absent	Absent	Absent	Absent	Absent	Absent

Epilepsy	Absent	Absent	Absent	Absent	Absent	Present	Absent	Absent	Absent
Arm-reflexes	Hyper	Vivid	Normal	Normal	Normal	Vivid	Vivid	Vivid	Vivid
Leg-reflexes	Hyper	Vivid	Hyper	Hyper	Hyper	Hyper	Hyper	Hyper	Hyper
Hoffman (R)	Absent	Present	Present	Absent	Absent	Absent	Not done	Not done	Not done
Hoffman (L)	Absent	Present	Present	Absent	Absent	Absent	Not done	Not done	Not done
Trommer (R)	Absent	Absent	Present	Absent	Absent	Present	Not done	Not done	Not done
Trommer (L)	Absent	Absent	Present	Absent	Absent	Present	Not done	Not done	Not done
Babinsky (R)	Present	Absent	Absent	Absent	Present	Present	Not done	Not done	Not done
Babinsky (L)	(+)	Absent	Absent	Absent	Present	Absent	Not done	Not done	Not done
Clonus (R)	Absent	Absent	Absent	Present	Absent	Absent	Not done	Not done	Not done
Clonus (L)	Absent	Absent	Absent	Present	Absent	Absent	Not done	Not done	Not done
Spasticity	Absent	Absent	Absent	Absent	Absent	Absent	Absent	Absent	Absent

Force (arms)	Normal	Normal	Normal	Normal	Normal	Normal	Normal	Normal	Normal
Force (legs)	Normal	Normal	Normal	Normal	Normal	Normal	Normal	Normal	Normal
Int.tremor(R)	Absent	Absent	Absent	Present	Absent	Present	Absent	Absent	Absent
Int.tremor(L)	Absent	Absent	Absent	Present	Absent	Absent	Absent	Absent	Absent
Dysmetria(R)	Mild	Mild	Absent	Mild	No response	Absent	Not done	Not done	Not done
Dysmetria(L)	Mild	Mild	Absent	Mild	No response	Mild	Not done	Not done	Not done
Head (cm)	53	55	52.5	53	51	54	Not done	Not done	Not done
Menstruation	n.a.	n.a.	n.a.	n.a	Premenstrual	(+)	n.a	Post-menopausal	n.a.
Cal. Nys. (R)	> 2 min	> 2 min	> 2 min	> 2 min	> 2 min	> 2 min	Not done	Not done	Not done
Cal. Nys. (L)	> 2 min	> 2 min	> 2 min	> 2 min	> 2 min	> 2 min	Not done	Not done	Not done

Mental status as measured by Developmental Quotient (DQ) estimated by clinical history was judged as severe retardation (DQ 20 to 34) and profound retardation (DQ < 20). Dysmetria as measured by finger chase test judged as mild when under/overshooting target < 5 cm.
R, right; L, left; Cal. Nys., caloric nystagmus; n.a., not applicable.

*Detailed clinical information can be obtained from: family A: Tan *et al*., 2008a; family D: Tan, 2008b

Neuroradiological examination revealed that the cerebellum and the cerebellar vermis of the quadrupedal individuals are hypoplastic. Inferior portion is completely lost and midline is fissured in the vermis (Figure 3.2). These findings can be accompanied by small brainstem and the pons, simplification of the cortical gyri, and hypoplasia of corpus callosum in some patients (Tan, 2006a; Ozcelik *et al.*, 2008a). Similar signs except for hypoplasia of the corpus callosum are also observed in the MRI scans of two siblings walking bipedally in family B (Turkmen *et al.*, 2006).

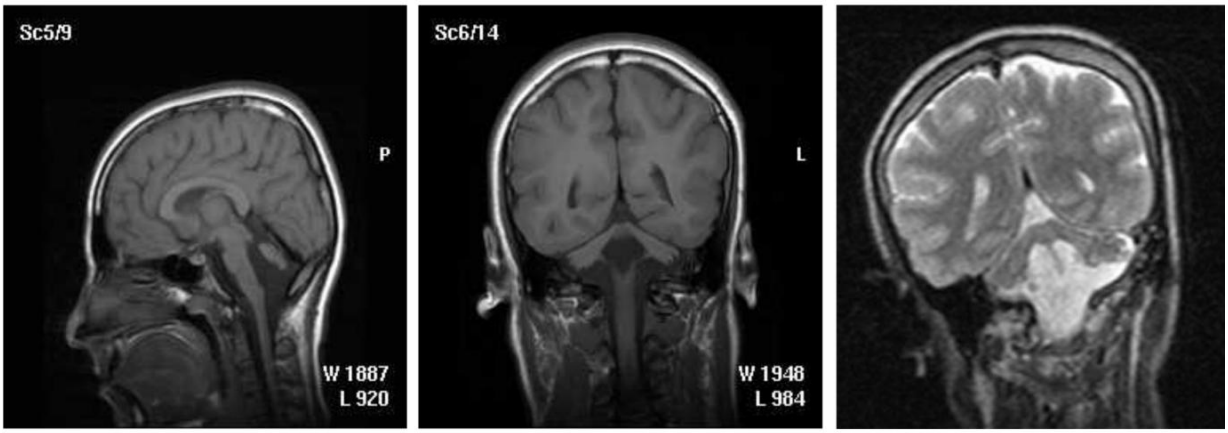

Figure 3.2 Neuroradiological images of affected individuals. Hypoplasia of the vermis which lacks inferior part, and the cerebellar hemispheres is seen in coronal and midsagittal MRI sections of VI:20 in family A. Cortical gyral simplification, and small brainstem and the pons are other findings (*left* and *center*). II:2 in family D displays similar signs (*right*). (Ozcelik *et al*., 2008a)

3.2 Chromosomal Loci Associated With Quadrupedal Locomotion

In family A, Affymetrix 250K GeneChip® was used for genome wide linkage analysis which revealed two regions on chromosomes 9p and 15q with positive lod scores (Appendix A). MERLIN or other linkage programs test for co-segregation between the disease allele and the DNA markers selected from the region of interest. It does not detect homozygosity information in the region. Therefore, for recessive disorders all regions providing positive lod scores should also be tested for homozygosity by inspecting haplotypes. With this aim, informative markers covering the regions with positive location scores were selected. Further haplotype analysis and homozygosity mapping with these markers confirmed linkage of the disease loci to a 1.032-Mb region between rs7847373 and rs10968723 markers on chromosome 9p24 (Figure 3.3) and exclude the locus in chromosome 15q (Figure 3.4).

Disease loci in family B was linked to chromosome 17p13, confirming a previous study (Turkmen *et al*., 2006). In family C, no homozygosity was identified for the critical regions on chromosomes 9p24 (Figure 3.5) and 17p13 (Figure 3.6) and multipoint linkage analysis yielded highly negative lod scores, excluding both loci; gene mapping in this family is ongoing.

Figure 3.3 Homozygosity mapping of cerebellar hypoplasia and quadrupedal locomotion to chromosome 9p24. Affected individuals were indicated with filled symbols in the pedigree of family A. Regions associated with the disease allele of Unertan syndrome was represented with black bars. Boundaries for the disease locus were defined between markers rs7847373 and rs10968723 by recombination events in individuals VI:16 (obligate carrier) and VII:4 (normal sibling). Physical positions and pairwise lod scores for each marker are shown on the upper left. Zmax represents the maximum lod score obtained at Θ=0.00 cM (Ozcelik *et al*., 2008a).

Chromosome 9p24

SNP ID	Position (Mb)	Z_{max}
rs519864	1.72	0.823
rs7847373	1.83	-infi
rs4740653	1.88	0.749
rs7857865	1.94	3.185
rs1572747	1.95	1.431
rs7040968	2.13	2.027
rs10491695	2.15	1.606
rs7044488	2.24	1.124
rs16906885	2.48	3.185
rs10967598	2.69	2.583
rs10968723	2.86	-infi
rs10813058	2.93	-infi

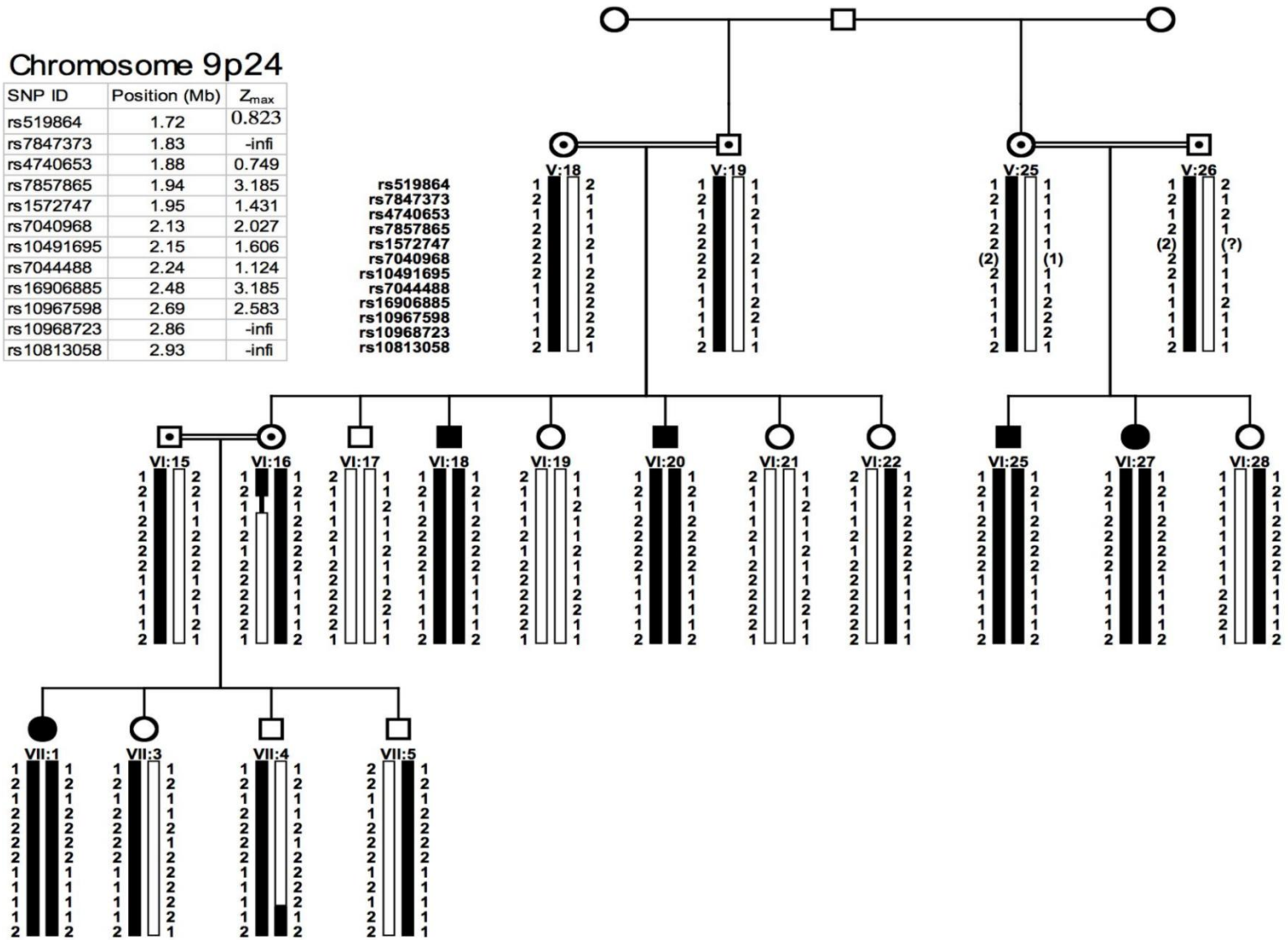

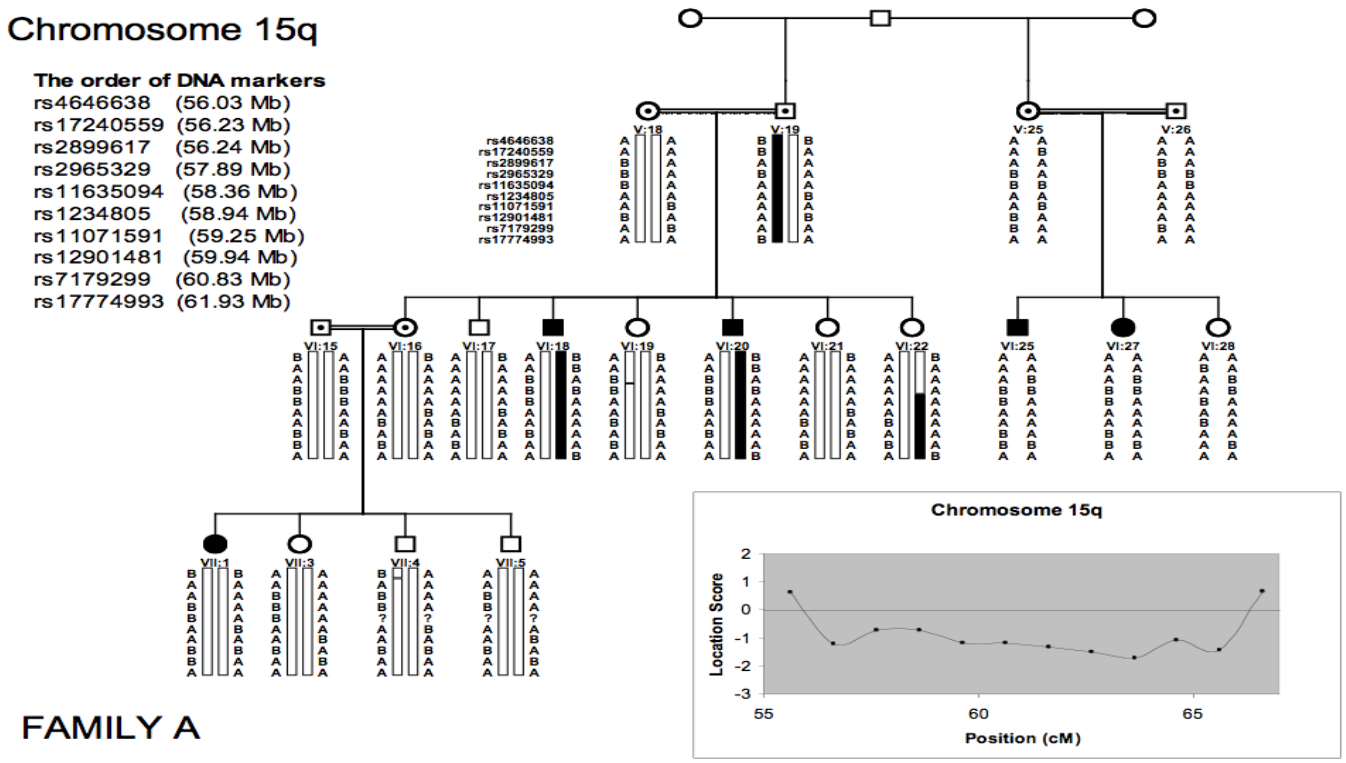

Figure 3.4 Haplotype analysis of family A using SNP markers from 15q residing between the 55- and 65-Mb region. The order of SNP markers based on physical positions is shown on the upper left. Although whole genome SNP genotyping gave positive lod scores for that region, homozygosity was not detected among affected individuals in the haplotype analysis of the entire pedigree. Absence of consensus between the branches in the haplotype and negative scores in multipoint linkage analysis (*bottom right*) confirmed exclusion of the 15q region (Ozcelik *et al*., 2008a).

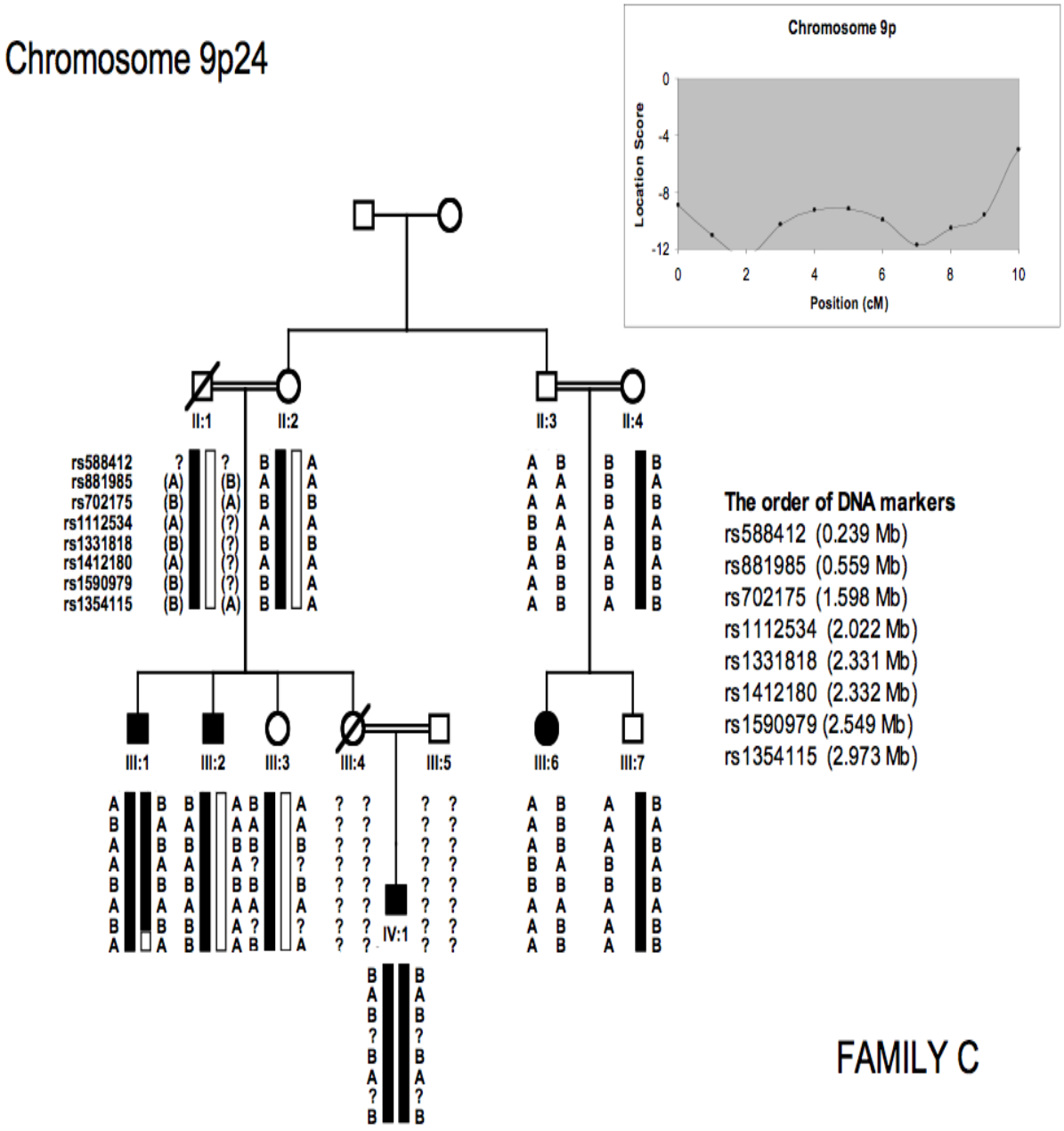

Figure 3.5 Exclusion of chromosome 9p24 in family C. SNP markers in the critical interval were tested in haplotype and multipoint linkage analysis (Ozcelik *et al*., 2008a).

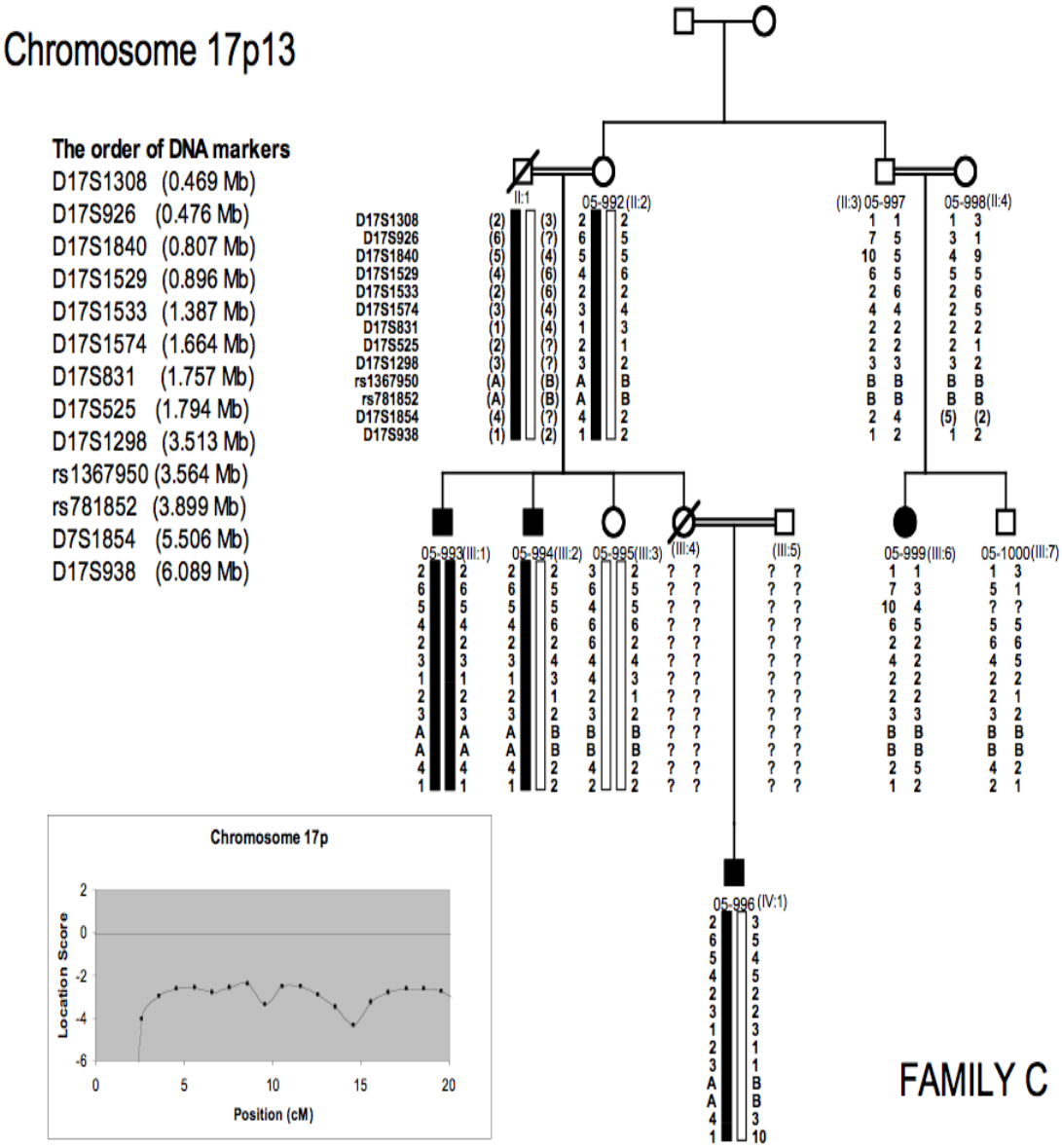

Figure 3.6 Haplotype and exclusion analyses of family C using polymorphic markers from 17p13 critical region. Graphical presentation of the multipoint linkage analysis using the information obtained from 10K SNP array is shown on the bottom left. Haplotype was constructed with the polymorphic markers selected from the same critical region (Ozcelik *et al*., 2008a).

In family D, whole genome SNP genotyping was not done. Instead, polymorphic markers from the critical intervals of chromosomes 9p24 and 17p13 were tested. The pedigree showed homozygosity in chromosome 9p24.

3.2.1 Genetic heterogeneity; Unertan syndrome type I

The families exhibiting Unertan syndrome are living in isolated villages apart from each other and there is no documented ancestral relationship between the families. However, Unertan syndrome is a very rare disease, only six families reported until now. Because of this we expected a single locus shared by affected individuals in all families. But, mapping studies resulted in three different chromosomal localizations in our families. These are chromosome 9p24 in family A and family D, and chromosome 17p13 in family B (Turkmen *et al*., 2006; Ozcelik *et al*., 2008a). Disease trait of family C could not be linked to either 17p13 or 9p24 regions (Ozcelik *et al*., 2008a). These results revealed genetic heterogeneity in Unertan syndrome.

Hence, the condition in families A and D is proposed as "Unertan syndrome type 1" (Ozcelik *et al*., 2008a).

3.3 Candidate Gene Analysis in 9p24

3.3.1 *VLDLR* as a candidate gene

The critical region on chromosome 9p24 includes *SMARCA2* (SWI/SNF-related, matrix-associated, actin-dependent regulator of chromatin, subfamily A, member 2), *VLDLR* (very low density lipoprotein receptor), *KCNV2* (potassium channel, voltage-gated, subfamily V, member 2), and *KIAA0020* (minor histocompatibility antigen HA-8) genes.

Among these genes *VLDLR* was selected as a prime positional candidate. The rationale behind this selection was that a gene involved in nervous system development, neuronal migration, and cerebellar maturation could be involved in the pathogenesis of quadrupedal gait. Additionally, it was previously shown that a genomic deletion including *VLDLR* causes cerebellar hypoplasia with cerebral gyral simplification (Boycott *et al*., 2005)

3.3.2 *VLDLR* sequencing in families A and D

37-year-old male of family A (VI:20) was studied as index patient. He ambulates in a quadrupedal manner. His speech is dysarthric and cognitive abilities are severely reduced with no conscious experience. Hypoplasia of the cerebellum and the cerebellar vermis with complete loss of inferior vermis, moderately simplified cerebral cortical gyri, and small brainstem and the pons are his MRI scan findings.

Index patient of Family D (II:2) was a 38-year-old male. Profound mental retardation, dysarthria, and truncal ataxia accompany his quadrupedal locomotion. His cerebellum and vermis are hypoplastic and can be observed along with moderate simplification of cortical gyri in MRI brain scans.

Sequencing of *VLDLR* gene exons from genomic DNA of these affected individuals revealed a homozygous c769C->T mutation in family A and a homozygous c2339delT mutation in family D (Figure 3.7; Ozcelik *et al*., 2008a).

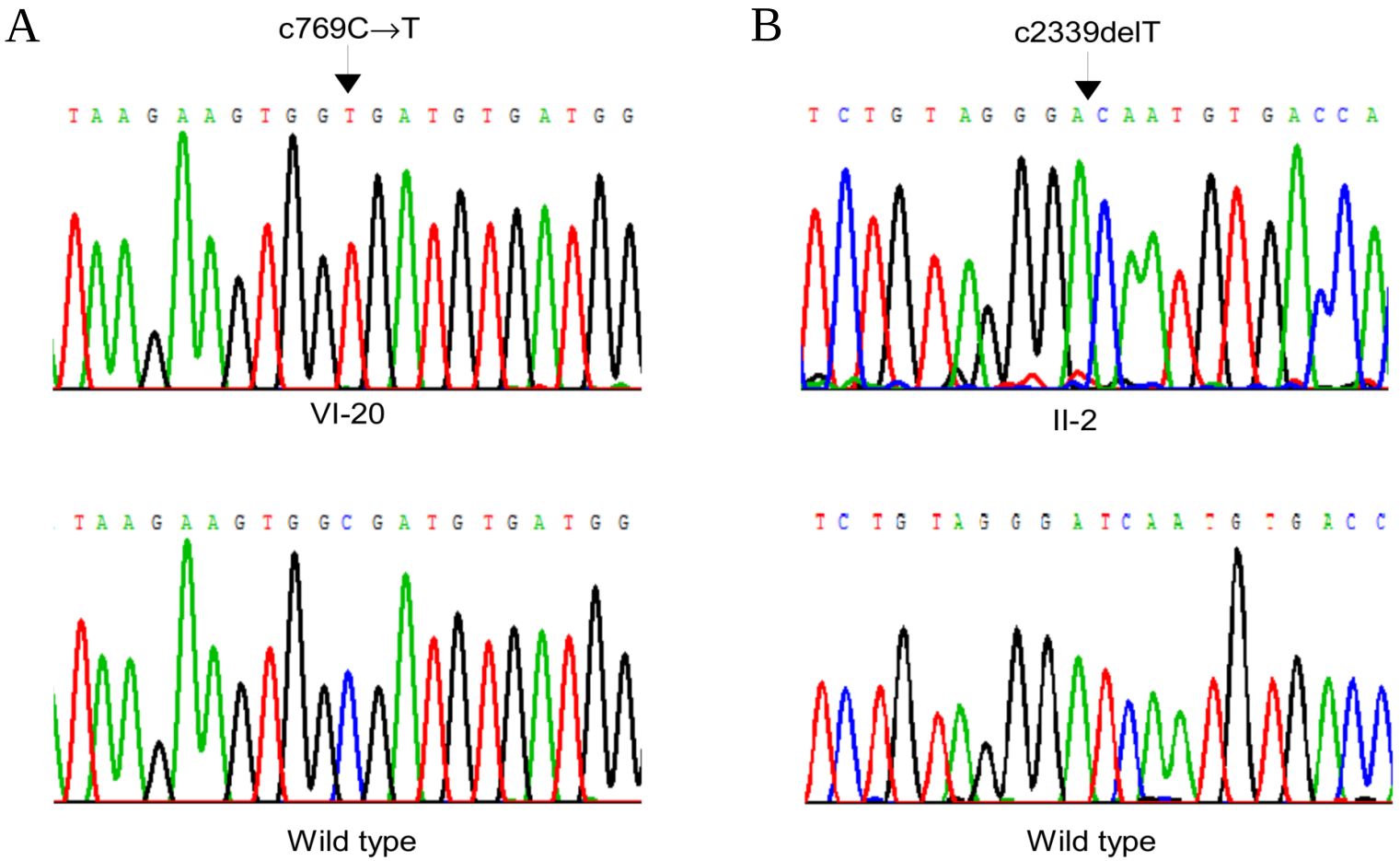

Figure 3.7 Chromatograms presenting *VLDLR* c769C->T mutation in family A (A) and *VLDLR* c2339delT mutation in family D (B) (Ozcelik *et al*., 2008a).

3.3.3 Restriction endonuclease based mutation screening in families A and D

Family A was screened for c769C->T mutation. There is no restriction site for *Hph*I enzyme (5'-GGTGA $(N)_8$↓-3') in the respective amplicon of DNA of a homozygous normal individual, and c769 C -> T mutation introduces a restriction site. Single band at 659 bp was observed for homozygous normal individuals, two bands of 463 and 196 were observed in homozygous mutant individuals as expected.

Family D members were genotyped with the particular primers to screen c2339delT mutation. Respective amplicon of DNA of a homozygous normal individual contains two restriction sites for *Mbo*I enzyme (5'-G↓ATC -3'), one of which would be eliminated by c2339delT mutation. The corresponding band sizes at the result of digestion were 217 and 106 bp bands for homozygous mutant individuals, and 181, 106 and 37 bp bands for homozygous normal individuals.

VLDLR mutation segregates with the disease in the members of both families (Figure 3.8). All patients are homozygous mutant, and all tested parents are heterozygous for the wild-type allele. Carriers of the families A and D were identified with this assay.

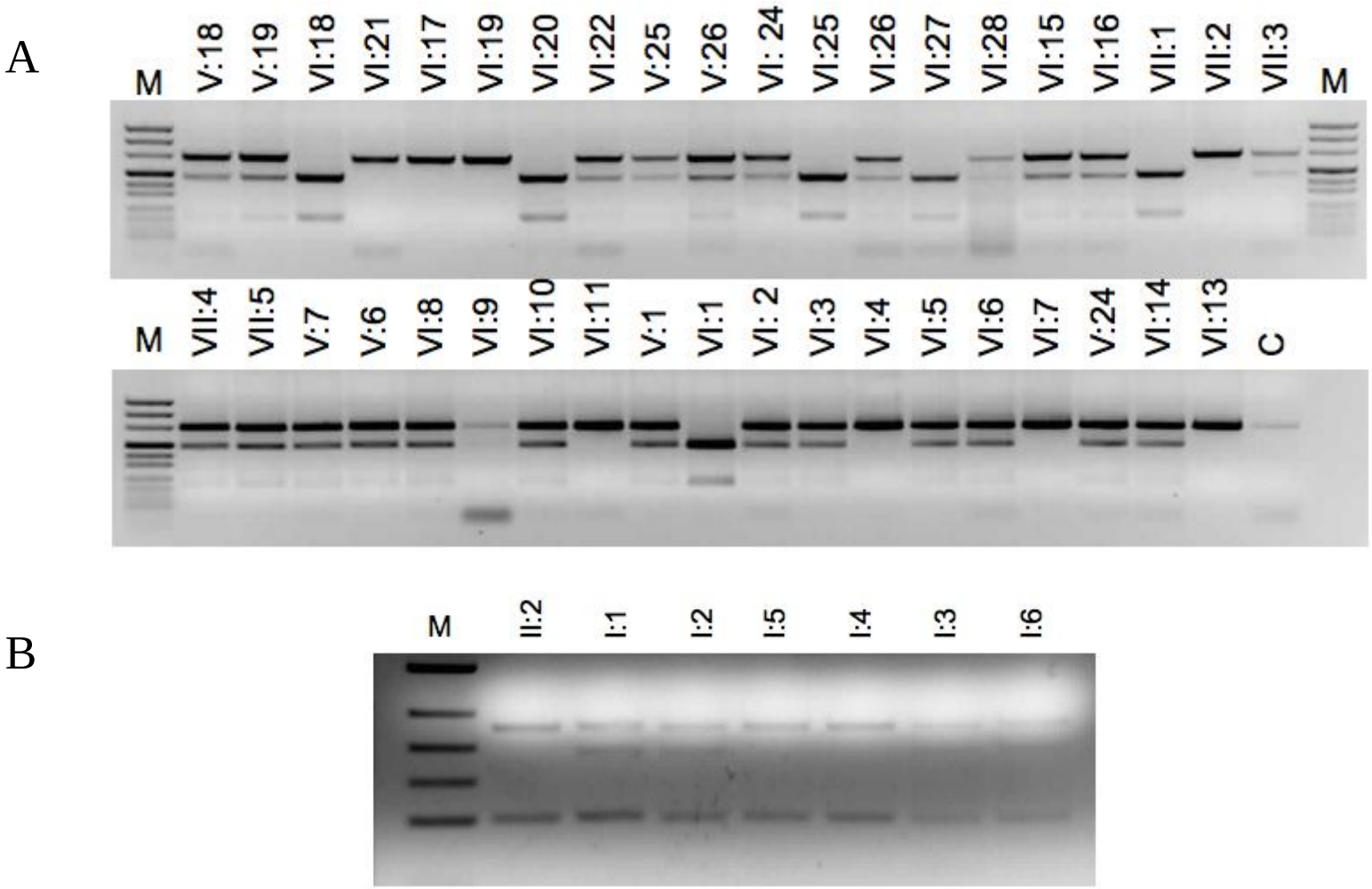

Figure 3.8 Restriction enzyme based mutation screening in family A (A) and family D (B). Fragment sizes of the DNA size marker (M) are 1118, 881, 692, 501, 404, 331, 242, and 190 bp in (A), and 331, 242, 190, 147, and 111 bp in (B). (Ozcelik *et al*., 2008a)

3.3.4 *VLDLR* sequencing in family B and C

Family B and family C did not share homozygosity for chromosome 9p24. Yet, certain human genetic traits can be caused by compound heterozygous mutations – presence of two different mutant alleles at the same gene.

To exclude the possibility of compound heterozygosity, *VLDLR* gene exons were sequenced from genomic DNA of the probands of Family B (V:11) and Family C (III:2). Sequencing of *VLDLR* did not reveal any mutations in both patients (Appendix B; Ozcelik *et al*., 2008a).

3.3.5 Restriction enzyme based mutation screening in control individuals

200 individuals including 50 individuals from southeast, 50 individuals from west and remaining 100 individuals from different geographical locations in Turkey were selected to screen both mutations in normal population. *Hph*I and *Mbo*I enzymes were used to screen c769C -> T and c2339delT mutations respectively, following genotyping of individuals with the particular primer pairs. Single band at 659 bp was observed for homozygous normal individuals with *Hph*I digestion and three bands with 181, 106 and 37 bp sizes were observed for homozygous normal individuals with *Mbo*I digestion. DNA of an affected individual in Family A (VI:1) was used as *Hph*I digestion control. Positive control was not necessary for *Mbo*I digestion since it has already restriction sites in homozygous normal genotype. All control individuals were homozygous normal for both mutations (Figure 3.9).

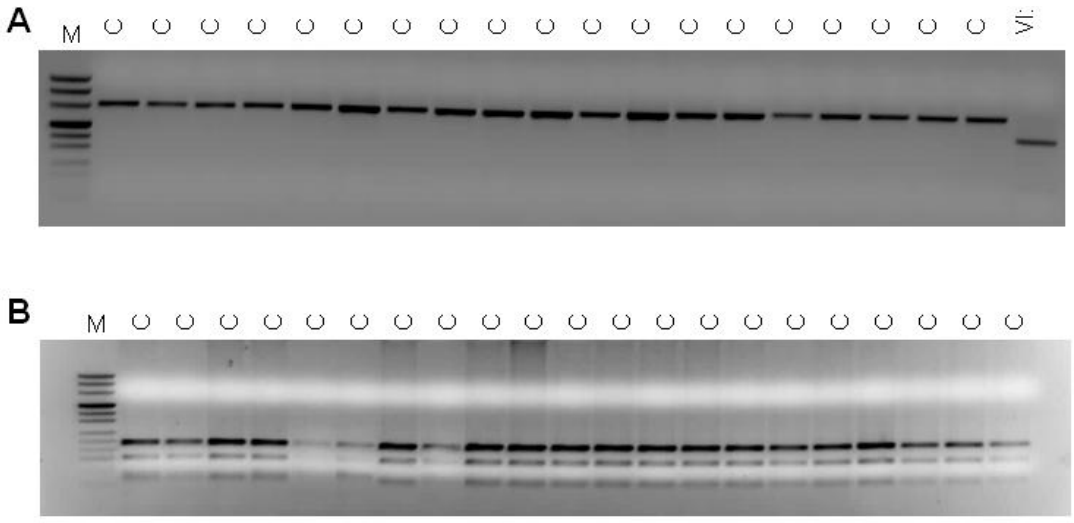

Figure 3.9 Screening of c769C->T (A) and c2339delT (B) mutations in control individuals. (Ozcelik *et al*., 2008a)

3.4 Quantitative Analysis of *VLDLR* Expression in Affected and Unaffected Individuals

Expression levels of *VLDLR* gene in affected individuals of families A and D (8 patients; 6 patients from family A and 2 patients from family D), and in 4 control individuals were compared using Q-PCR (Figure 3.10 and 3.11).

VLDLR gene is very lowly expressed in blood and primers specific for *VLDLR* cDNA were normalized by diluting cDNAs from 1µl to 2^{-3}µl. Relative expression levels were calculated according to the formula:

$$\text{Expression change} = n^{-(\Delta CT \text{ patient} - \Delta CT \text{ control})}$$

Where; n is the normalization number (depends on efficiency of the primers), CT is the threshold cycle for each sample, and ΔCT represents the difference between threshold cycles of *VLDLR* and *GAPDH* or *VLDLR* and *KDR*.

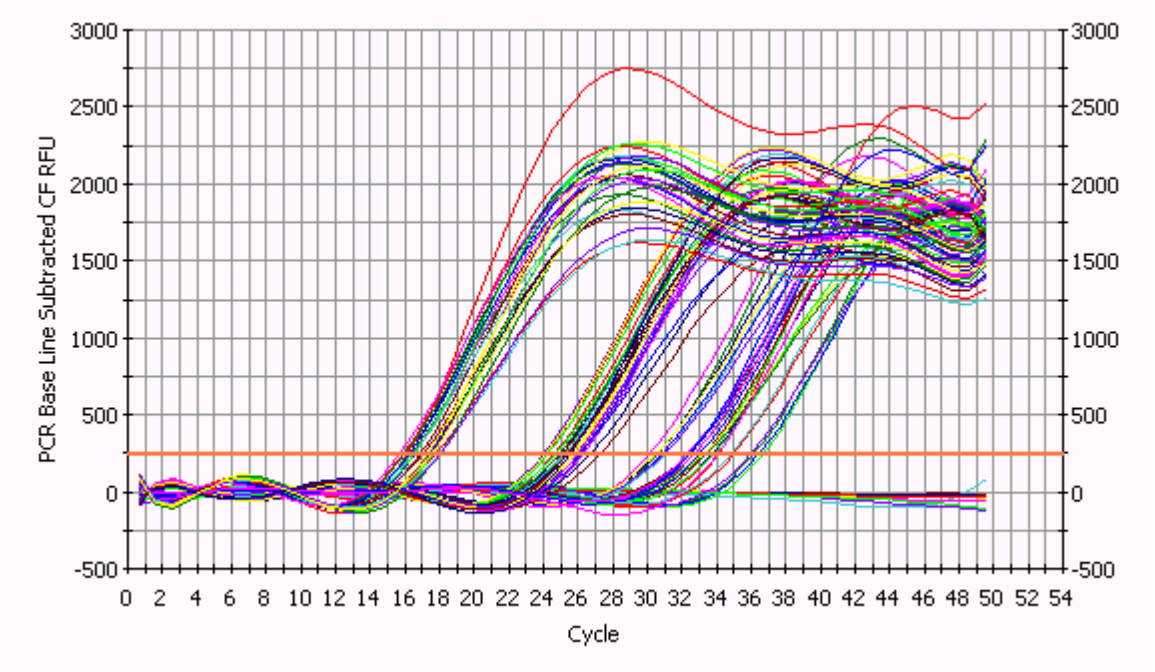

Figure 3.10 PCR amp/cycle graph for *VLDLR*.

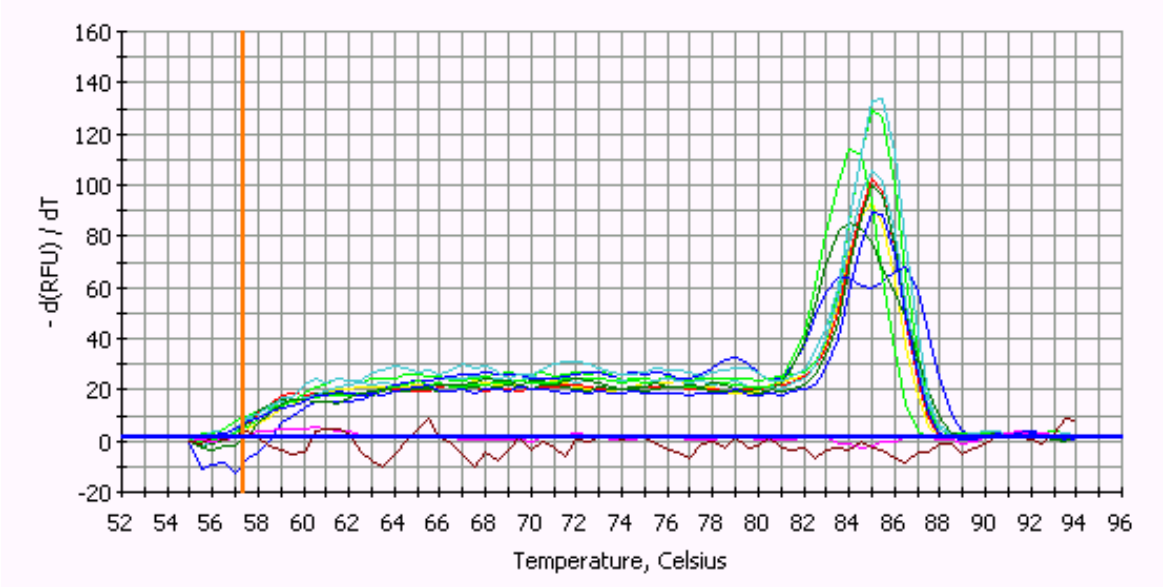

Figure 3.11 Melt curve graph for *VLDLR*.

There was no considerable difference for VLDLR expression between patients and controls (Figure 3.12; Ozcelik *et al*., 2008a).

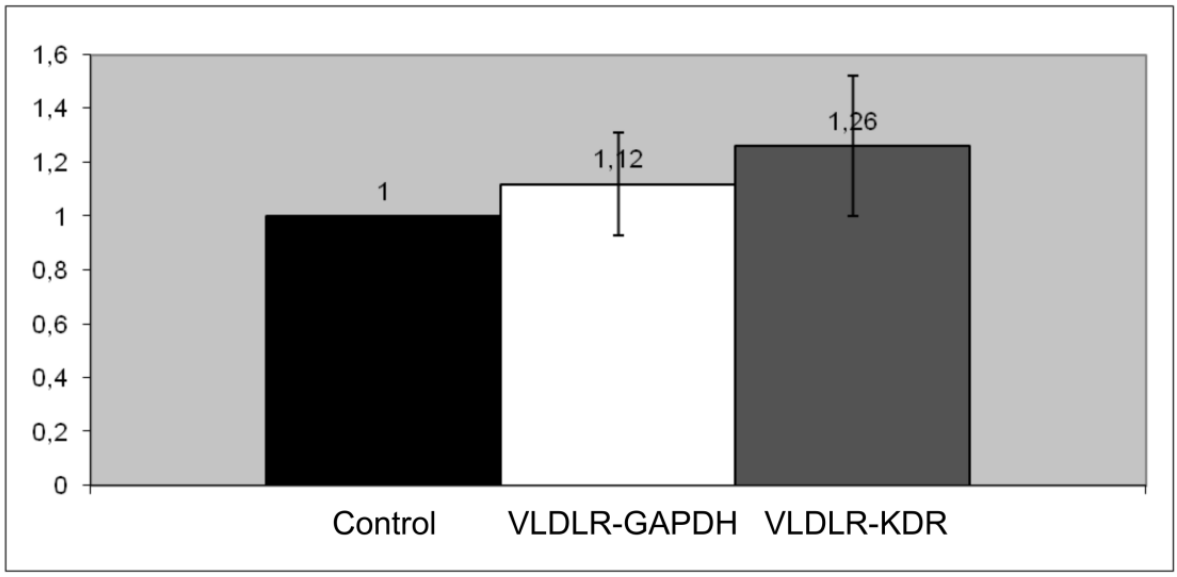

Figure 3.12 Quantitative analysis of *VLDLR* expression in patients and controls. Normalization number is 1.15 for *VLDLR* cDNA primers. When *VLDLR* expression in controls (Control) is assumed as 1, VLDLR expression in patients normalized to GAPDH (VLDLR-GAPDH) would be 1.12 ± 0.19, and VLDLR expression in patients normalized to KDR (VLDLR-KDR) would be 1.26 ± 0.26. (Ozcelik *et al*., 2008a)

PART IV: DISCUSSION and CONCLUSION

In the context of this research, homozygosity mapping and candidate gene sequencing were performed in four consanguineous families diagnosed with Unertan syndrome. Cerebellar hypoplasia, quadrupedal locomotion and mental retardation are the trademarks of this recessively inherited disorder.

Homozygosity mapping linked Unertan syndrome to three different loci, demonstrating genetic heterogeneity in the disease. Genetic heterogeneity is frequently observed in numerous several human genetic diseases. For example there are more than 130 different autosomal recessive, autosomal dominant and X-linked loci, and countless distinct mutations leading to hereditary deafness.

The loci linked to Unertan syndrome are chromosome 9p24 in families A and D, 17p13 in family B, and neither loci in family C. The minimal regions in 9p24 and 17p13 were found to be 1.032-Mb and 7.116-Mb intervals, respectively. Since the 17p13 interval is large and contains at least 150 genes, our efforts first targeted 9p24. There are 4 genes in the 9p24 region. Of these, very low density lipoprotein receptor (*VLDLR*) appeared as a prime positional candidate because of its expression in the cerebellum. Sequencing of *VLDLR* exons from genomic DNA revealed two distinct mutations that lead to truncated *VLDL* receptors; c769C->T, results in a stop codon, R257X, in ligand binding type repeats, and c2339delT mutation causes a frameshift, I780TfsX3 and generates a stop codon in *O*-linked sugar domain (Figure 4.1; Ozcelik *et al*., 2008a). These mutations prevent the receptor to be inserted into membrane and to transmit Reelin signal to

intracellular partners. During brain development, these disruptions in *VLDLR* preclude formation of the neural structures that are critical for gait. Same phenotype caused by different mutations in the same gene implies allelic heterogeneity in the disorder. Allelic heterogeneity can also be observed in numerous human genetic disorders. Hypercholesterolemia, which was linked to >300 different mutations in the LDL receptor, can be given as an example for a disorder with allelic heterogeneity (Ozcelik *et al*., 2008b).

As a consequence of genetic heterogeneity and identified genetic changes, the condition in families A and D is proposed as "VLDLR-associated Quadrupedal Locomotion" (VLDLR-QL) or Unertan Syndrome Type 1.

Identification of *VLDLR* mutations in Unertan syndrome extends the knowledge about the role of Reelin signaling pathway in neuronal migration disorders and in pathogenesis of neurodevelopmental movement diseases. Reelin signaling pathway is involved in lamination of neurons into distinct cortical layers, and disruptions of certain proteins in the pathway are implicated in specific cortical dysgenesis disorders. Homozygous mutations have been identified in the human Reelin (*RELN*) gene producing Norman-Roberts type lissencephaly syndrome (OMIM 257320; Hong *et al*., 2000). This type of lissencephaly syndrome is characterized with moderately thickened cortex and pachygyria, abnormalities in the hippocampus, and severe cerebellar hypoplasia with absent folia (Ross & Walsh, 2001). Mutations in the human *RELN* are similar to naturally occurring mouse *Reln* alleles that lead to reeler phenotype in mice with ataxic gait and trembling (Hong *et al*., 2000; D'Arcangelo *et al*., 1995). Mouse deficient for *VLDLR* was also studied. Engineered mouse lacking *VLDL* receptor appear grossly normal and has a normal life span (Frykman *et al*., 1995). Nonetheless, similar to the hypoplastic cerebellum in humans with *VLDLR* mutation (Ozcelik *et al*., 2008), the mouse cerebellum is smaller and has less folium, where Purkinje cells have failed to form the Purkinje cell plate, in the absence of *VLDL* receptor (Trommsdorff *et al*., 1999).

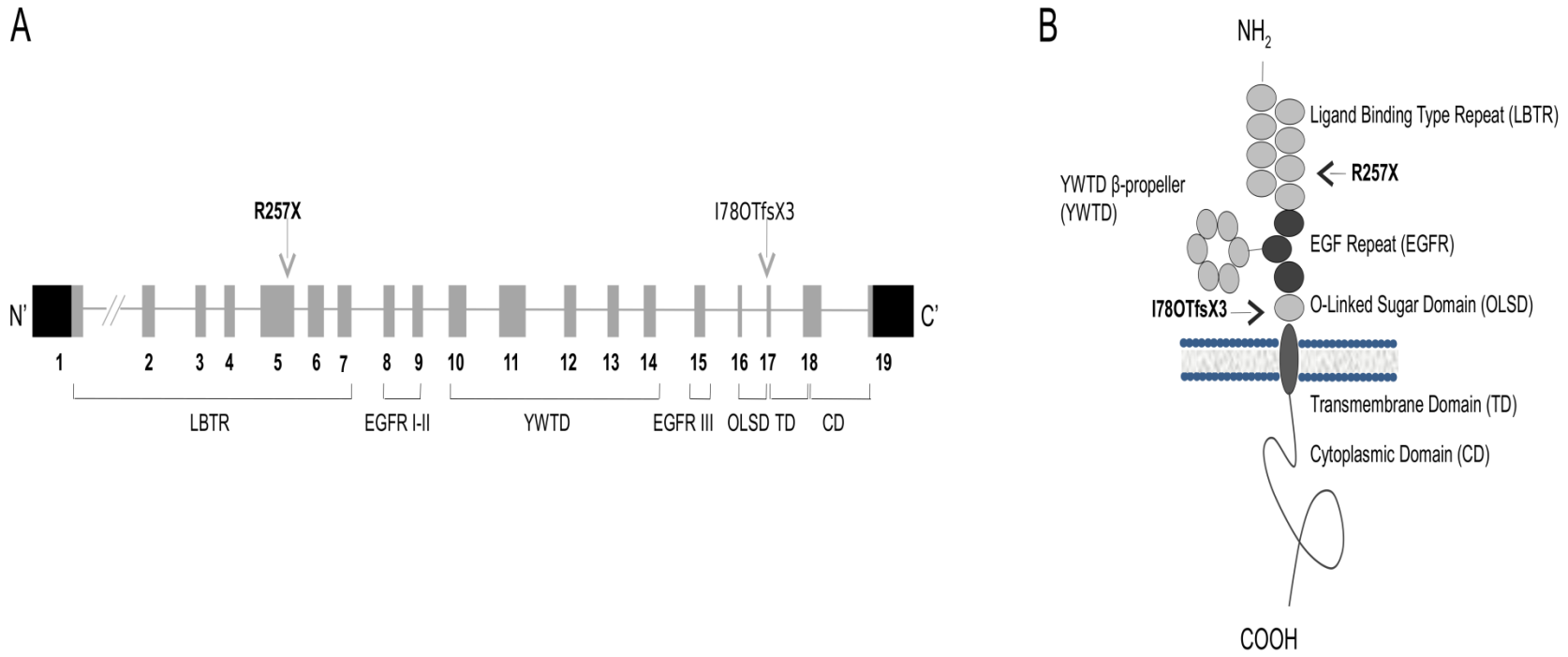

Figure 4.1 Schematic representation of the mutations in exons (A) and functional domains (B) of *VLDLR*. *VLDLR* gene consists of 19 exons and encodes a protein of 873 amino acids. Locations of the mutations are shown with arrows. LBTR, ligand-binding type repeat; EGFR, epidermal growth factor repeat I–III; YWTD, YWTD –propeller; OLSD, *O*-linked sugar domain; TD, transmembrane domain; CD, cytoplasmic domain (Ozcelik *et al*., 2008a; Herz & Bock, 2002; www.expasy.org/uniprot/P98155).

4.1 Unertan Syndrome vs. Disequilibrium Syndrome

Another disorder caused by *VLDLR*-associated genomic abnormalities is a form of disequilibrium syndrome described in the Hutterite population of North America (DES-H, OMIM 224050; Boycott *et al*. 2005). Disequilibrium syndrome was initially described as an autosomal recessive disorder of cerebral palsy associated with a variety of developmental abnormalities involving disturbed equilibrium, severe motor retardation, impaired cognitive skills, muscular hypotonia, and perceptual abnormalities (Hagberg *et al*., 1972; Sanner, 1973). Disequilibrium syndrome found in the Hutterites manifests itself with nonprogressive hypoplasia of the cerebellum, simplification of cerebral gyri, moderate-to-profound mental retardation, truncal ataxia and delayed ambulation, and caused by a homozygous deletion of a 199-kb region encompassing *VLDLR* gene (Boycott *et al*. 2005).

Affected individuals of Unertan syndrome and disequilibrium syndrome have quite similar clinical findings. Nevertheless, habitual and efficient quadrupedal locomotion is distinctive feature of Unertan syndrome patients (Table 4.1; Ozcelik *et al*., 2008a). Most of the disequilibrium patients cannot walk independently and others learn to walk very late. Those who can walk have a wide based, non tandem gait. Yet, they do not ambulate in a quadrupedal fashion. This is also the case for DES-H patients (Glass *et al*., 2005). On the other hand, individuals with Unertan syndrome ambulate in a quadrupedal manner with their hands and feet in both diagonal and lateral sequence gaits. Among patients in families A and D, independent bipedal gait can be achieved only by two affected individuals whom; however, prefers quadrupedal walking most of the time (Ozcelik *et al*., 2008b; Turkmen *et al*. 2008).

Table 4.1 Physical, radiological, and genetic characteristics of the Turkish families in this study and of Hutterite family DES-H (Glass *et al*., 2005; Ozcelik *et al*., 2008a). Cvs, central vestibular system; Pvs, peripheral vestibular system..

	Family A	Family B	Family C	Family D	DES-H
Chromosomal location	9p24	17p	Not 9p or 17p	9p24	9p24
Gene and mutation	*VLDLR* (c769C→T)	unknown	unknown	*VLDLR* (c2339delT)	Deletion including *VLDLR* and *LOC401491*
Gait	quadrupedal	quadrupedal	quadrupedal	quadrupedal	bipedal
Speech	dysarthric	dysarthric	dysarthric	dysarthric	dysarthric
Hypotonia	absent	absent	absent	absent	present
Barany caloric nystagmus	normal	Cvs defect	Pvs defect	not done	not done
Mental retardation	profound	severe to profound	profound	profound	moderate to profound
Ambulation	delayed	delayed	delayed	delayed	delayed
Truncal ataxia	severe	severe	severe	severe	severe
Lower leg reflexes	hyperactive	hyperactive	hyperactive	hyperactive	hyperactive
Upper extremity reflexes	vivid	vivid	vivid	vivid	vivid
Tremor	very rare	mild	present	absent	present
Pes-planus	present	present	present	present	present
Seizures	very rare	rare	rare	absent	observed in 40% of cases
Strabismus	present	present	present	present	present
Inferior cerebellum	hypoplasia	hypoplasia	mild hypoplasia	hypoplasia	hypoplasia
Inferior vermis	absent	absent	normal	absent	absent
Cortical gyri	mild simplification	mild simplification	mild simplification	mild simplification	mild simplification
Corpus callosum	normal	reduced	normal	normal	normal

A possible explanation for the gait difference between these two syndromes may be impairment of motor skills required for quadrupedal gait in the DES-H patients. This type of motor retardation can prevent them to perform quadrupedal locomotion and force them to walk bipedally. Such a severe phenotype seen in the Hutterite patients can be due to 199-kb deletion including the entire *VLDLR* gene and part of a hypothetical gene, *LOC401491*. Also, since the deleted region is a large interval, expression of neighboring genes can be affected due to the absence of intergenic regulatory elements (Boycott *et al*., 2005).

When genotype-phenotype correlations of Unertan syndrome and DES-H are compared, clinical heterogeneity should also be considered. Conclusion of different mutation in the same gene with different clinical phenotypes is not a rare situation in medical genetics. For example, certain mutations in cadherin 23 result in blindness and deafness, whereas other mutations in the same gene cause hearing loss with normal vision. Clinical heterogeneity is also applicable for Unertan syndrome and disequilibrium syndrome phenotypes (Ozcelik *et al*., 2008b). The Hutterite families in North America, families A and D in Turkey, and a family diagnosed with disequilibrium syndrome in Iran, all have different genomic abnormalities of *VLDLR* gene. Whereas DES-H patients lack the entire *VLDLR* gene (Boycott *et al*., 2005), Iranian patients have a nonsense change in exon 10 of the same gene (Moheb *et al*., 2008). On the other hand, the mutations in Turkish families A and D are, respectively, a nonsense change in exon 5 and a single-base-pair deletion in exon 17 leading to a frameshift in *VLDLR* (Ozcelik *et al*., 2008a). These different abnormalities of *VLDLR* gene have resulted in different movement disorders including late bipedal ambulation (Boycott *et al*., 2005), ataxic gait (Moheb *et al*., 2008), and quadrupedal locomotion (Ozcelik *et al*., 2008a) along with cerebellar hypoplasia in all three cases.

4.2 Is Quadrupedal Locomotion an Environmental Adaptation?

Quadrupedal locomotion of the affected individuals in Turkish families can be considered as an adaptation to their congenital cerebellar ataxia because of poor environmental conditions, including lack of access to proper medical care, local cultural environment, or religious beliefs of the parents.

Inadequate medical care would not lead to quadrupedality in the patients because we have already known that families A and D looked for medical treatments to improve gait of their affected children. In addition to discouragement of affected children from quadrupedal walking by their parents, there is a physician who participated in medical interventions in family A. On the other hand, mother of the index patient in family D consulted with private medical practices and two major academic medical centers for a definitive diagnosis and correction of the disorder in her son. Unfortunately, all these efforts did not prevent quadrupedal locomotion in the affected individuals (Ozcelik *et al*., 2008a).Zimmer frames that were provided to certain affected individuals during studies helped them in upright walking. However, this does not eradicate genetic basis of quadrupedal walking since for example the correction of myopia with help of glasses does not mean that near-sightedness is not a genetic condition

Local cultural environment and religious beliefs are also highly unlikely to lead to quadrupedal walking of the patients. It would not be true to assume that walking in a quadrupedal manner was suppressed in the Hutterites, and yet it was tolerated and was not corrected in the Turkish families due to certain cultural and religious factors. This assumption has been falsified by families who did not tolerate quadrupedal walking, but instead searched for medical therapies. Also, recently described family with quadruped members in Brazil (Garcias & Roth, 2007) demonstrates that quadrupedal gait is rather a distinct phenotype than an adaptation mechanism.

4.5 Future Prospects

Cerebellar hypoplasia and quadrupedal locomotion in humans was linked to at least three different chromosomes with our studies. Gene in one of these chromosomal loci, 9p24, was identified as *VLDLR*. It would be interesting to identify genes responsible for the disorder in other families.

After the identification of causative mutations in a disease, easy and affordable DNA-based diagnostic testing becomes possible. This is indeed true for *VLDLR* since both mutations can be detected by specific PCR and restriction endonuclease cleavage, thus giving us the opportunity to perform carrier identification and population screening.

Observing development of animals with mutant *VLDL* receptors could give further details about the pathogenesis of this syndrome, and also about the role of *VLDLR* in development of nervous system required for gait in humans.

PART V: REFERENCES

Abecasis GR, Cherny SS, Cookson WO, Cardon LR (2002). Merlin--rapid analysis of dense genetic maps using sparse gene flow trees. *Nat Genet.* 30:97-101.

Abecasis GR & Wigginton JE (2005). Handling marker-marker linkage disequilibrium: pedigree analysis with clustered markers. *Am J Hum Genet.* 77:754-67.

Angevine JB Jr & Sidman RL (1961). Autoradiographic study of cell migration during histogenesis of cerebral cortex in the mouse. *Nature*. 192:766-8.

Arnaud L, Ballif BA, Förster E, Cooper JA (2003). Fyn tyrosine kinase is a critical regulator of disabled-1 during brain development. *Curr Biol*. 13:9-17.

Assadi AH, Zhang G, Beffert U, McNeil RS, Renfro AL, Niu S, Quattrocchi CC, Antalffy BA, Sheldon M, Armstrong DD, Wynshaw-Boris A, Herz J, D'Arcangelo G, Clark GD (2003). Interaction of reelin signaling and Lis1 in brain development. *Nat Genet*. 35:270-6.

Ballif BA, Arnaud L, Arthur WT, Guris D, Imamoto A, Cooper JA (2004). Activation of a Dab1/CrkL/C3G/Rap1 pathway in Reelin-stimulated neurons. *Curr Biol*. 14:606-10. Erratum in: *Curr Biol*. 2004. 14:742.

Banfi S & Zoghbi HY (1994). Molecular genetics of hereditary ataxias. *Baillieres Clin Neurol*. 3:281-95.

Bock HH & Herz J (2003). Reelin activates SRC family tyrosine kinases in neurons. *Curr Biol*. 13:18-26.

Boycott KM, Flavelle S, Bureau A, Glass HC, Fujiwara TM, Wirrell E, Davey K, Chudley AE, Scott JN, McLeod DR, Parboosingh JS (2005). Homozygous deletion of the very low density lipoprotein receptor gene causes autosomal recessive cerebellar hypoplasia with cerebral gyral simplification. *Am J Hum Genet.* 77:477–483.

Caviness VS Jr (1982). Neocortical histogenesis in normal and reeler mice: a developmental study based upon [3H]thymidine autoradiography. *Brain Res*. 256:293-302.

Chae T, Kwon YT, Bronson R, Dikkes P, Li E, Tsai LH (1997). Mice lacking p35, a neuronal specific activator of Cdk5, display cortical lamination defects, seizures, and adult lethality. Neuron. 18:29-42.

Cottingham RW Jr, Idury RM, Schäffer AA (1993). Faster sequential genetic linkage computations. *Am J Hum Genet*. 53:252-63.

D'Arcangelo G, Miao GG, Chen SC, Soares HD, Morgan JI, Curran T (1995). A protein related to extracellular matrix proteins deleted in the mouse mutant *reeler*. *Nature*. 374:719-23.

D'Arcangelo G, Nakajima K, Miyata T, Ogawa M, Mikoshiba K, Curran T (1997). Reelin is a secreted glycoprotein recognized by the CR-50 monoclonal antibody. *J Neurosci*. 17:23-31.

D'Arcangelo G, Homayouni R, Keshvara L, Rice DS, Sheldon M, Curran T (1999). Reelin is a ligand for lipoprotein receptors. *Neuron*. 24:471-9.

Derer P (1985). Comparative localization of Cajal-Retzius cells in the neocortex of normal and reeler mutant mice fetuses. *Neurosci Lett*. 54:1-6.

Di Donato S (1998). The complex clinical and genetic classification of inherited ataxias. I. Dominant ataxias. *Ital J Neurol Sci*. 19:335-43.

Di Donato S, Gellera C, Mariotti C (2001). The complex clinical and genetic classification of inherited ataxias. II. Autosomal recessive ataxias. *Neurol Sci*. 22:219-28.

Dueñas AM, Goold R, Giunti P (2006). Molecular pathogenesis of spinocerebellar ataxias. *Brain*. 129:1357-70.

Dulabon L, Olson EC, Taglienti MG, Eisenhuth S, McGrath B, Walsh CA, Kreidberg JA, Anton ES (2000). Reelin binds alpha3beta1 integrin and inhibits neuronal migration. *Neuron*. 27:33-44.

Espinós-Armero C, González-Cabo P, Palau-Martínez F (2005). Autosomal recessive cerebellar ataxias. Their classification, genetic features and pathophysiology. *Rev Neurol*. 41:409-22.

Falconer DS (1951). Two new mutants *trembler* and *reeler*, with neurological actions in the house mouse. *J. Genet*. 50:192-201

Fogel BL & Perlman S (2007). Clinical features and molecular genetics of autosomal recessive cerebellar ataxias. *Lancet Neurol*. 6:245-57.

Frost DO, Edwards MA, Sachs GM, Caviness VS Jr (1986). Retinotectal projection in reeler mutant mice: relationships among axon trajectories, arborization patterns and cytoarchitecture. *Brain Res*. 393:109-20.

Frykman PK, Brown MS, Yamamoto T, Goldstein JL, Herz J (1995). Normal plasma lipoproteins and fertility in gene-targeted mice homozygous for a disruption in the gene encoding very low density lipoprotein receptor. *Proc Natl Acad Sci U S A.* 92:8453-7.

Gallagher E, Howell BW, Soriano P, Cooper JA, Hawkes R (1998). Cerebellar abnormalities in the disabled (mdab1-1) mouse. *J Comp Neurol*. 402:238-51.

Garcias Gde L & Roth Mda G (2007). A Brazilian family with quadrupedal gait, severe mental retardation, coarse facial characteristics, and hirsutism. *Int J Neurosci*. 117:927-33.

Gatchel JR & Zoghbi HY (2005).Diseases of unstable repeat expansion: mechanisms and common principles. *Nat Rev Genet*. 6:743-55.

Gilmore EC & Herrup K (2000). Cortical development: receiving reelin. *Curr Biol*. 10:R162-6.

Glass HC, Boycott KM, Adams C, Barlow K, Scott JN, Chudley AE, Fujiwara TM, Morgan K, Wirrell E, McLeod DR (2005). Autosomal recessive cerebellar hypoplasia in the Hutterite population. *Dev Med Child Neurol.* 47:691–695.

Gleeson JG & Walsh CA (2000). Neuronal migration disorders: from genetic diseases to developmental mechanisms. *Trends Neurosci*. 23:352-9.

Goffinet AM (1979). An early development defect in the cerebral cortex of the reeler mouse. A morphological study leading to a hypothesis concerning the action of the mutant gene. *Anat Embryol (Berl).* 157:205-16.

Goffinet AM (1984). Abnormal development of the facial nerve nucleus in reeler mutant mice. *J Anat*. 138:207-15.

Goffinet AM, So KF, Yamamoto M, Edwards M, Caviness VS Jr (1984). Architectonic and hodological organization of the cerebellum in reeler mutant mice. *Brain Res*. 318:263-76.

Goldowitz D, Cushing RC, Laywell E, D'Arcangelo G, Sheldon M, Sweet HO, Davisson M, Steindler D, Curran T (1997). Cerebellar disorganization characteristic of reeler in scrambler mutant mice despite presence of reelin. *J Neurosci*. 17:8767-77.

Goldowitz D & Hamre K (1998). The cells and molecules that make a cerebellum. *Trends Neurosci*. 21:375-82.

González JL, Russo CJ, Goldowitz D, Sweet HO, Davisson MT, Walsh CA (1997). Birthdate and cell marker analysis of scrambler: a novel mutation affecting cortical development with a reeler-like phenotype. *J Neurosci*. 17:9204-11.

Hack I, Bancila M, Loulier K, Carroll P, Cremer H (2002). Reelin is a detachment signal in tangential chain-migration during postnatal neurogenesis. *Nat Neurosci*. 5:939-45.

Hack I, Hellwig S, Junghans D, Brunne B, Bock HH, Zhao S, Frotscher M (2007). Divergent roles of ApoER2 and Vldlr in the migration of cortical neurons. *Development*. 134:3883-91.

Hagberg B, Sanner G, Steen M (1972). The dysequilibrium syndrome in cerebral palsy. Clinical aspects and treatment. *Acta Paediatr Scand Suppl*. 226:1-63.

Harding AE (1993) in *Inherited Ataxias*, ed Harding AE & Deufel T (New York: Raven) Vol 61, pp 1–14.

Hatten ME (1999). Central nervous system neuronal migration. *Annu Rev Neurosci*. 22:511-39.

Herz J & Bock HH (2002). Lipoprotein receptors in the nervous system. *Annu Rev Biochem*. 71:405-34.

Hiesberger T, Trommsdorff M, Howell BW, Goffinet A, Mumby MC, Cooper JA, Herz J (1999). Direct binding of Reelin to VLDL receptor and ApoE receptor 2 induces tyrosine phosphorylation of disabled-1 and modulates tau phosphorylation. *Neuron*. 24:481-9.

Hirotsune S, Takahara T, Sasaki N, Hirose K, Yoshiki A, Ohashi T, Kusakabe M, Murakami Y, Muramatsu M, Watanabe S, Nakao K, Katsuki M, Hayashizaki Y (1995) The reeler gene encodes a protein with an EGF-like motif expressed by pioneer neurons. *Nat Genet*. 10:77-83.

Hoffarth RM, Johnston JG, Krushel LA, van der Kooy D (1995). The mouse mutation reeler causes increased adhesion within a subpopulation of early postmitotic cortical neurons. *J Neurosci*. 15:4838-50.

Hong SE, Shugart YY, Huang DT, Shahwan SA, Grant PE, Hourihane JO, Martin ND, Walsh CA (2000). Autosomal recessive lissencephaly with cerebellar hypoplasia is associated with human RELN mutations. *Nat Genet*. 26:93-6. Erratum in: *Nat Genet*. 2001. 27:225.

Howell BW, Hawkes R, Soriano P, Cooper JA (1997). Neuronal position in the developing brain is regulated by mouse disabled-1. *Nature*. 389:733-7.

Howell BW, Herrick TM, Cooper JA (1999). Reelin-induced tyrosine phosphorylation of disabled 1 during neuronal positioning. *Genes Dev*.13:643-8. Erratum in: *Genes Dev*. 13:1642.

Humphrey N, Skoyles JR, Keynes R (2005). Human hand-walkers: Five siblings who never stood up. Discussion paper, Centre for Philos of Nat and Soc Sci London.

Hunter-Schaedle KE (1997). Radial glial cell development and transformation are disturbed in reeler forebrain. *J Neurobiol*. 33:459-72.

Lathrop GM & Lalouel JM (1984). Easy calculations of lod scores and genetic risks on small computers. *Am J Hum Genet*. 36:460-5.

Marin-Padilla M (1998). Cajal-Retzius cells and the development of the neocortex. *Trends Neurosci*. 21:64-71.

Mariotti C & Di Donato S (2001). Cerebellar/spinocerebellar syndromes. *Neurol Sci*. 22 Suppl 2:S88-92.

Matsuzaki H, Dong S, Loi H, Di X, Liu G, Hubbell E, Law J, Berntsen T, Chadha M, Hui H, Yang G, Kennedy GC, Webster TA, Cawley S, Walsh PS, Jones KW, Fodor SP, Mei R (2004). Genotyping over 100,000 SNPs on a pair of oligonucleotide arrays. *Nat Methods*. 1:109-11.

Miyata T, Nakajima K, Aruga J, Takahashi S, Ikenaka K, Mikoshiba K, Ogawa M (1996). Distribution of a reeler gene-related antigen in the developing cerebellum: an immunohistochemical study with an allogeneic antibody CR-50 on normal and reeler mice. *J Comp Neurol*. 372:215-28.

Moheb LA, Tzschach A, Garshasbi M, Kahrizi K, Darvish H, Heshmati Y, Kordi A, Najmabadi H, Ropers HH, Kuss AW (2008). Identification of a nonsense mutation in the very low-density lipoprotein receptor gene (VLDLR) in an Iranian family with dysequilibrium syndrome. *Eur J Hum Genet*. 16:270-3

Ogawa M, Miyata T, Nakajima K, Yagyu K, Seike M, Ikenaka K, Yamamoto H, Mikoshiba K (1995). The reeler gene-associated antigen on Cajal-Retzius neurons is a crucial molecule for laminar organization of cortical neurons. *Neuron*. 14:899-912.

Ohshima T, Ward JM, Huh CG, Longenecker G, Veeranna, Pant HC, Brady RO, Martin LJ, Kulkarni AB (1996). Targeted disruption of the cyclin-dependent kinase 5 gene results in abnormal corticogenesis, neuronal pathology and perinatal death. *Proc Natl Acad Sci U S A*. 93:11173-8.

O'Rourke NA, Dailey ME, Smith SJ, McConnell SK (1992). Diverse migratory pathways in the developing cerebral cortex. *Science*. 258:299-302.

Orr HT & Zoghbi HY (2007). Trinucleotide repeat disorders. *Annu Rev Neurosci*. 30:575-621.

Ozcelik T, Akarsu N, Uz E, Caglayan S, Gulsuner S, Onat OE, Tan M, Tan U (2008a). Mutations in the very low-density lipoprotein receptor VLDLR cause cerebellar hypoplasia and quadrupedal locomotion in humans. *Proc Natl Acad Sci U S A.* 105:4232-6.

Ozcelik T, Akarsu N, Uz E, Caglayan S, Gulsuner S, Onat OE, Tan M, Tan U (2008b). Reply to Herz *et al*. and Humphrey *et al*.: Genetic heterogeneity of cerebellar hypoplasia with quadrupedal locomotion. *Proc Natl Acad Sci U S A.* 105:E32-3.

Palau F & Espinós C (2006). Autosomal recessive cerebellar ataxias. *Orphanet J Rare Dis*. 1:47.

Perlman SL (2004). Symptomatic and disease-modifying therapy for the progressive ataxias. *Neurologist*. 10:275-89.

Pfaffi MW (2004) in *A-Z of Quantitative PCR*, ed Bustin S (International University Line, La Jolla, CA), pp 89–120.

Pinto-Lord MC, Evrard P, Caviness VS Jr (1982). Obstructed neuronal migration along radial glial fibers in the neocortex of the reeler mouse: a Golgi-EM analysis. *Brain Res*. 256:379-93.

Rakic P & Caviness VS Jr (1995). Cortical development: view from neurological mutants two decades later. *Neuron*. 14:1101-4.

Rice DS & Curran T (1999). Mutant mice with scrambled brains: understanding the signaling pathways that control cell positioning in the CNS. *Genes Dev*. 13:2758-73.

Rice DS & Curran T (2001). Role of the reelin signaling pathway in central nervous system development. *Annu Rev Neurosci*. 24: 1005-039.

Rice DS, Nusinowitz S, Azimi AM, Martínez A, Soriano E, Curran T (2001). The reelin pathway modulates the structure and function of retinal synaptic circuitry. *Neuron*. 31:929-41.

Ross ME & Walsh CA (2001). Human brain malformations and their lessons for neuronal migration. *Annu Rev Neurosci*. 24:1041-70.

Sanada K, Gupta A, Tsai LH (2004). Disabled-1-regulated adhesion of migrating neurons to radial glial fiber contributes to neuronal positioning during early corticogenesis. *Neuron*. 42:197-211.

Sanner G (1973). The dysequilibrium syndrome. A genetic study. *Neuropadiatrie*. 4:403-13.

Schäffer AA, Gupta SK, Shriram K, Cottingham RW Jr (1994). Avoiding recomputation in linkage analysis. *Hum Hered*. 44:225-37.

Schöls L, Bauer P, Schmidt T, Schulte T, Riess O (2004). Autosomal dominant cerebellar ataxias: clinical features, genetics, and pathogenesis. *Lancet Neurol*. 3:291-304.

Senzaki K, Ogawa M, Yagi T (1999). Proteins of the CNR family are multiple receptors for Reelin. *Cell*. 99:635-47.

Sheldon M, Rice DS, D'Arcangelo G, Yoneshima H, Nakajima K, Mikoshiba K, Howell BW, Cooper JA, Goldowitz D, Curran T (1997). Scrambler and yotari disrupt the disabled gene and produce a reeler-like phenotype in mice. *Nature*. 389:730-3.

Sheppard AM & Pearlman AL (1997). Abnormal reorganization of preplate neurons and their associated extracellular matrix: an early manifestation of altered neocortical development in the reeler mutant mouse. *J Comp Neurol*. 378:173-9.

Strachan T & Read AP (2004). *Human Molecular Genetics* – 3rd ed., (Garland Science, New York, NY), pp 101-109.

Sweet HO, Bronson RT, Johnson KR, Cook SA, Davisson MT (1996). Scrambler, a new neurological mutation of the mouse with abnormalities of neuronal migration. *Mamm Genome*. 7:798-802.

Tan U (2005). Unertan syndrome: A new theory on the evolution of human mind. *Neuroquantology*. 4: 250-255.

Tan U (2006a). A new syndrome with quadrupedal gait, primitive speech, and severe mental retardation as a live model for human evolution. *Int J Neurosci.* 116:361-9.

Tan U (2006b). Evidence for "Unertan syndrome" and the evolution of the human mind. *Int J Neurosci*. 116:763-74.

Tan U, Karaca S, Tan M, Yilmaz B, Bagci NK, Ozkur A, Pence S (2008a). Unertan syndrome: a case series demonstrating human devolution. *Int J Neurosci.* 118:1-25.

Tan U (2008b). Unertan syndrome: review and report of four new cases. *Int J Neurosci.* 118:211-25.

Tissir F & Goffinet AM (2003). Reelin and brain development. *Nat Rev Neurosci*. 4:496-505.

Trommsdorff M, Gotthardt M, Hiesberger T, Shelton J, Stockinger W, Nimpf J, Hammer RE, Richardson JA, Herz J (1999). Reeler/Disabled-like disruption of neuronal migration in knockout mice lacking the VLDL receptor and ApoE receptor 2. *Cell*. 97:689-701.

Turkmen S, Demirhan O, Hoffmann K, Diers A, Zimmer C, Sperling K, Mundlos S (2006). Cerebellar hypoplasia and quadrupedal locomotion in humans as a recessive trait mapping to chromosome 17p. *J Med Genet.* 43:461-4.

Turkmen S, Hoffmann K, Demirhan O, Aruoba D, Humphrey N, Mundlos S (2008). Cerebellar hypoplasia, with quadrupedal locomotion, caused by mutations in the very low-density lipoprotein receptor gene. *Eur J Hum Genet*. 2008. [Epub ahead of print]

Wang VY & Zoghbi HY (2001). Genetic regulation of cerebellar development. *Nat Rev Neurosci*. 2:484-91.

Ware ML, Fox JW, González JL, Davis NM, Lambert de Rouvroit C, Russo CJ, Chua SC Jr, Goffinet AM, Walsh CA (1997). Aberrant splicing of a mouse disabled homolog, mdab1, in the scrambler mouse. *Neuron*. 19:239-49.

Wechsler-Reya RJ & Scott MP (1999). Control of neuronal precursor proliferation in the cerebellum by Sonic Hedgehog. *Neuron*. 22:103-14.

Yip JW, Yip YP, Nakajima K, Capriotti C (2000).Reelin controls position of autonomic neurons in the spinal cord. *Proc Natl Acad Sci U S A*. 97:8612-6.

Yoneshima H, Nagata E, Matsumoto M, Yamada M, Nakajima K, Miyata T, Ogawa M, Mikoshiba K (1997). A novel neurological mutant mouse, yotari, which exhibits reeler-like phenotype but expresses CR-50 antigen/reelin. *Neurosci Res*. 29:217-23.

Zhang G, Assadi AH, McNeil RS, Beffert U, Wynshaw-Boris A, Herz J, Clark GD, D'Arcangelo G (2007). The Pafah1b complex interacts with the Reelin receptor VLDLR. *PLoS ONE*. 2:e252.

Zoghbi HY (2000). Spinocerebellar ataxias. *Neurobiol Dis*. 7:523-7.

PART VI: APPENDICES

Appendix A: Genome Wide 250K SNP Genotyping Results

Appendix B: Exclusion of Compound Heterozygosity Possibility in Families B and C

Parametric Analysis for Recessive_Model

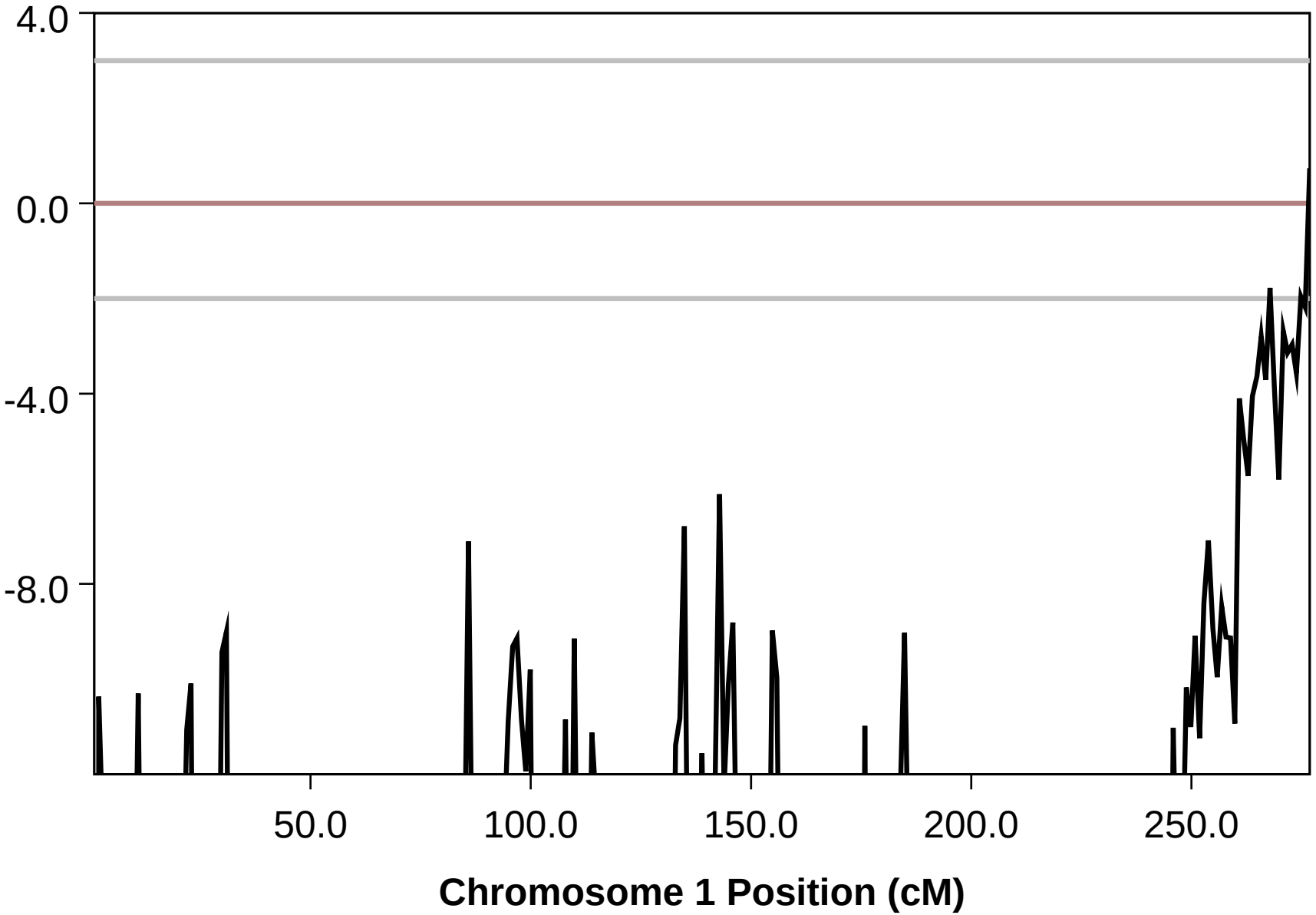

Parametric Analysis for Recessive_Model

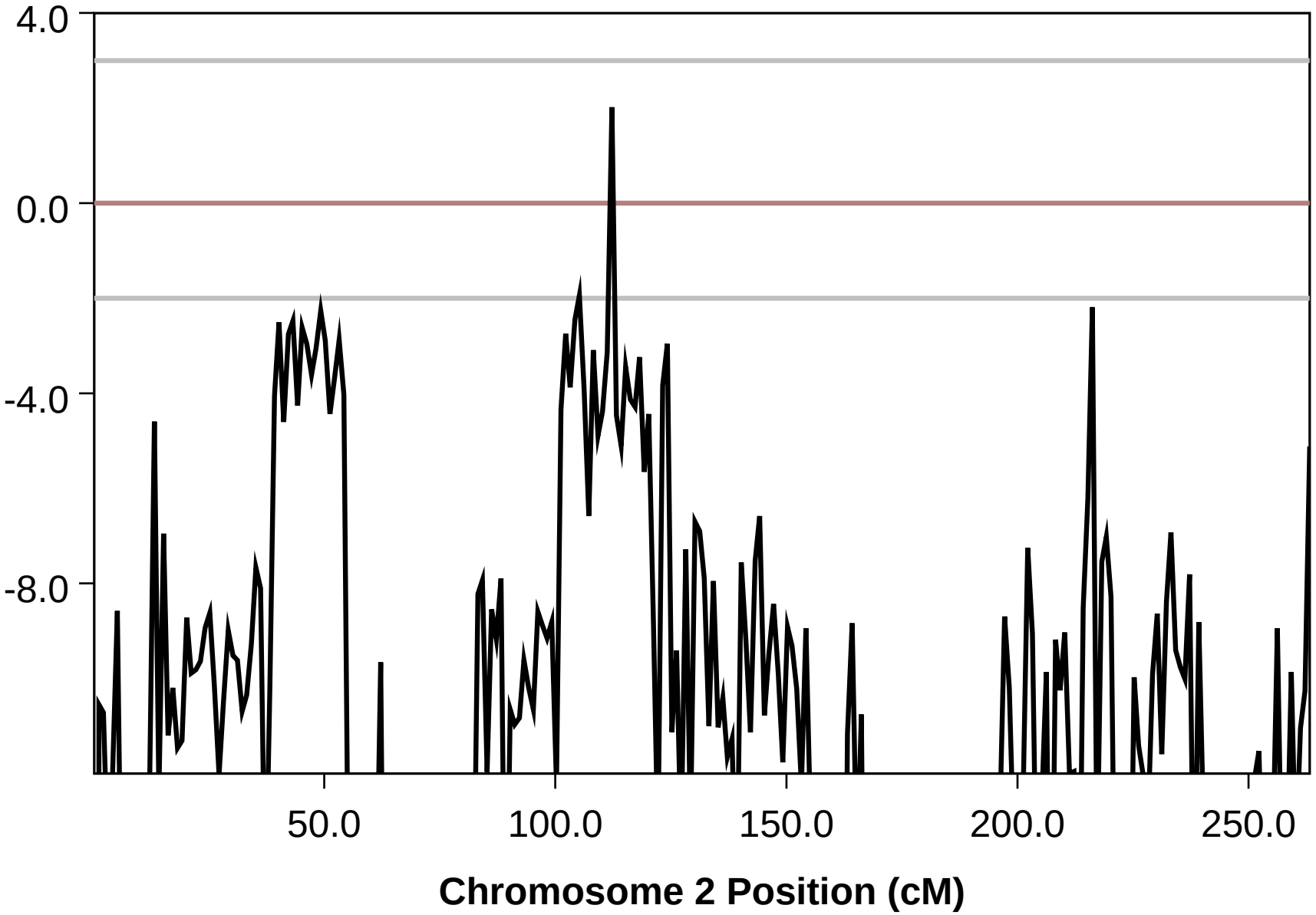

Parametric Analysis for Recessive_Model

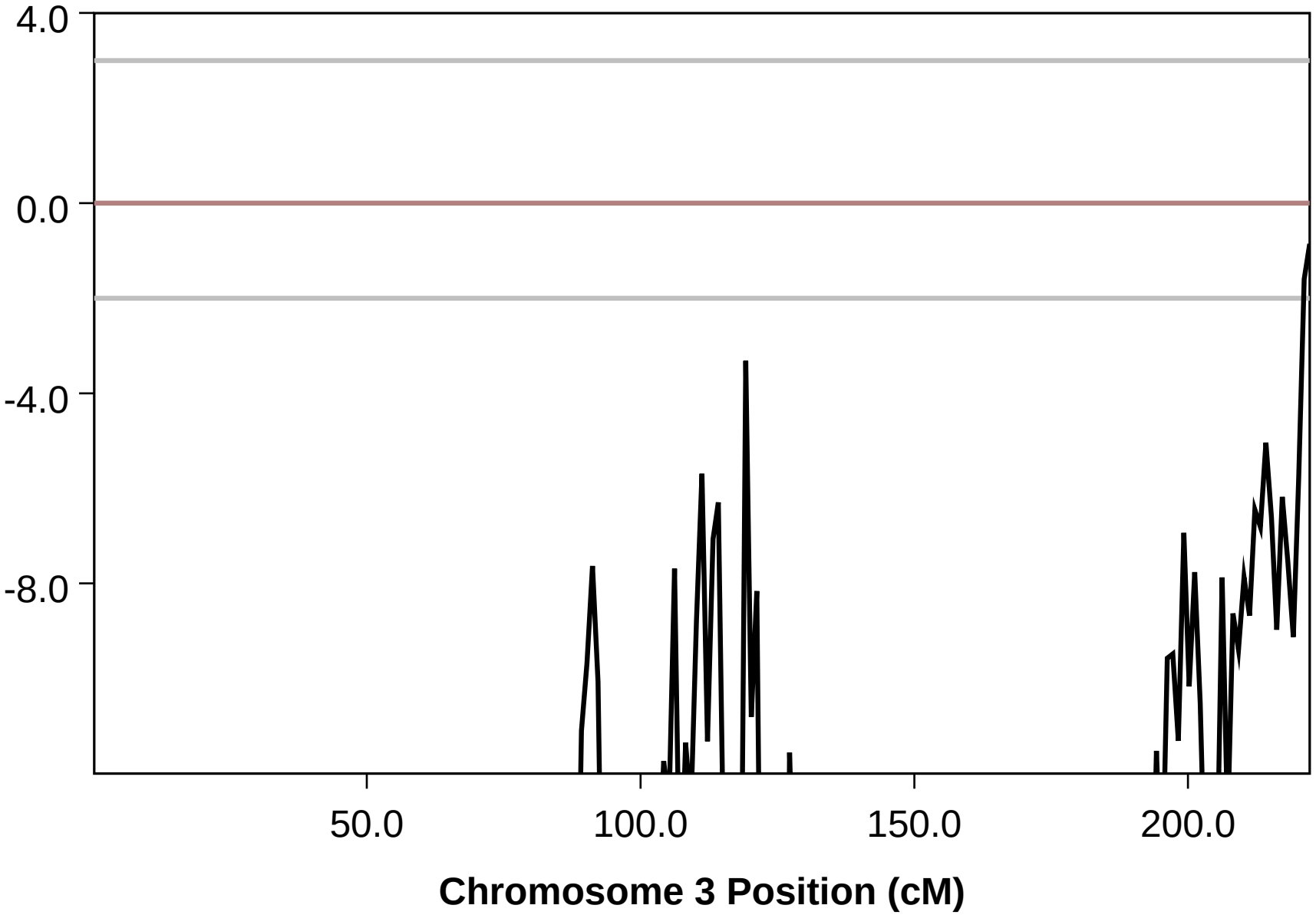

Parametric Analysis for Recessive_Model

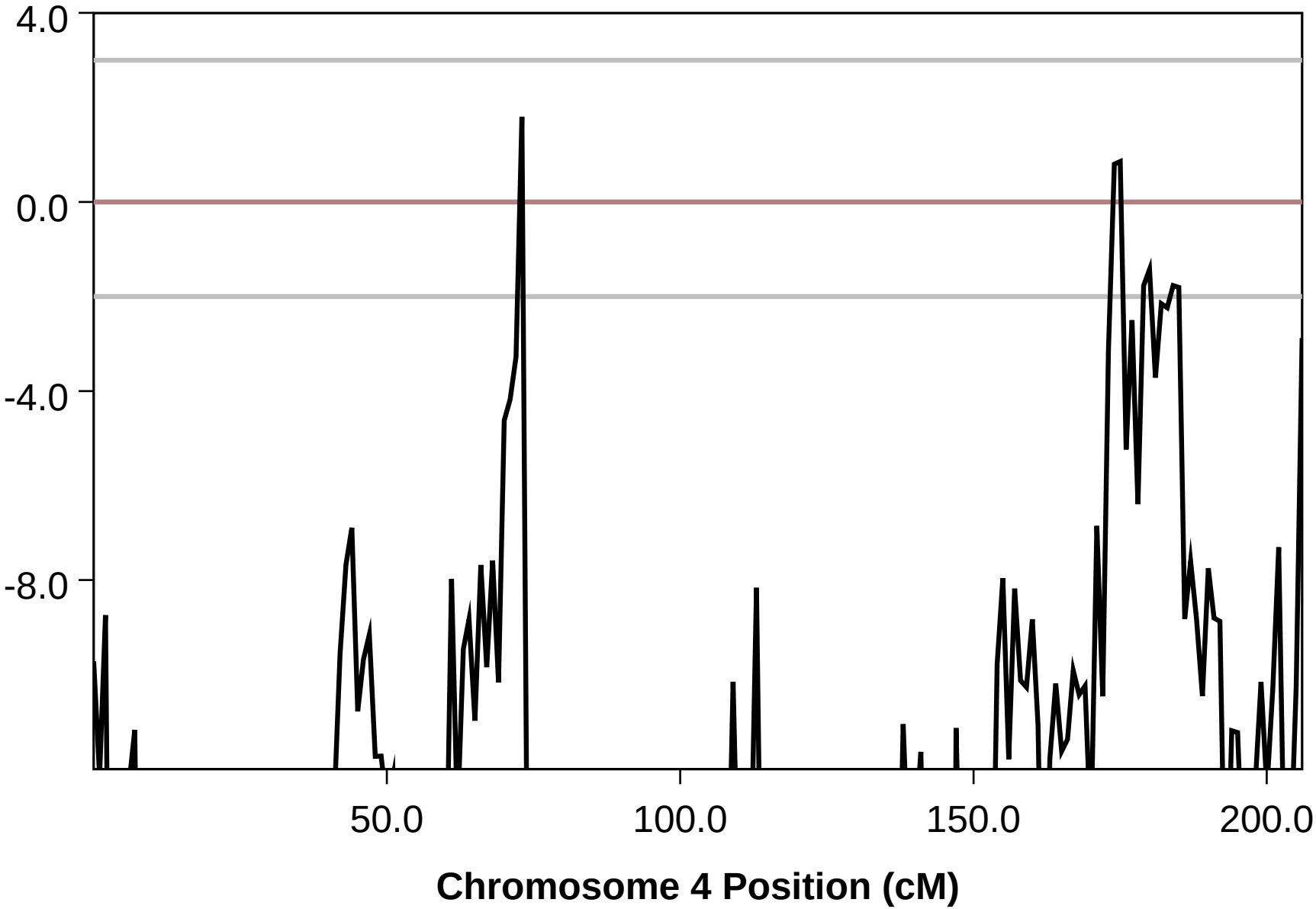

Parametric Analysis for Recessive_Model

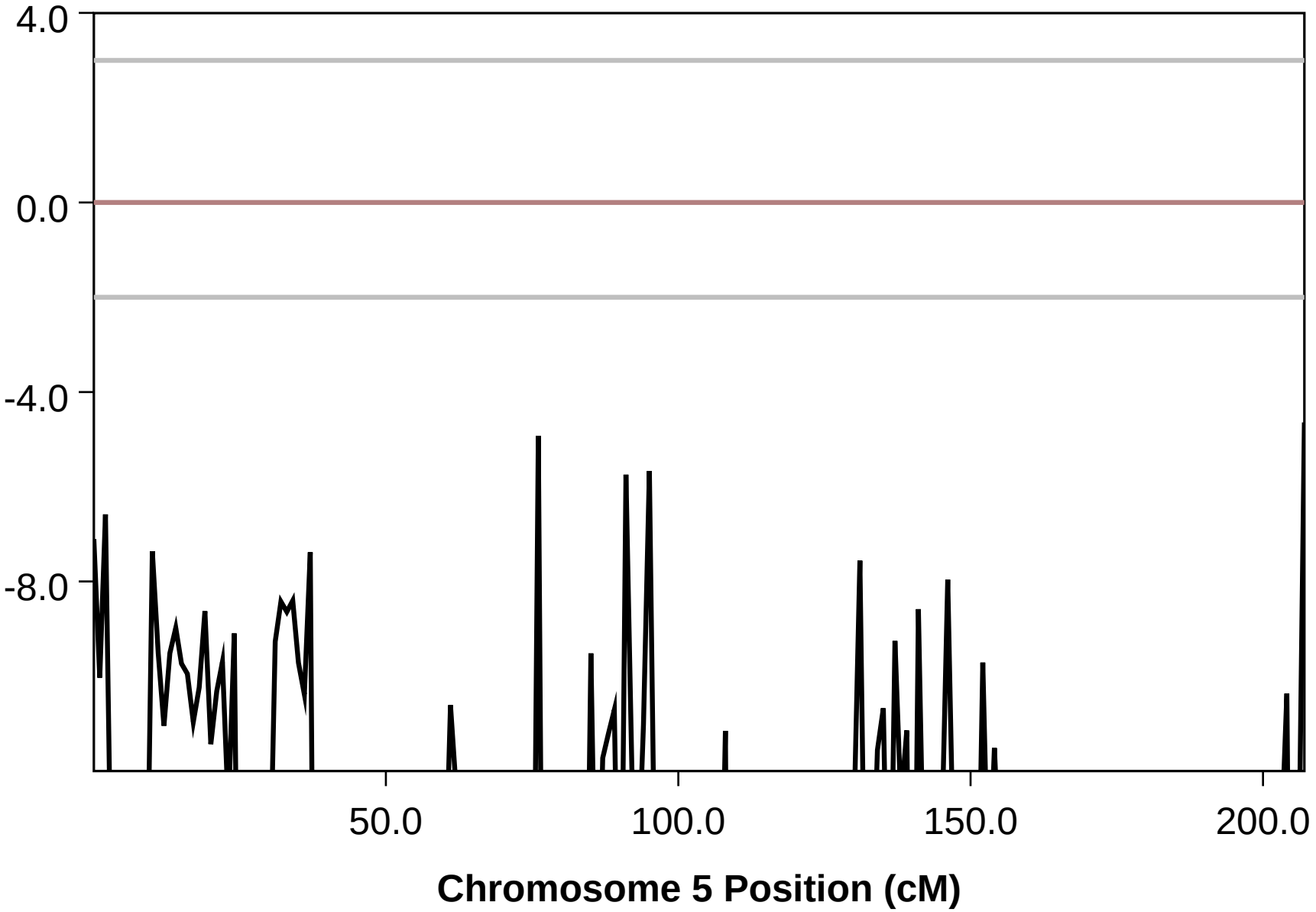

Parametric Analysis for Recessive_Model

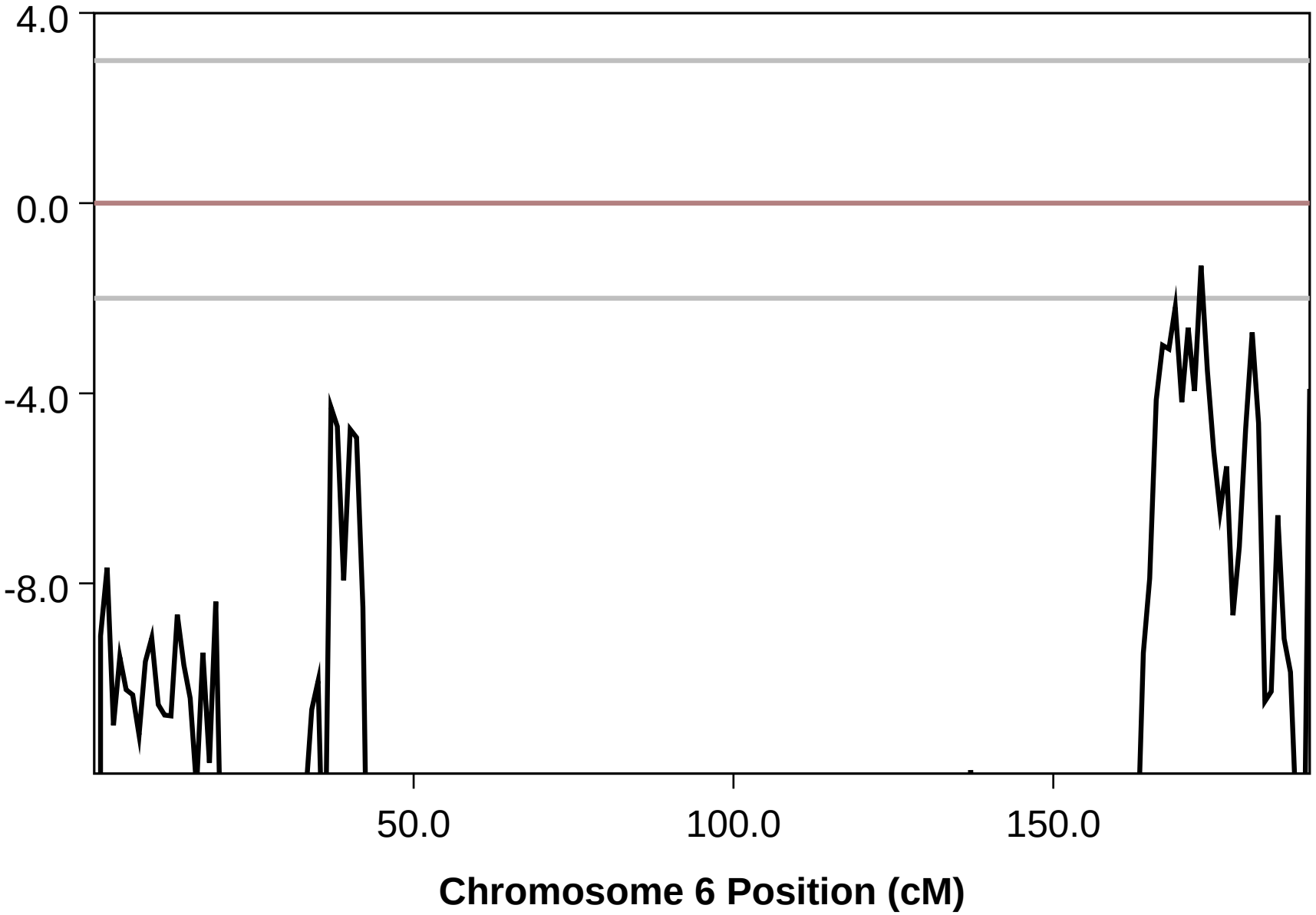

Parametric Analysis for Recessive_Model

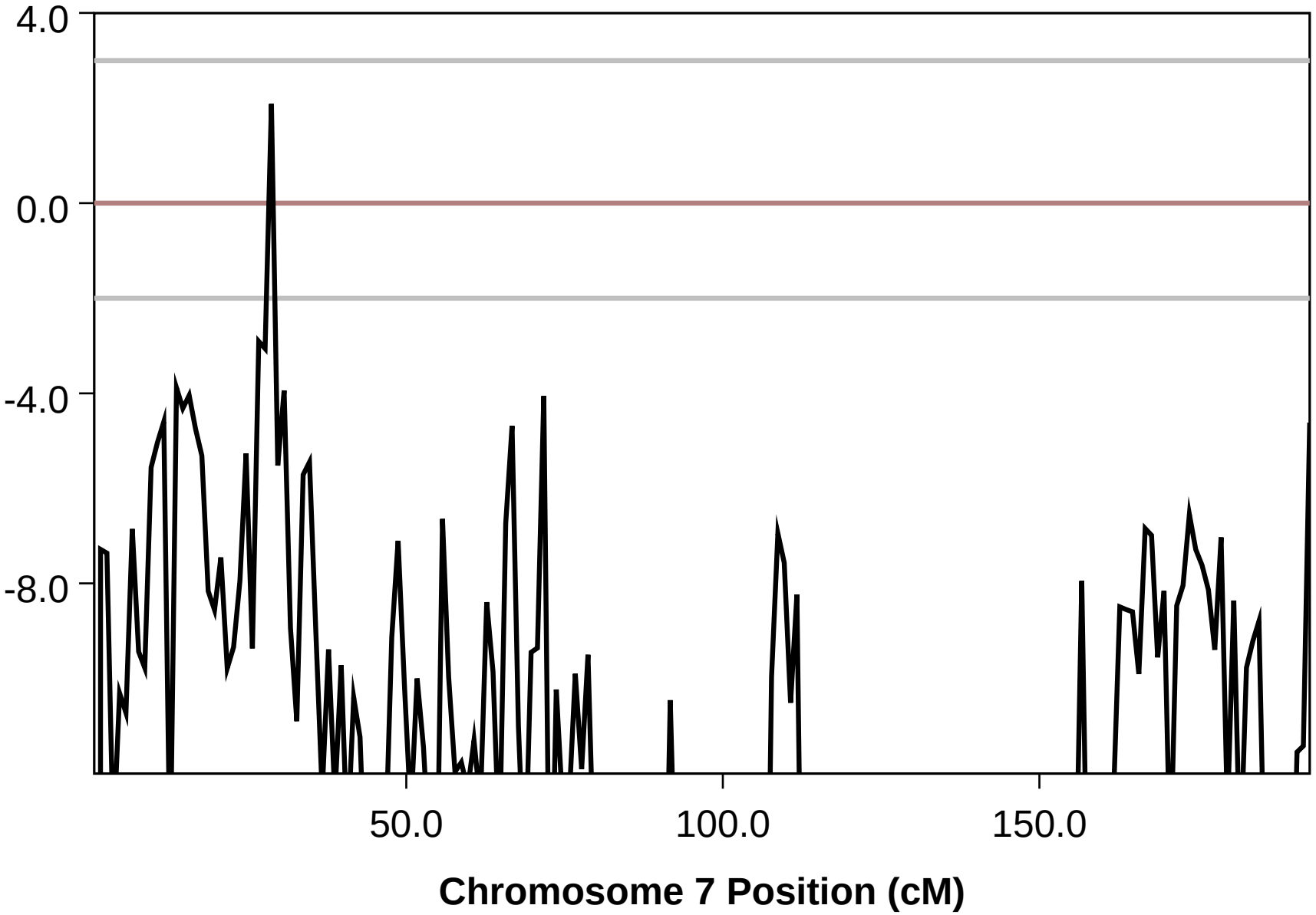

Parametric Analysis for Recessive_Model

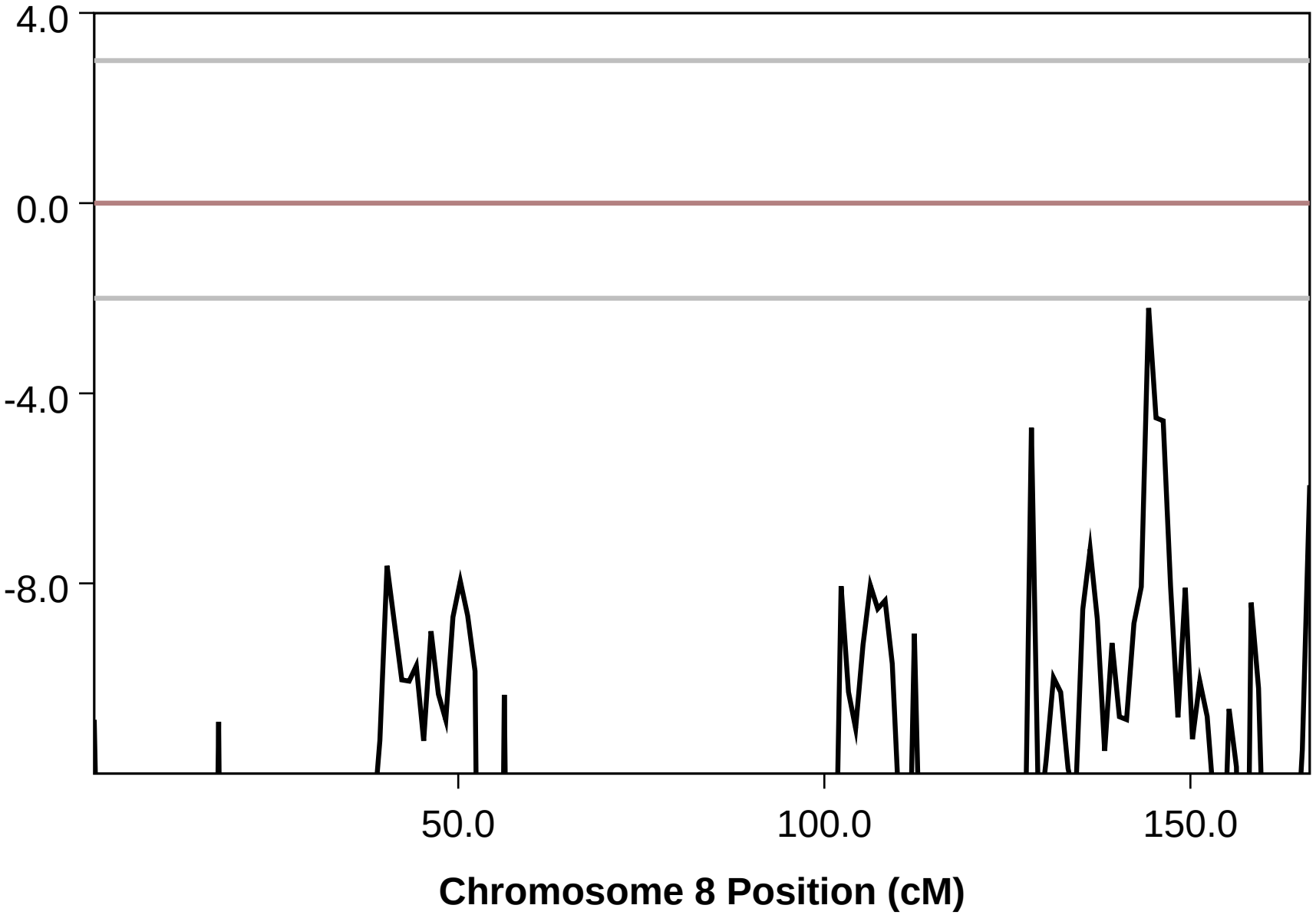

Parametric Analysis for Recessive_Model

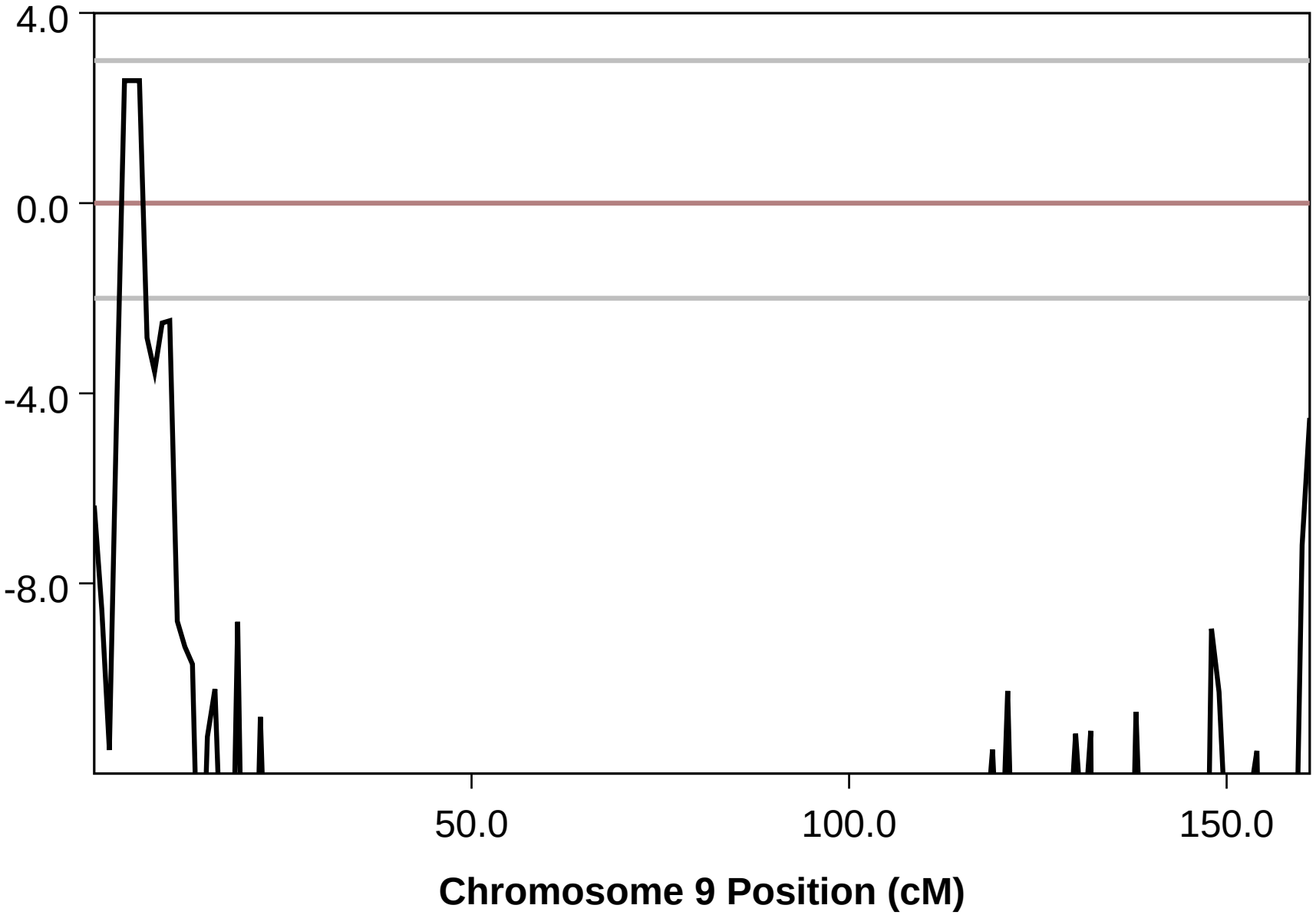

Parametric Analysis for Recessive_Model

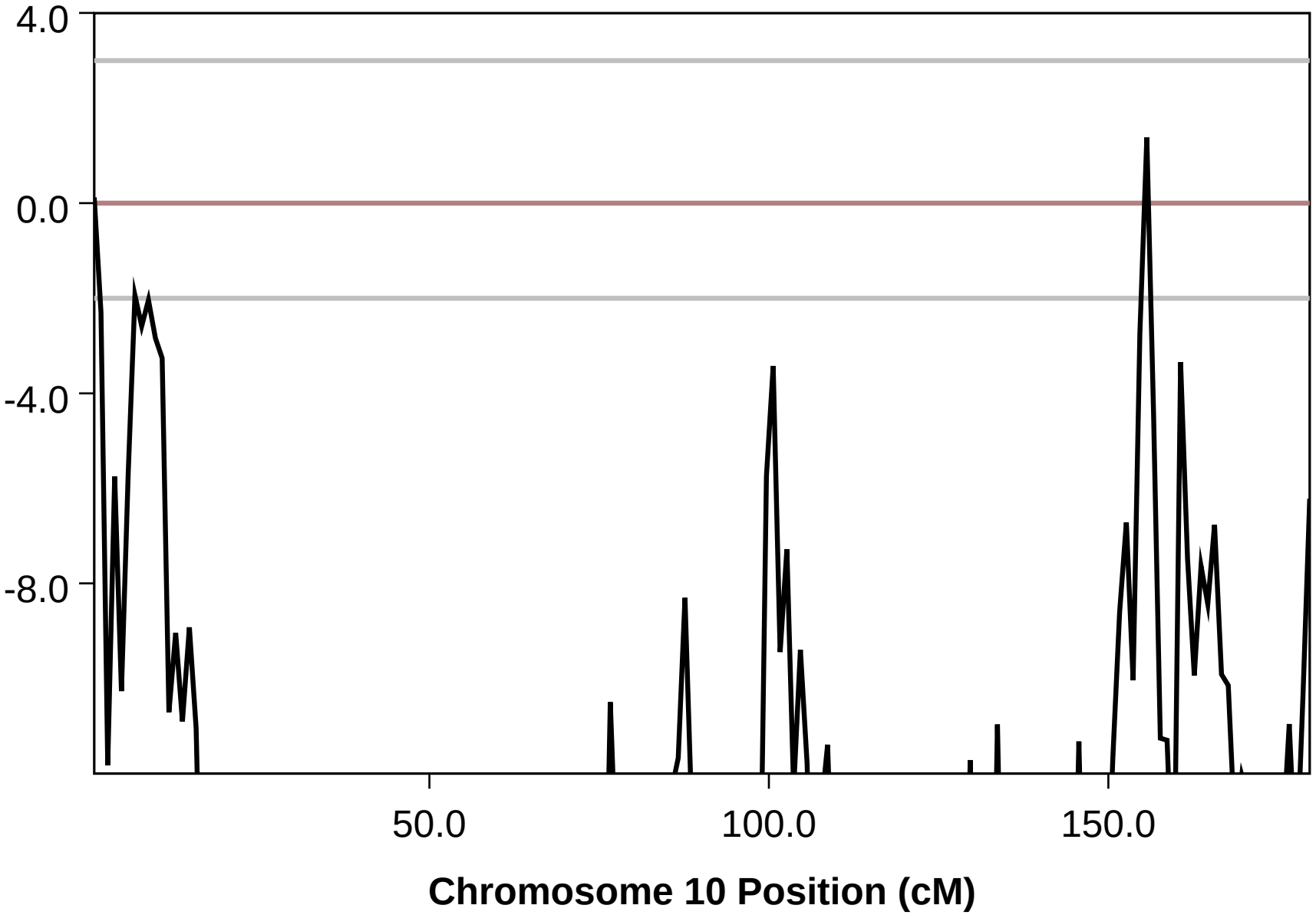

Parametric Analysis for Recessive_Model

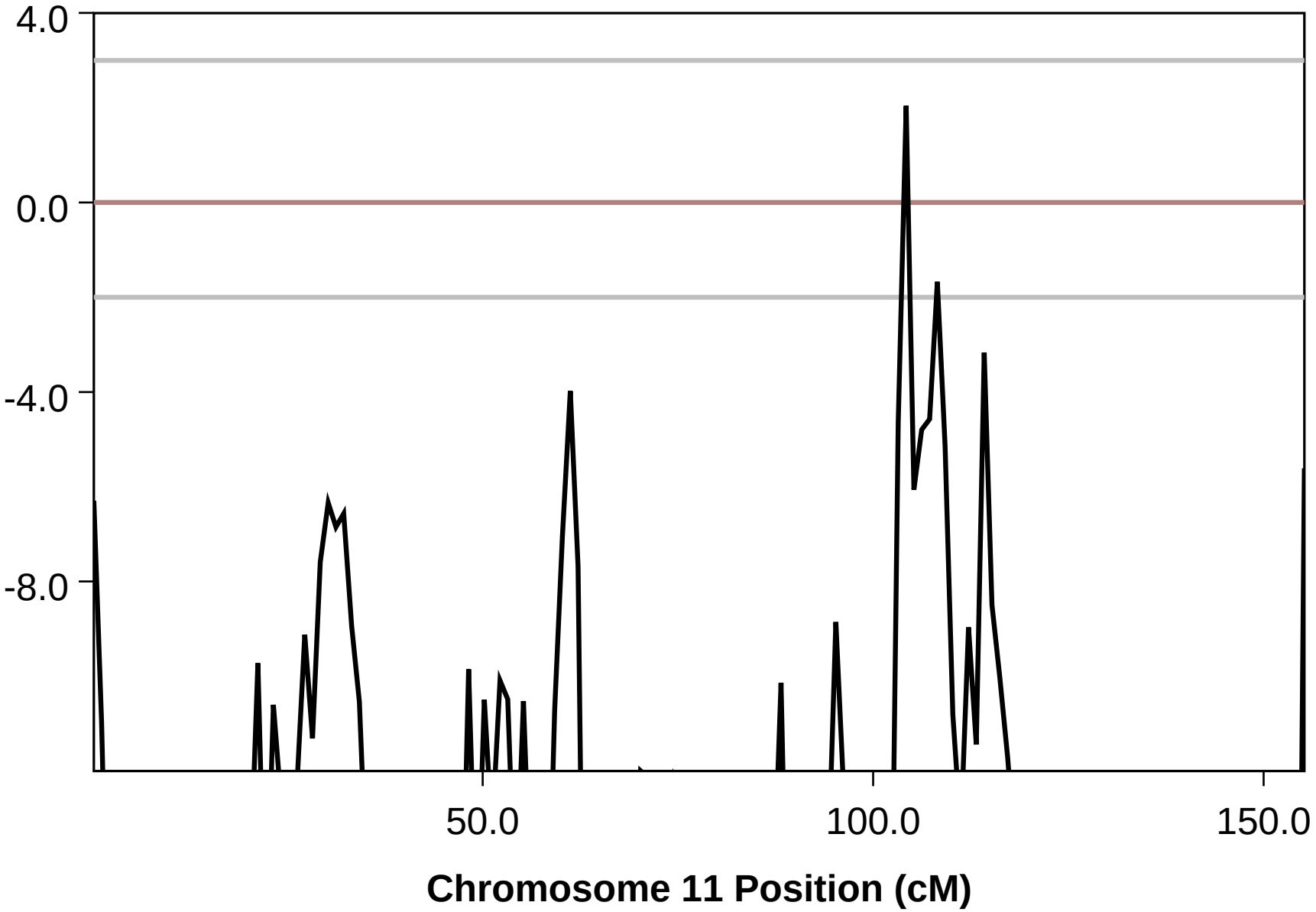

Parametric Analysis for Recessive_Model

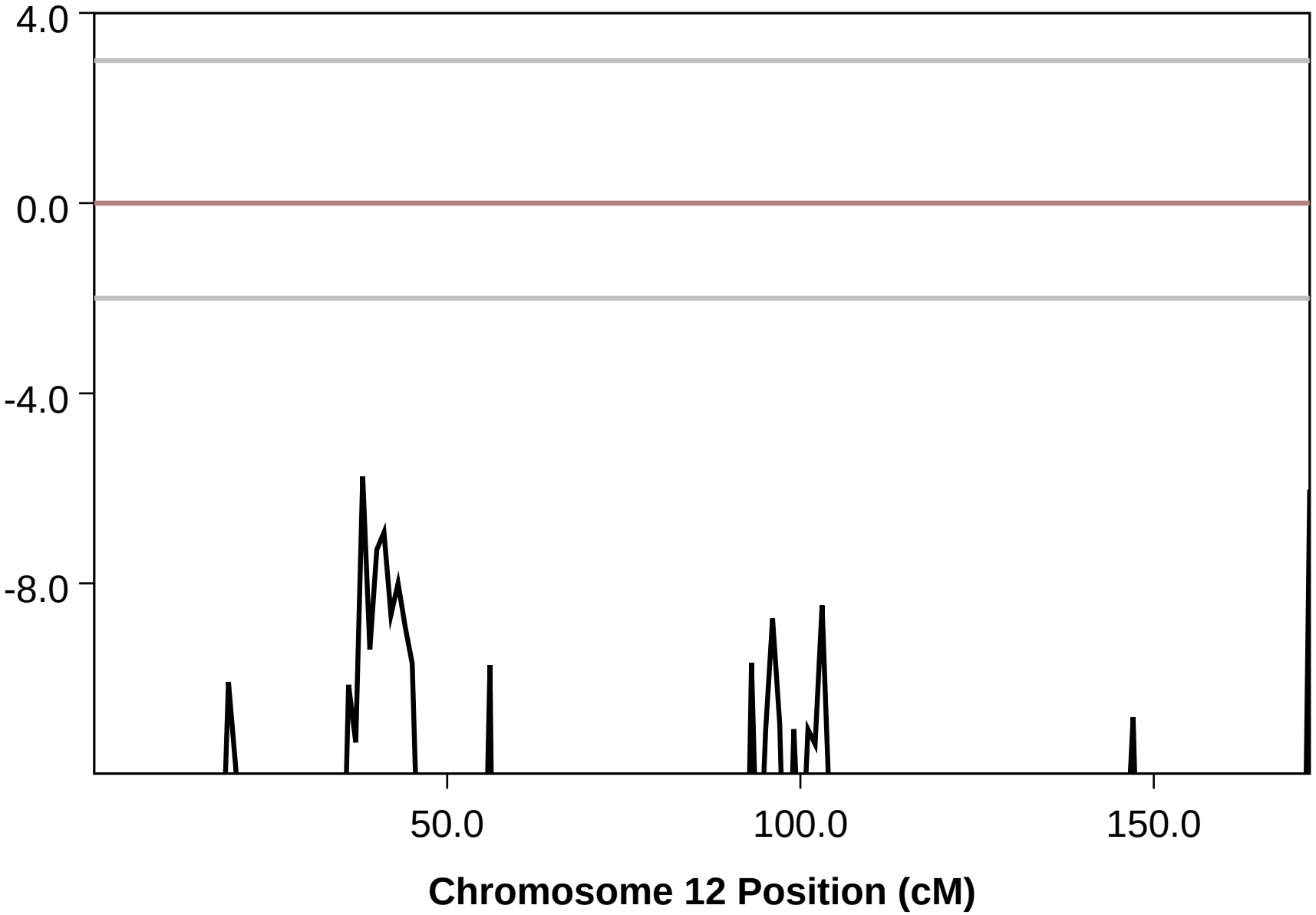

Parametric Analysis for Recessive_Model

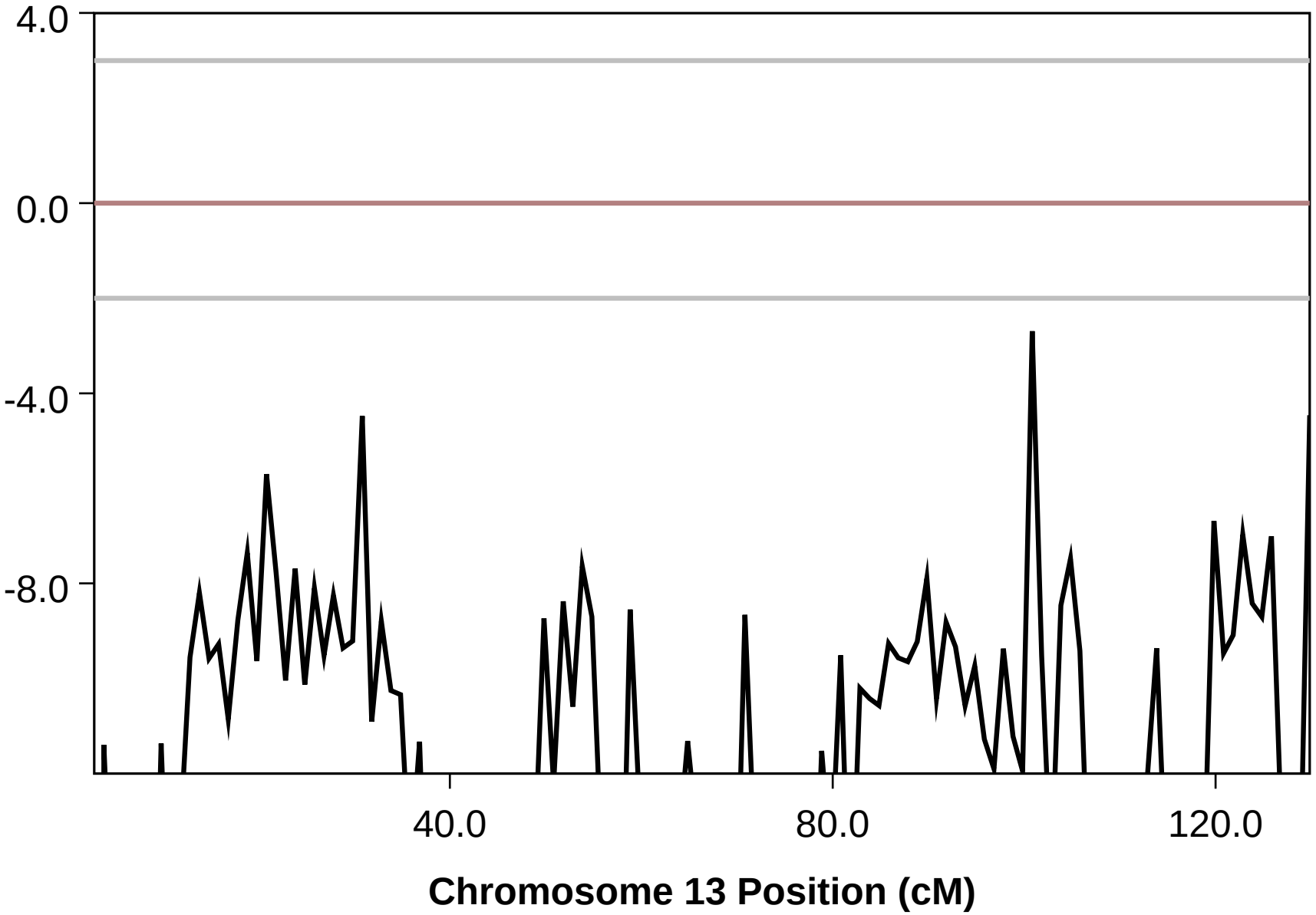

Parametric Analysis for Recessive_Model

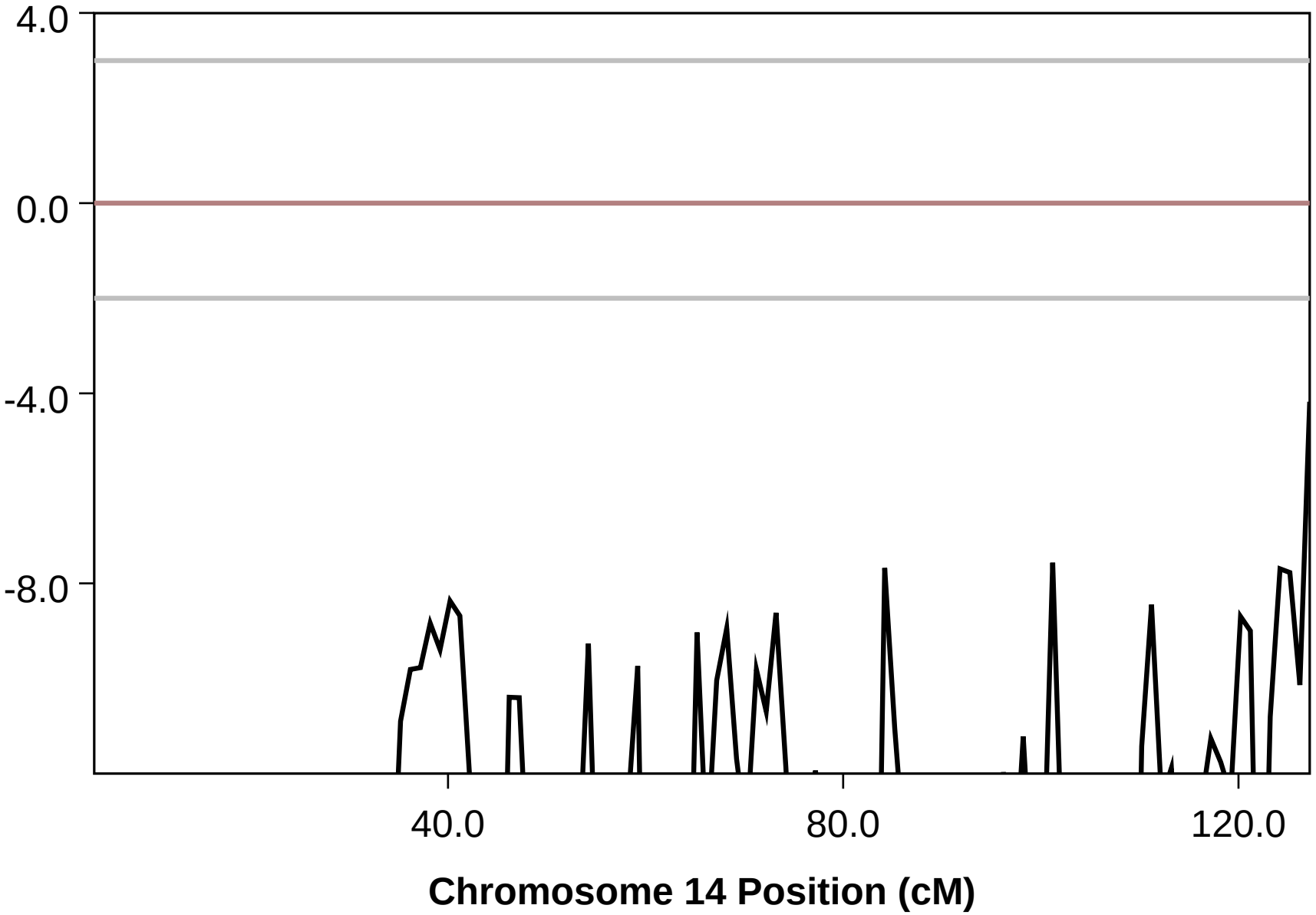

Parametric Analysis for Recessive_Model

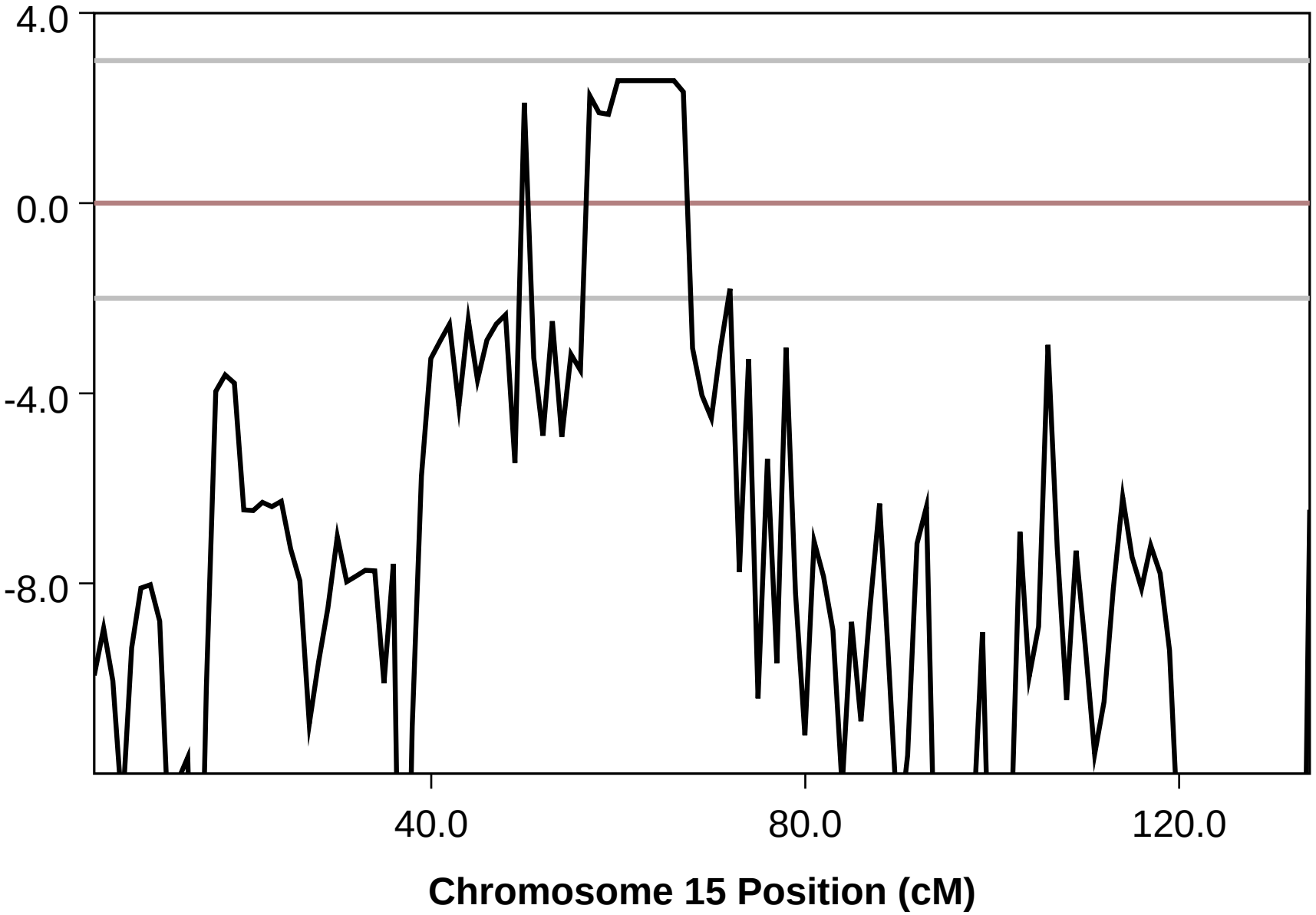

Parametric Analysis for Recessive_Model

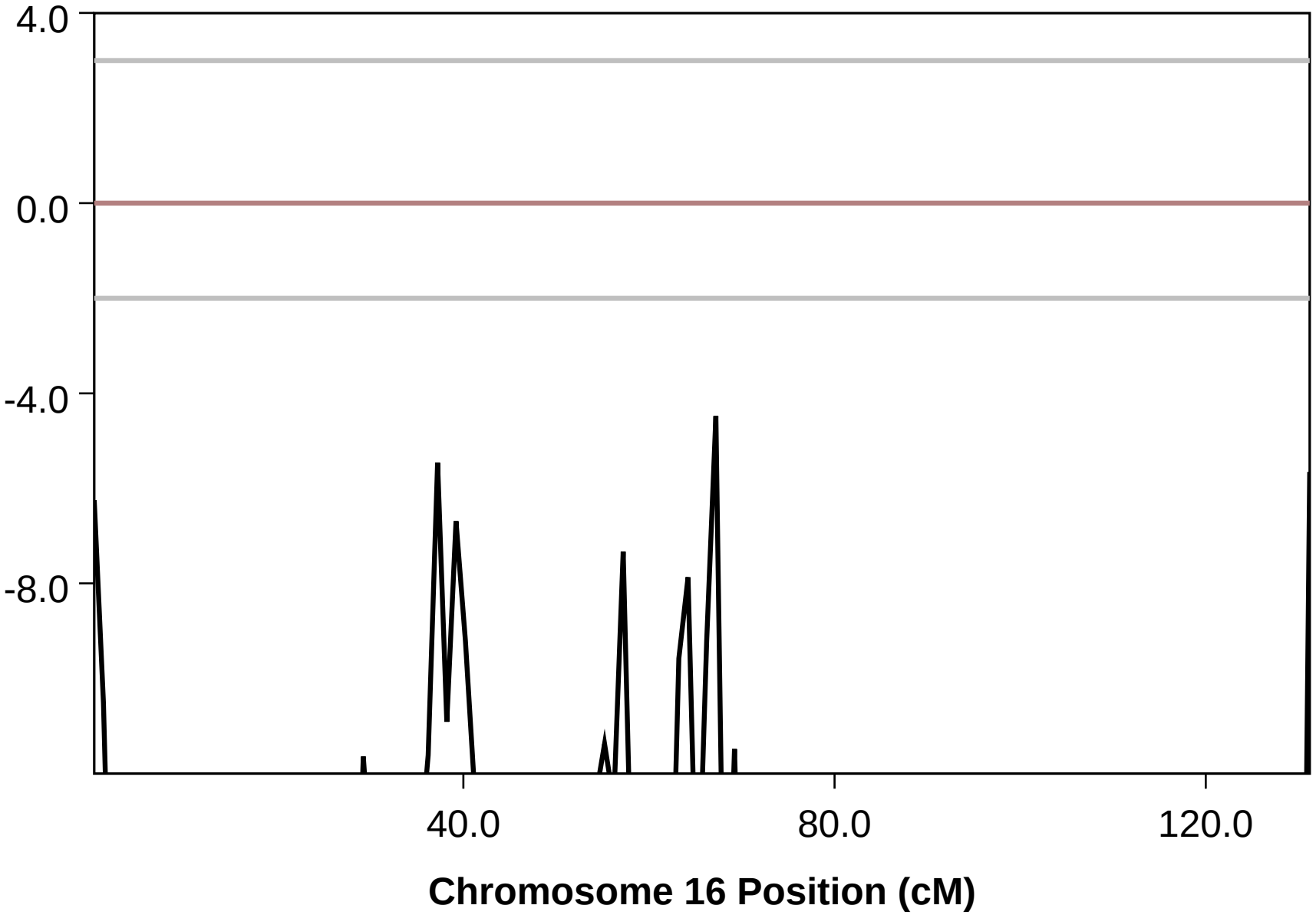

Parametric Analysis for Recessive_Model

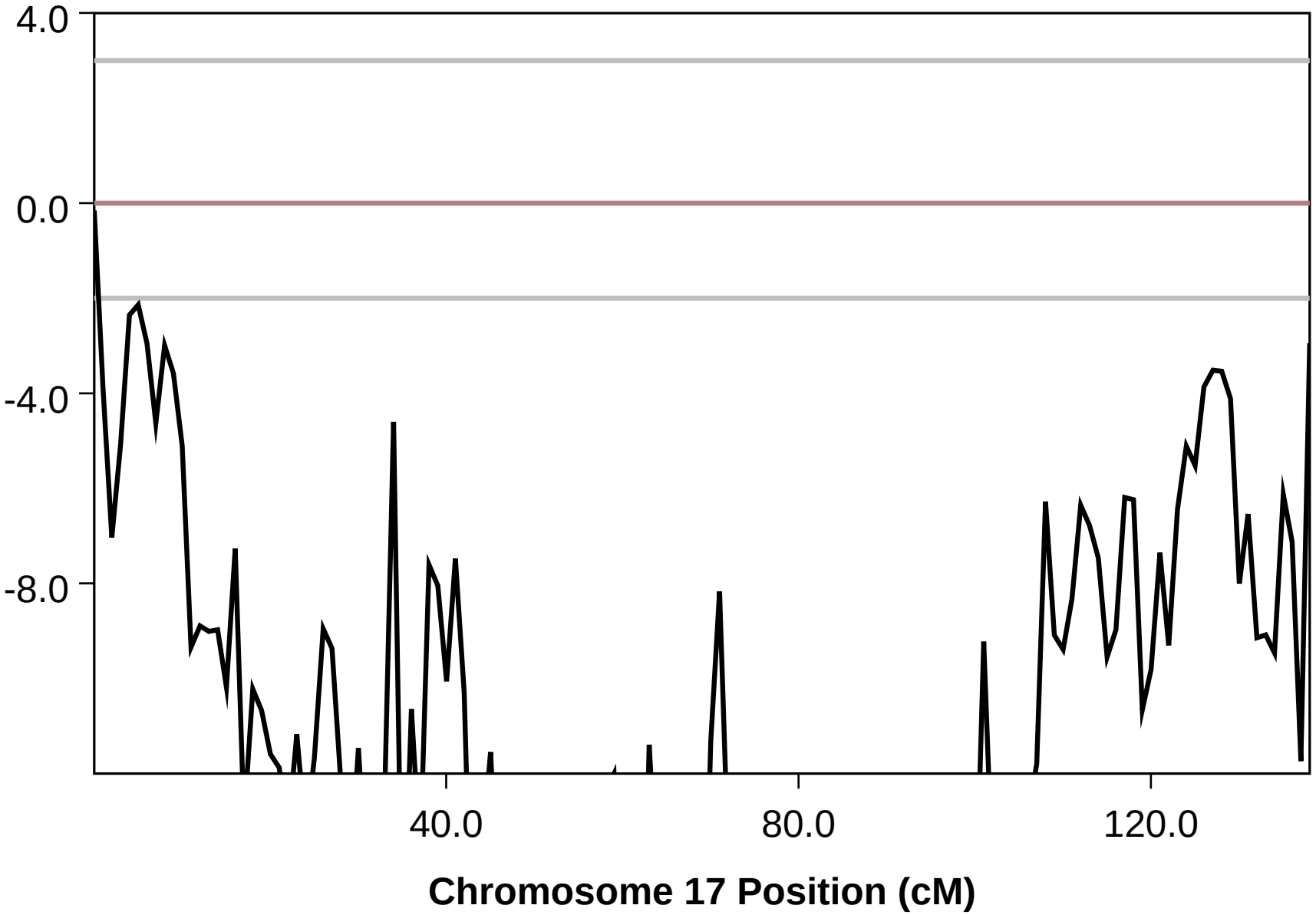

Parametric Analysis for Recessive_Model

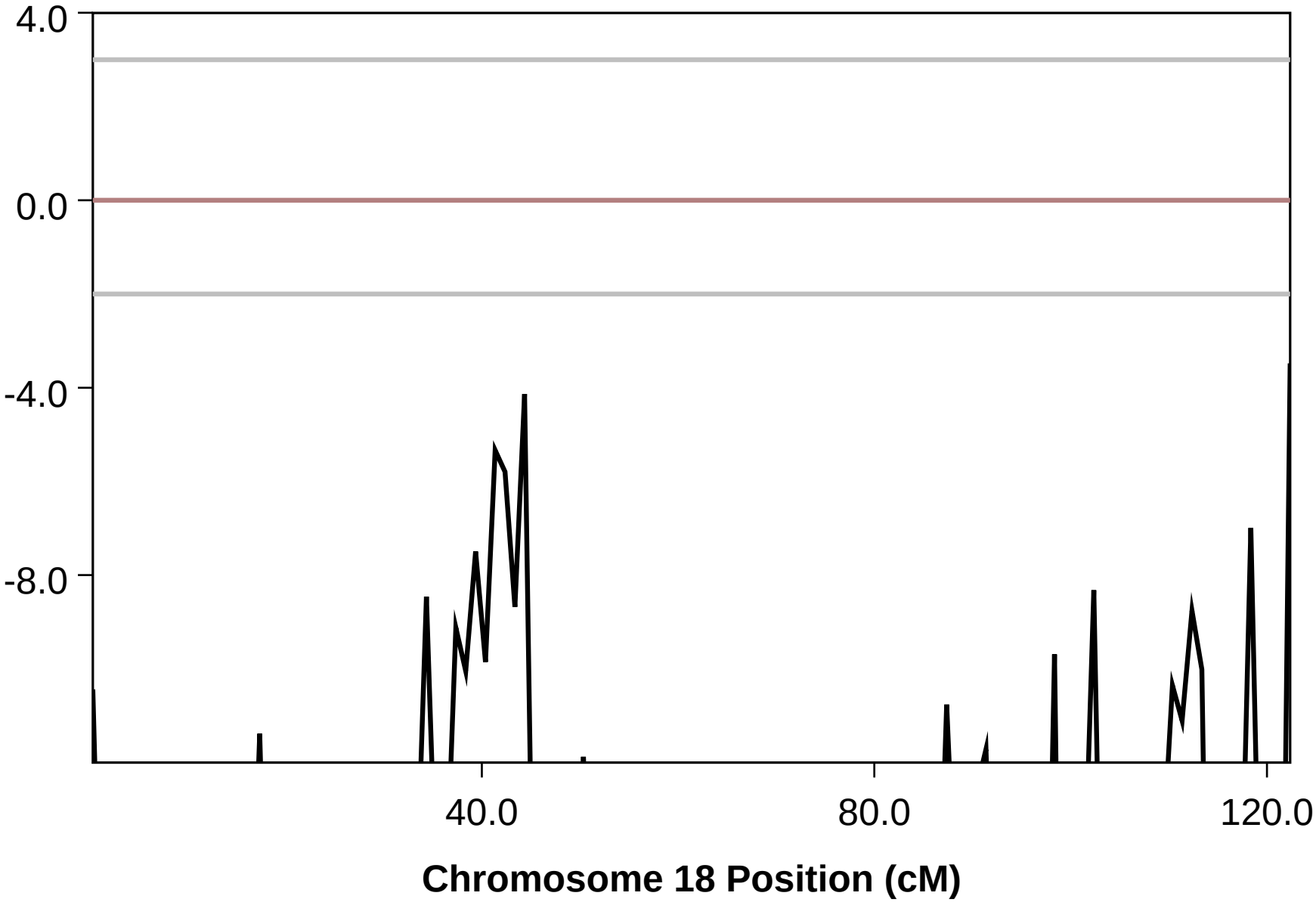

Parametric Analysis for Recessive_Model

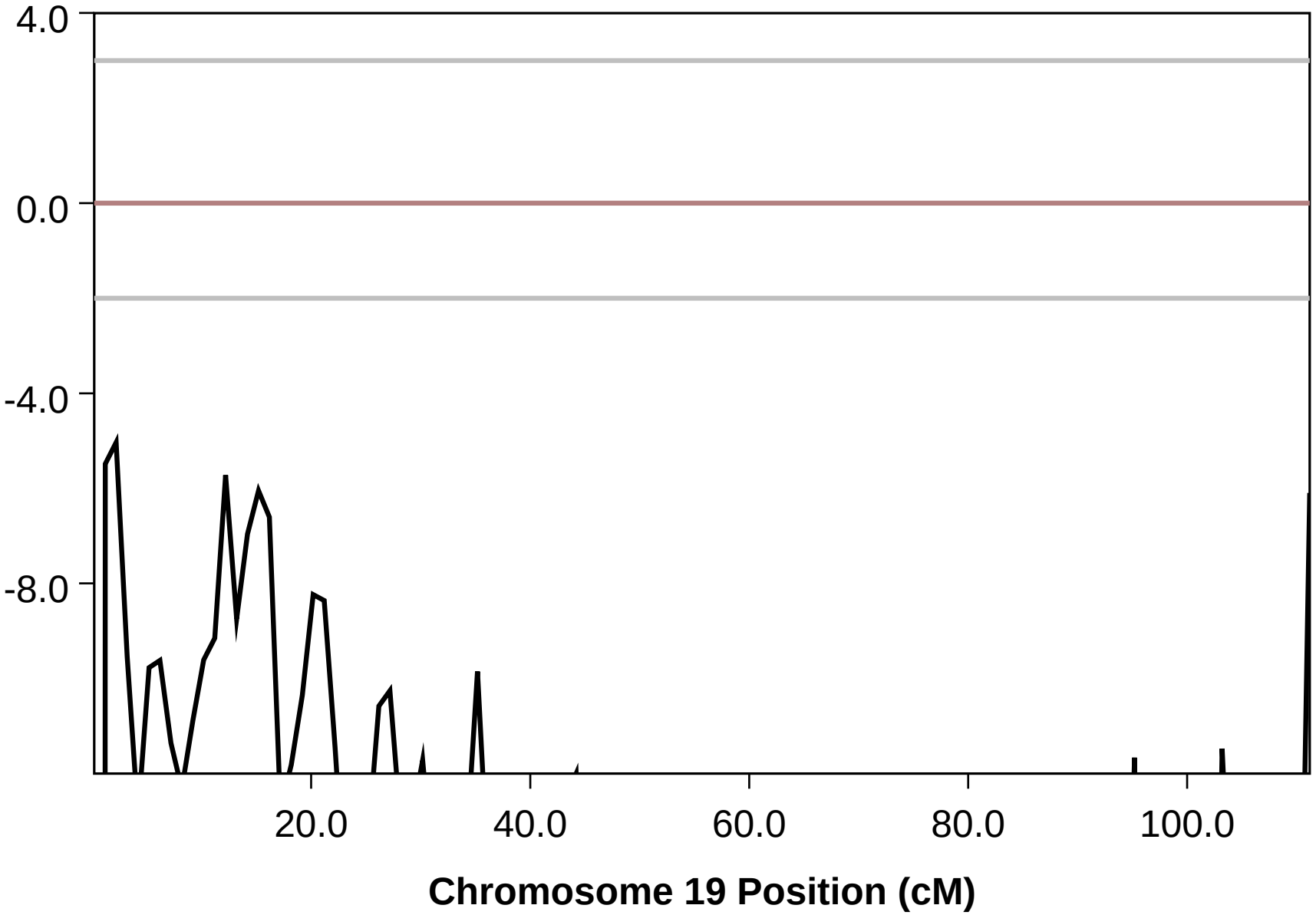

Parametric Analysis for Recessive_Model

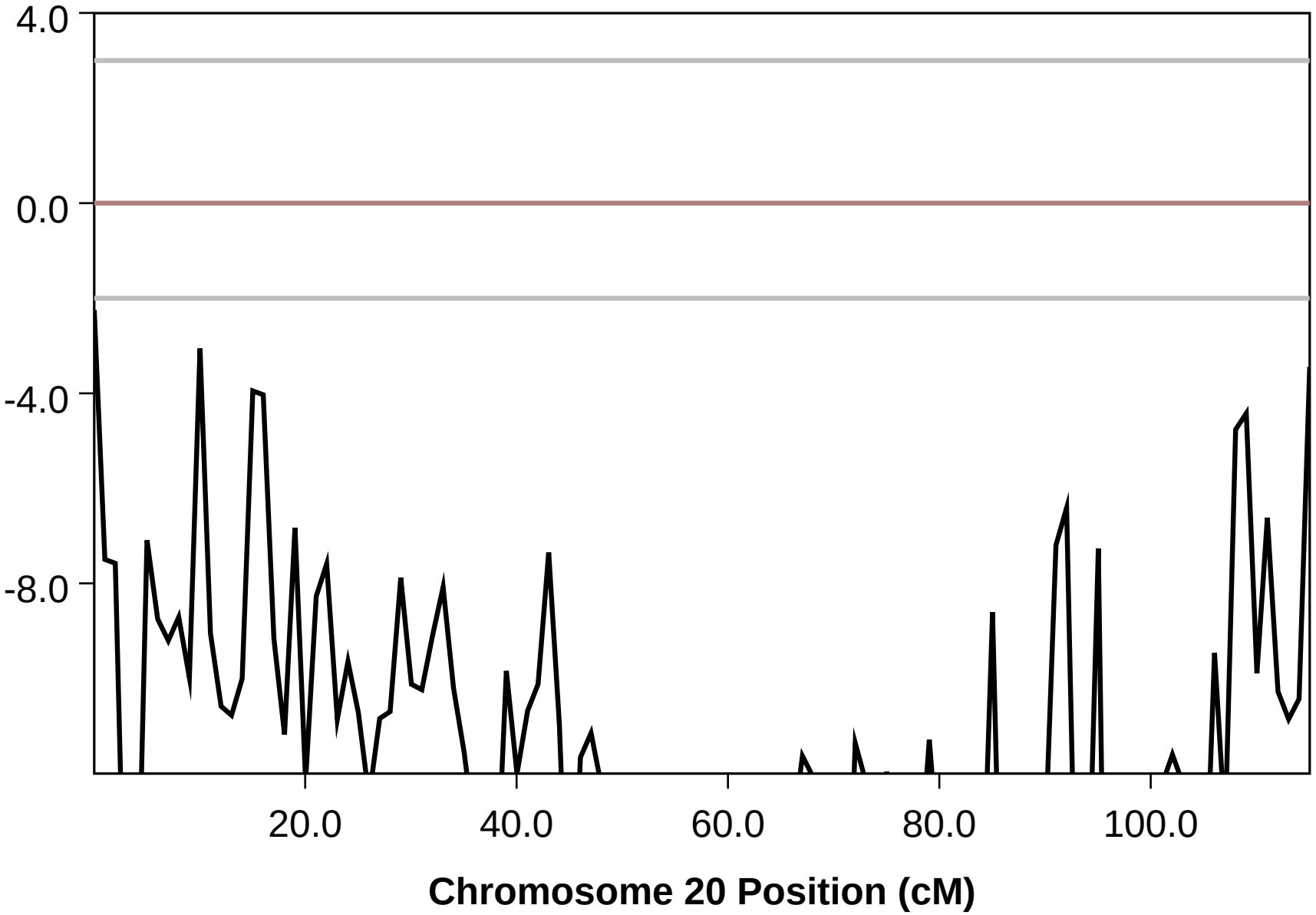

Parametric Analysis for Recessive_Model

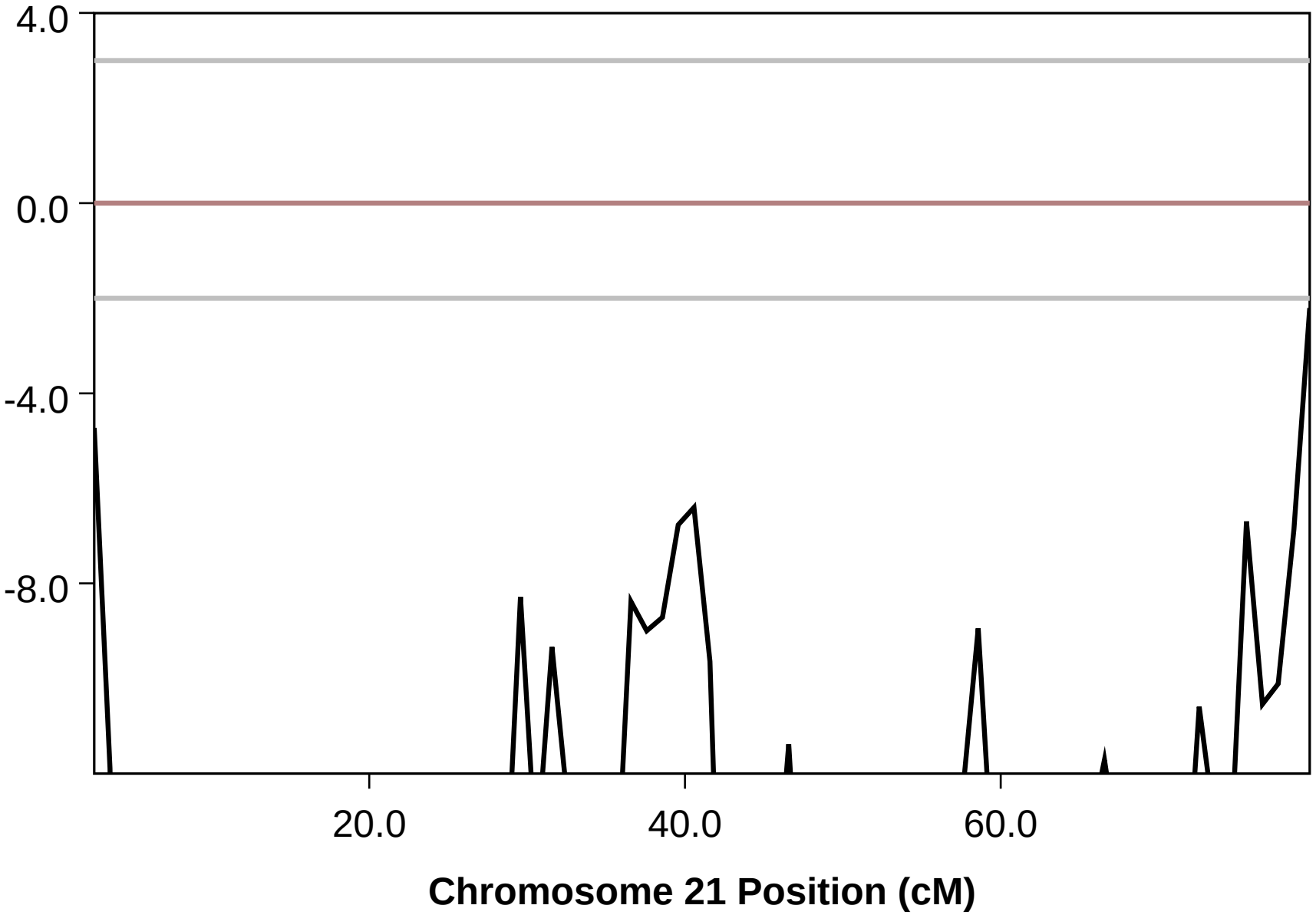

Parametric Analysis for Recessive_Model

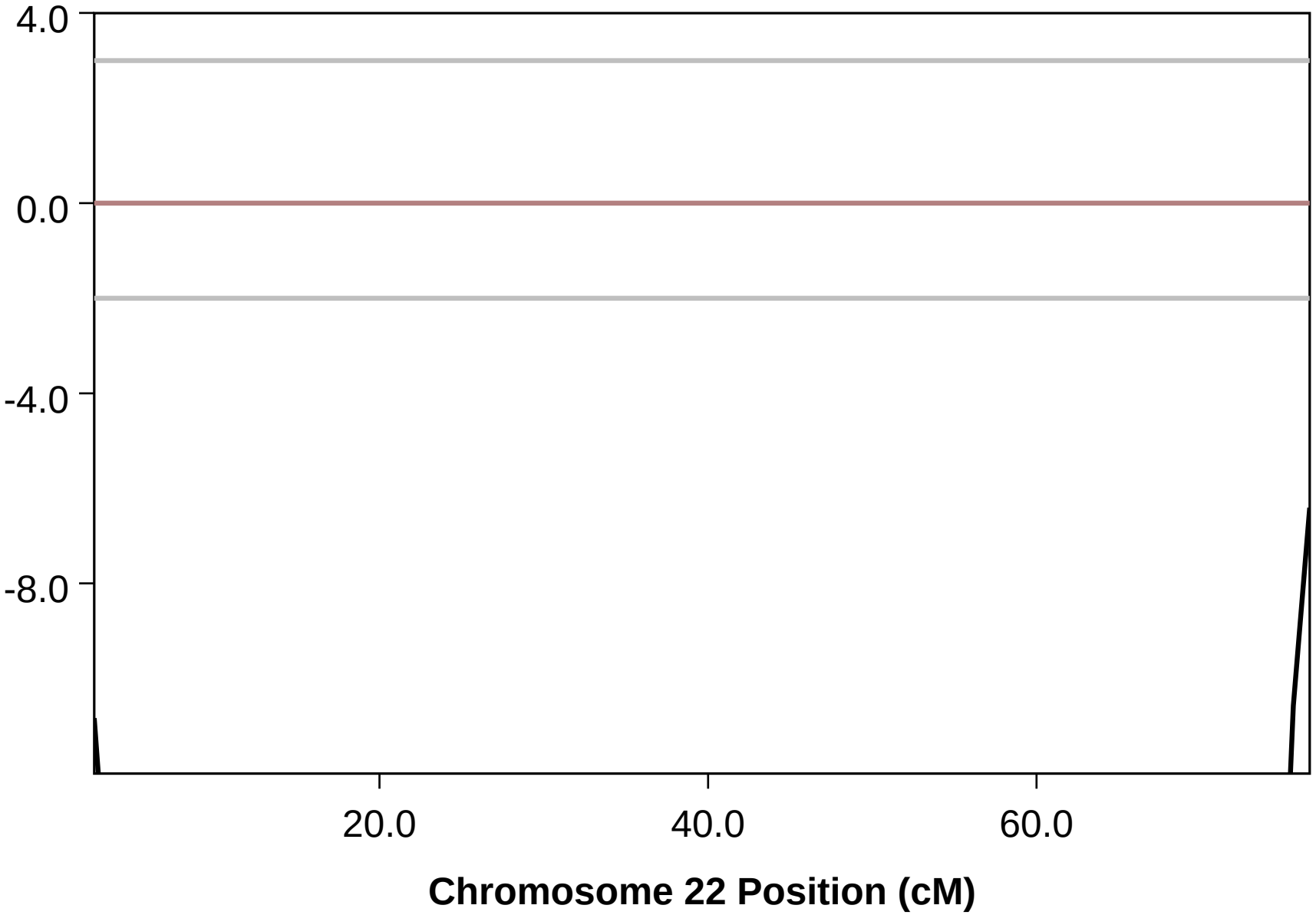

Parametric Analysis for Recessive_Model

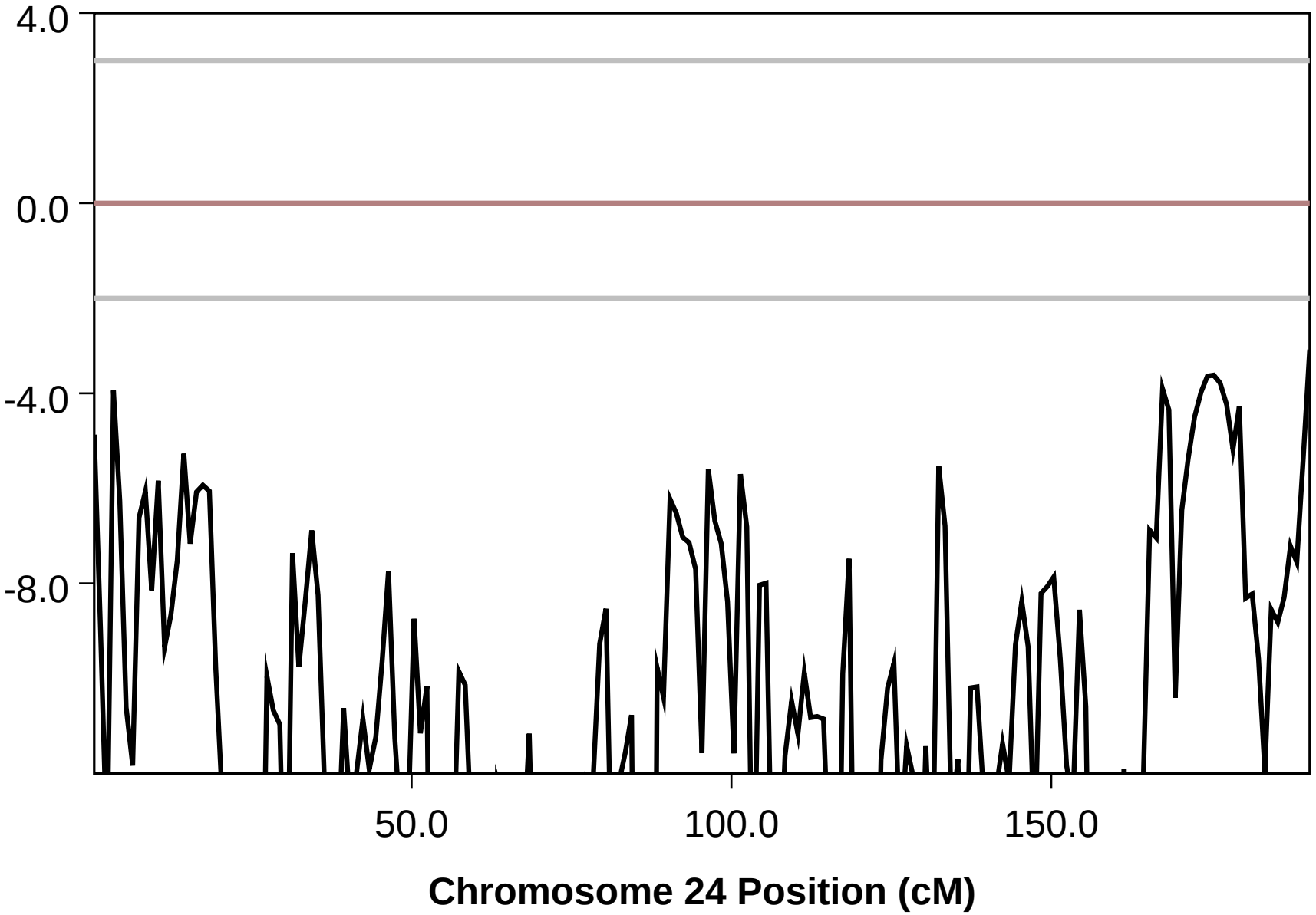

Appendix B

Affected Individual in Family B

5’UTR amplified with primer pair 1

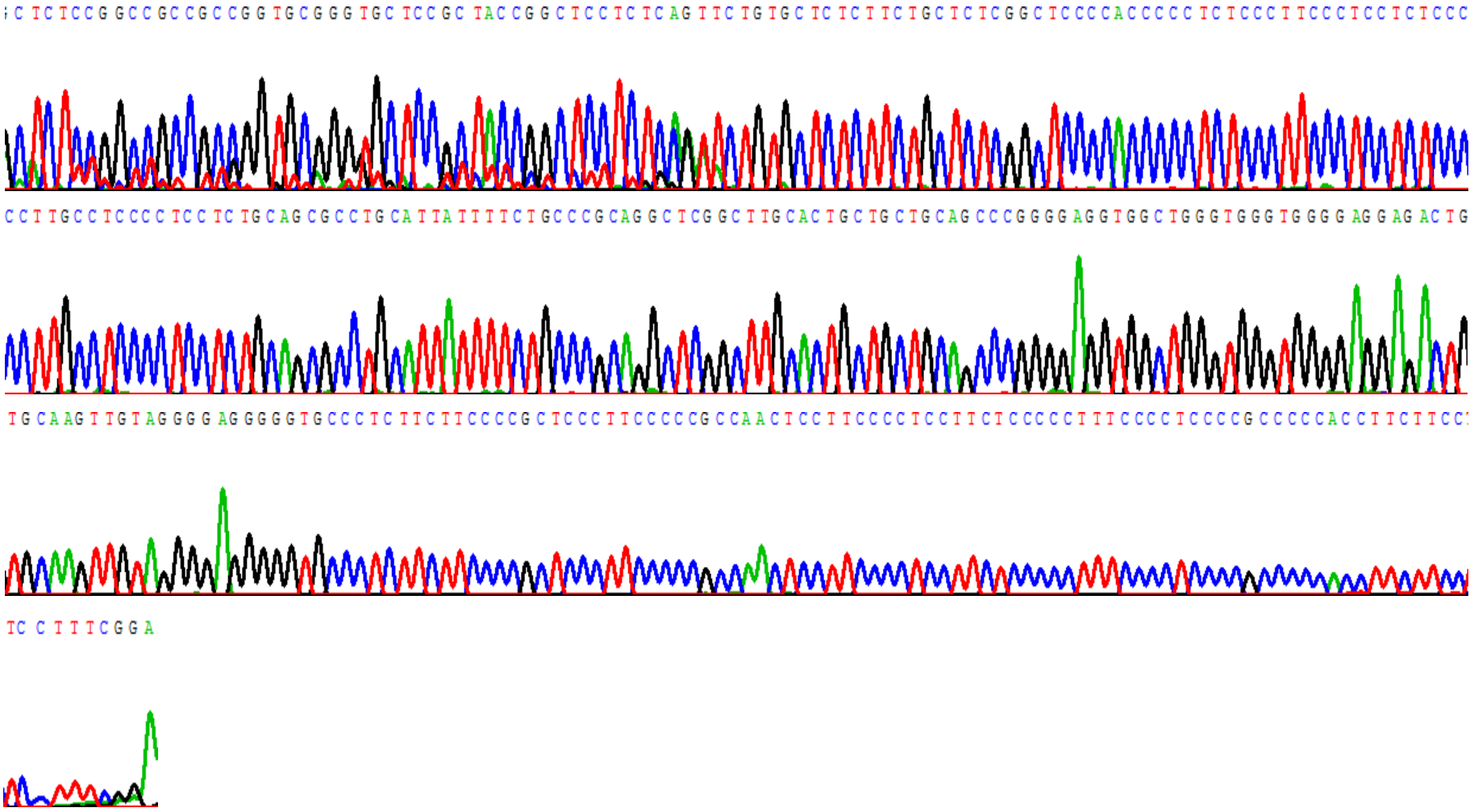

Exon 2 amplified with primer pair 3

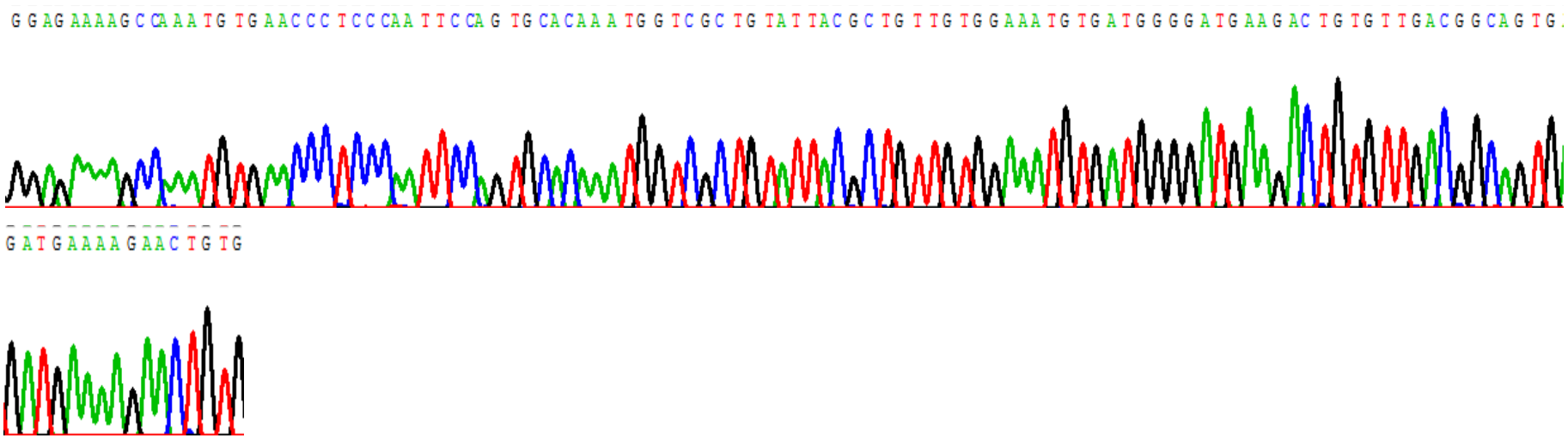

Exon 3 amplified with primer pair 4

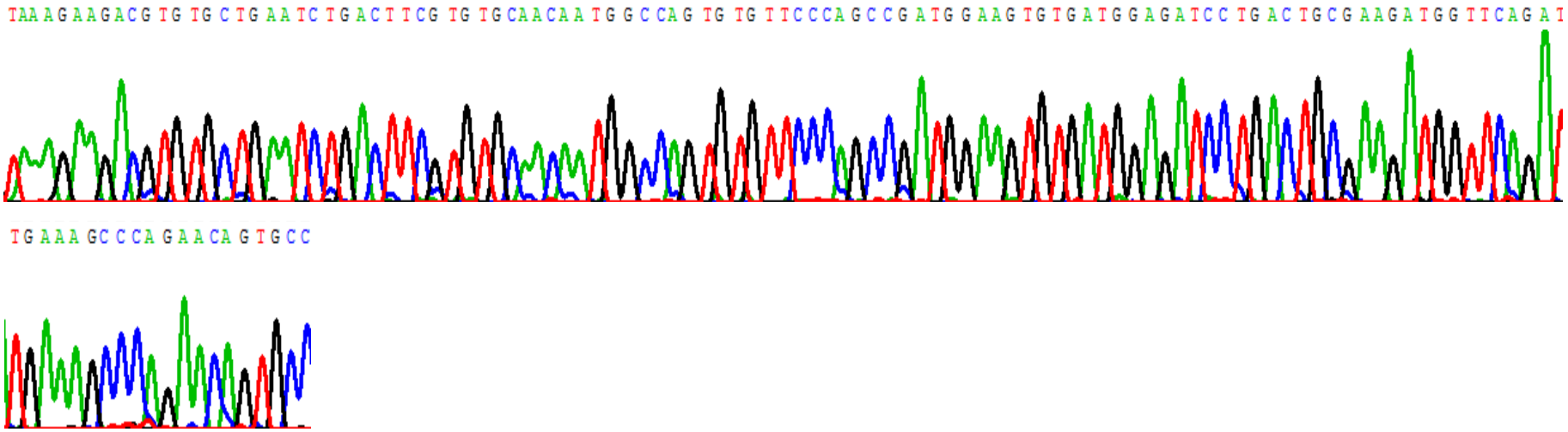

Exon 4 amplified with primer pair 5

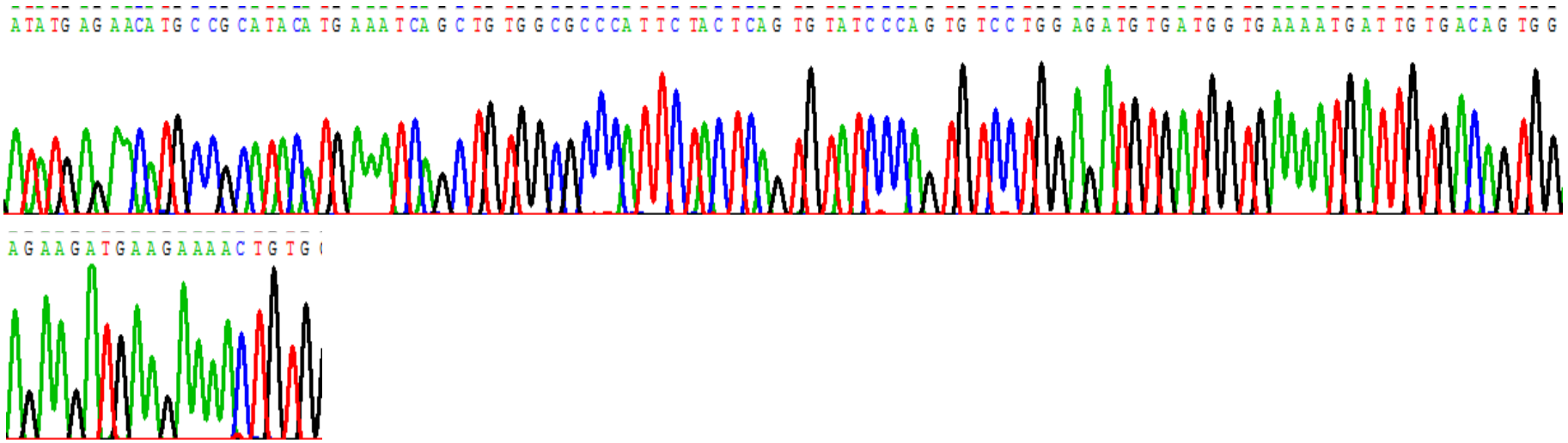

Exon 5 amplified with primer pair 6

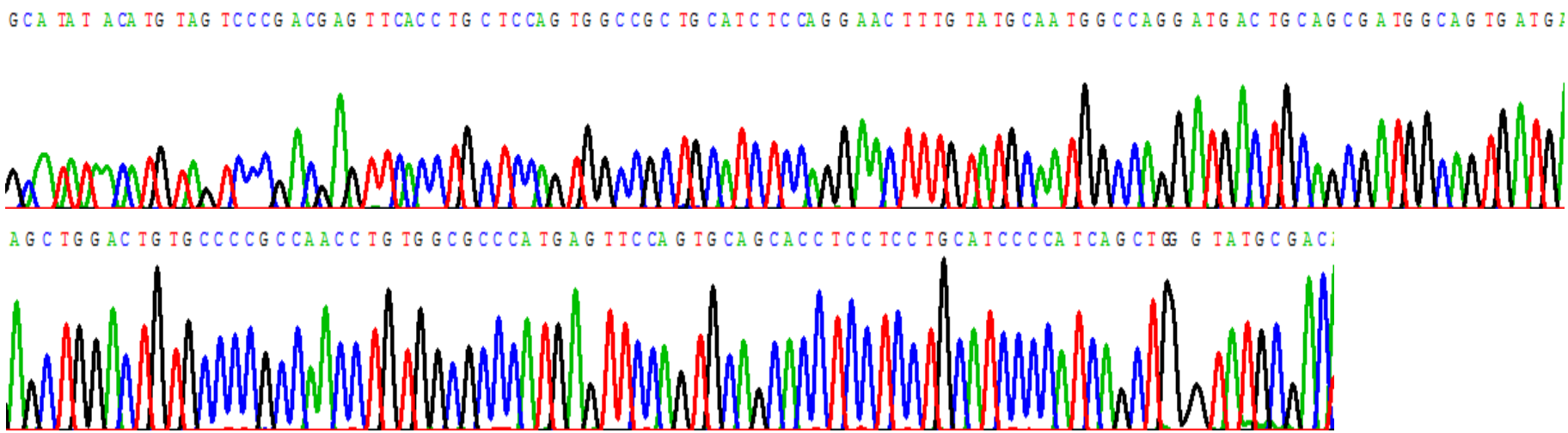

Exons 5 and 6 amplified with primer pair 7

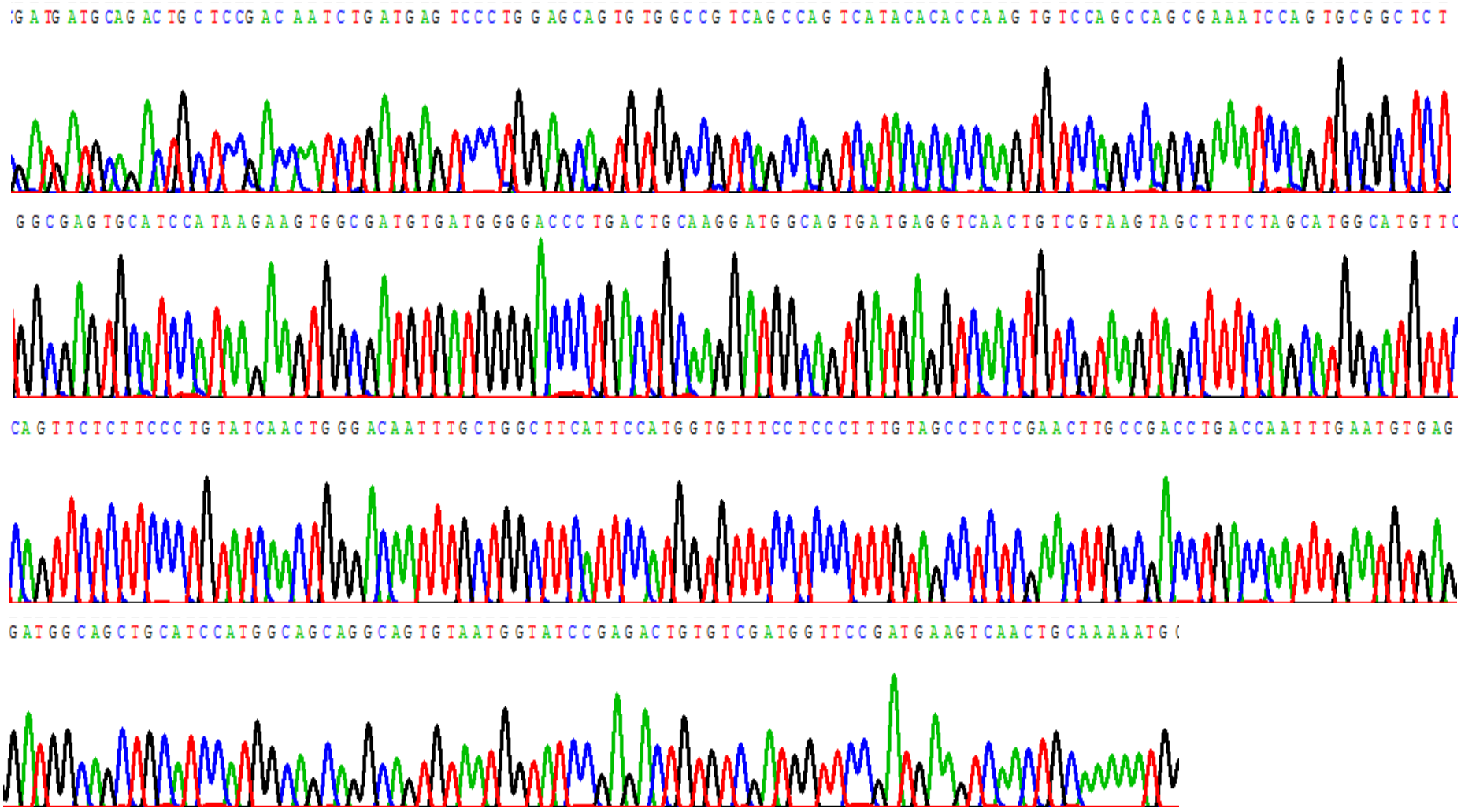

Exon 7 amplified with primer pair 8

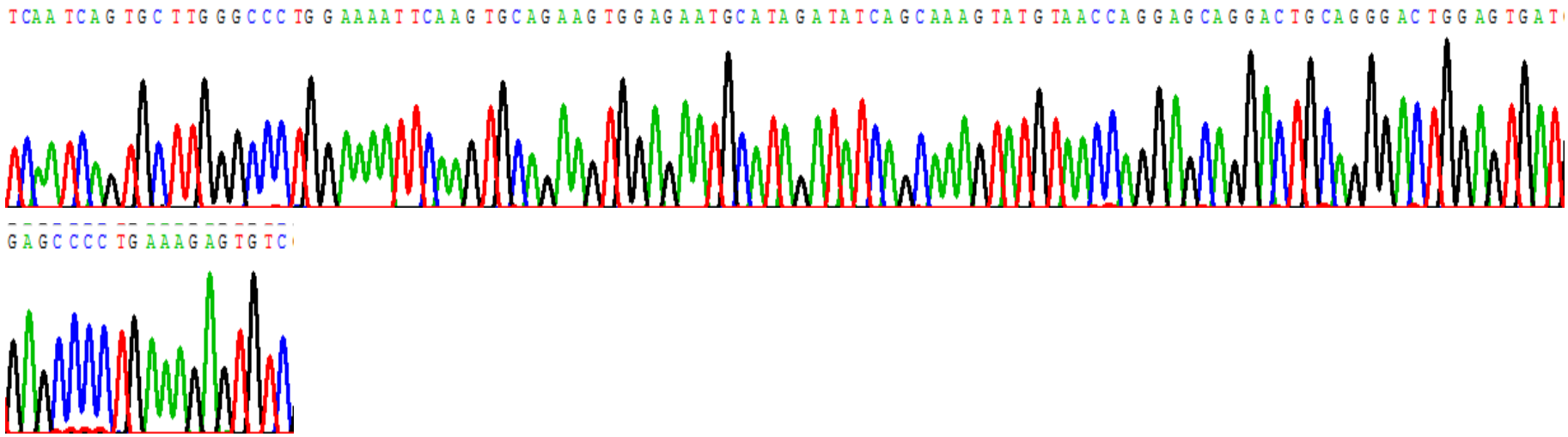

Exon 8 amplified with primer pair 9

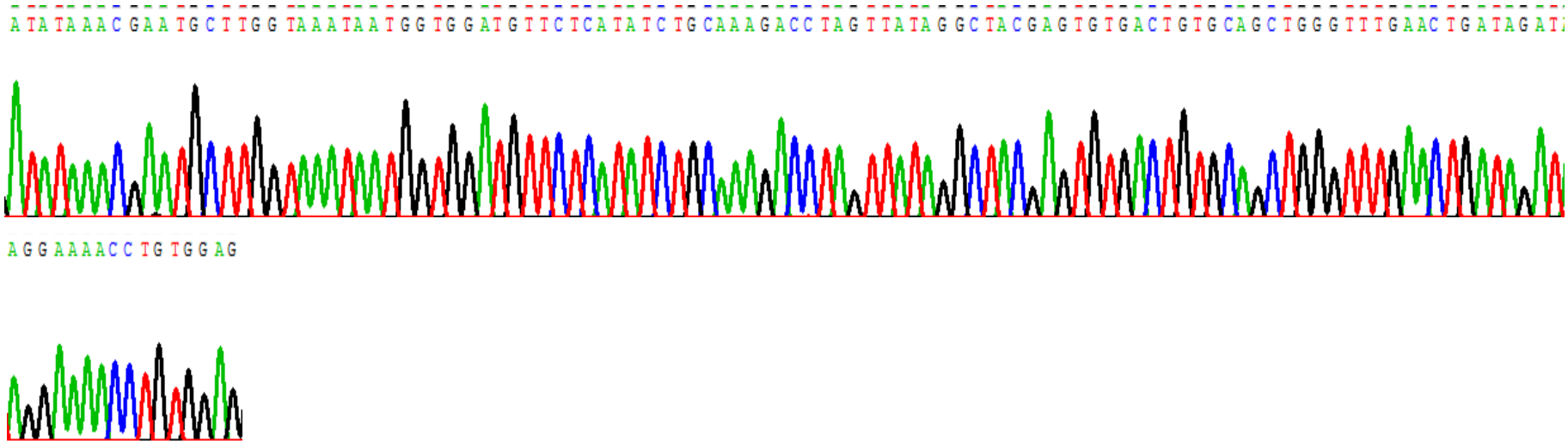

Exon 9 amplified with primer pair 10

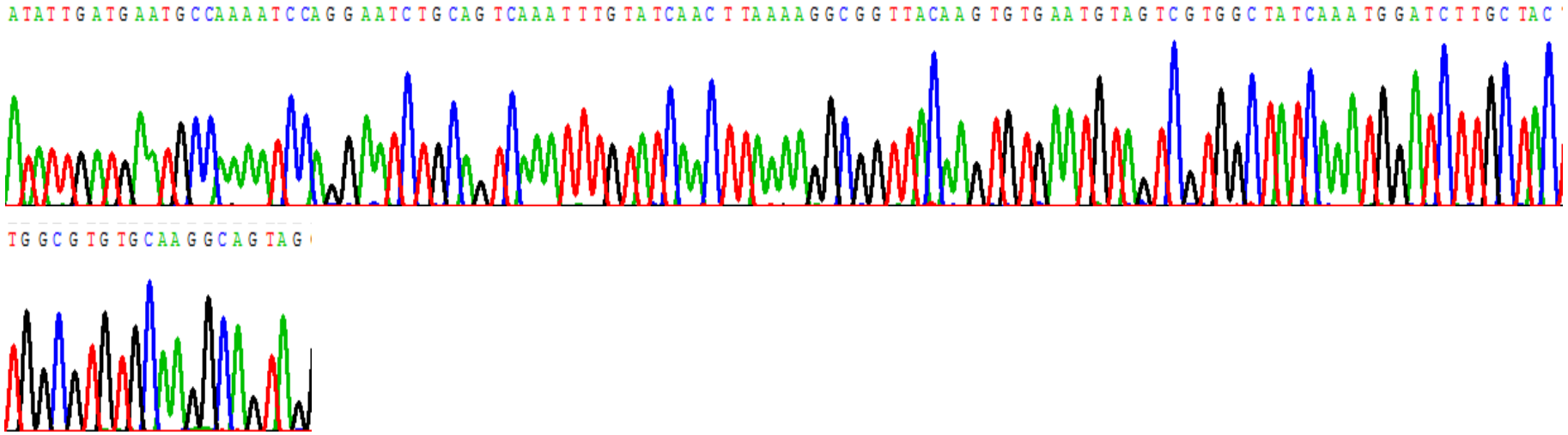

Exon 10 amplified with primer pair 11

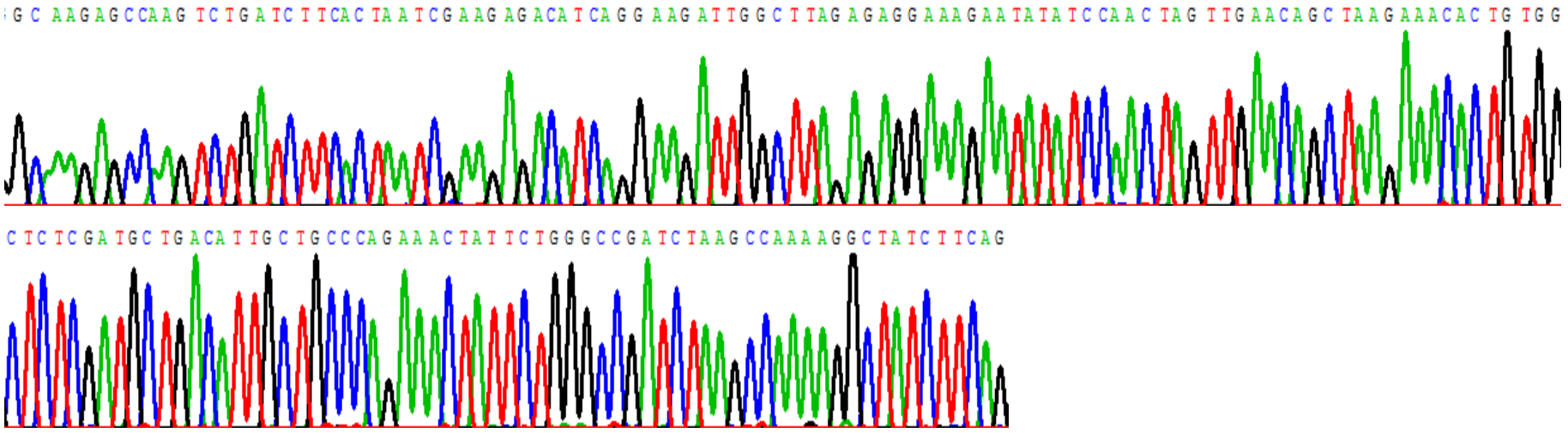

Exon 11 amplified with primer pair 12

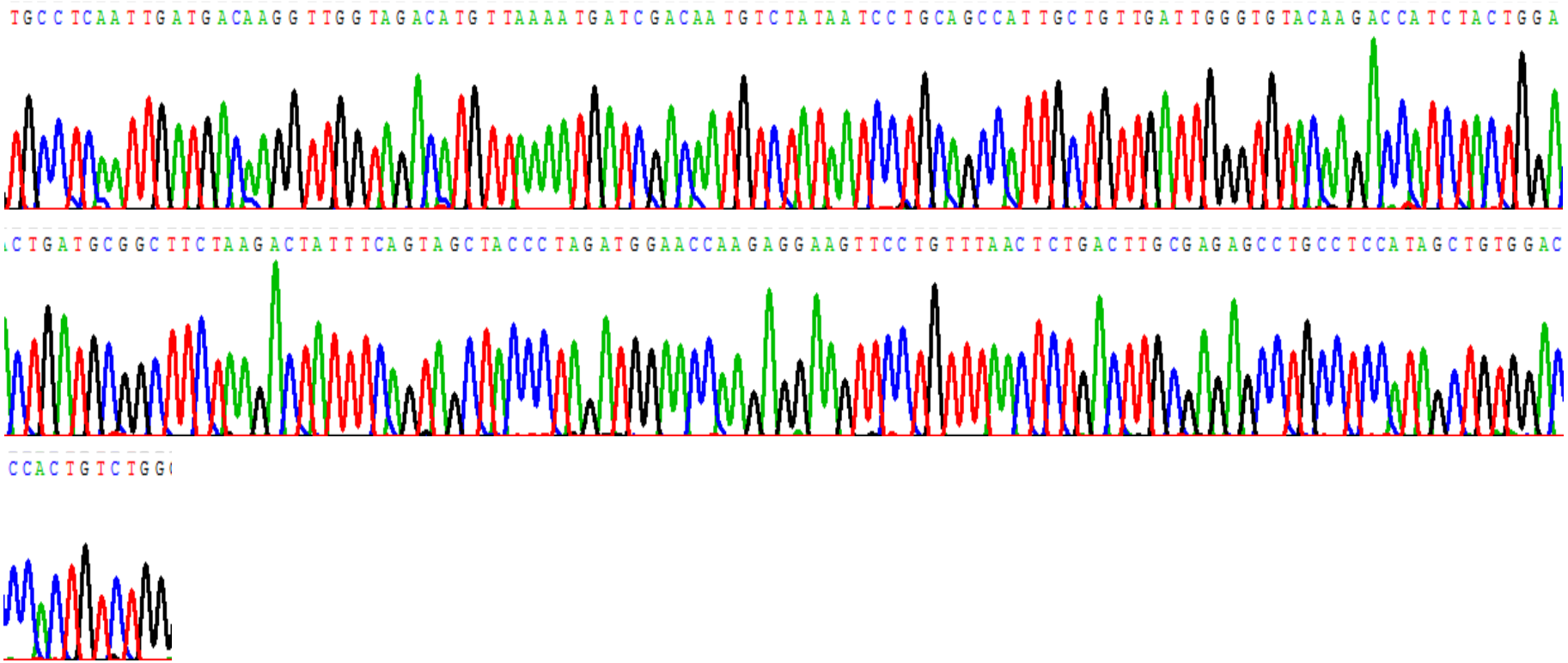

Exon 12 amplified with primer pair 13

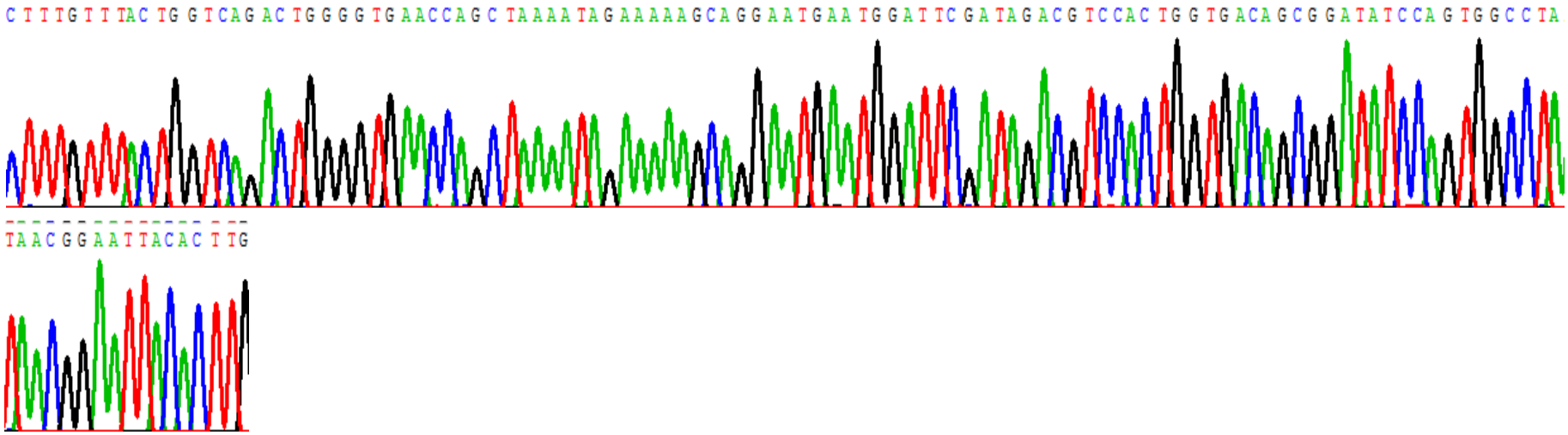

Exon 13 amplified with primer pair 14

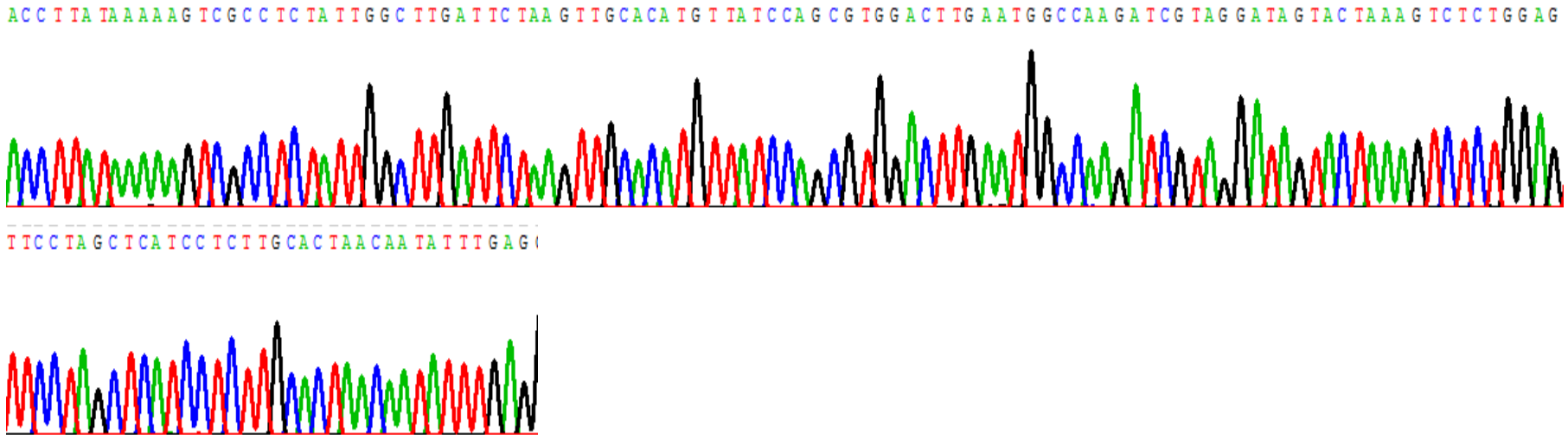

Exon 14 amplified with primer pair 15

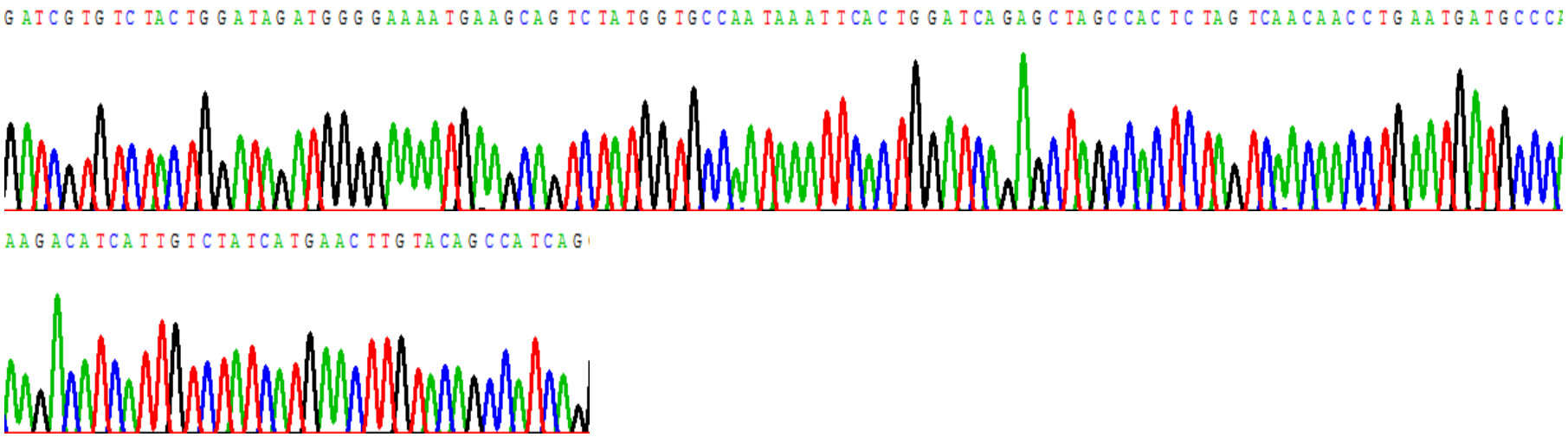

Exon 15 amplified with primer pair 16

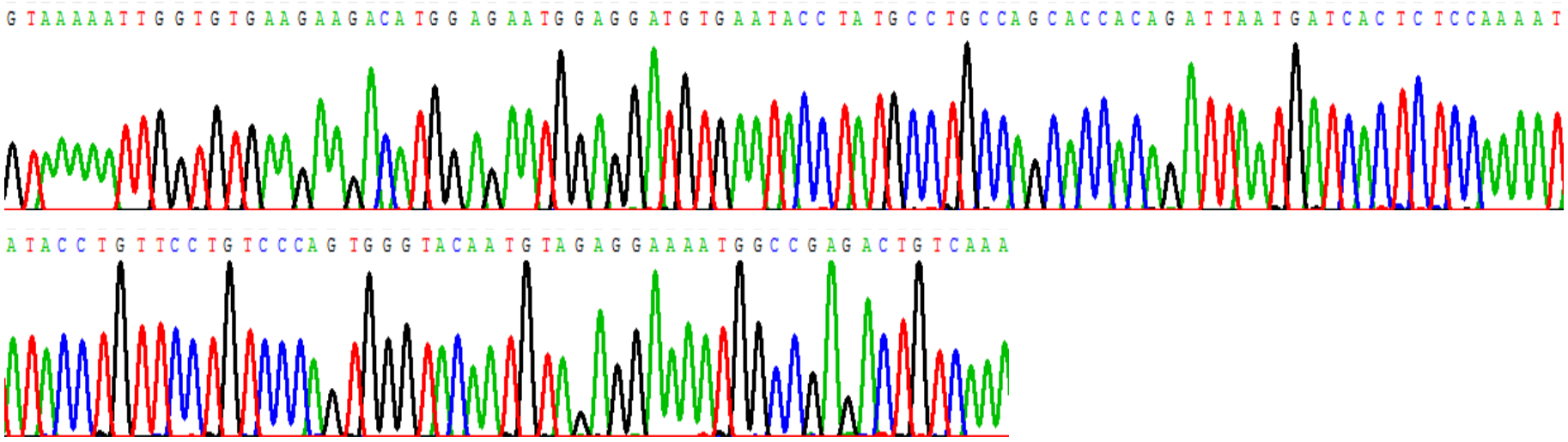

Exon 16 amplified with primer pair 17

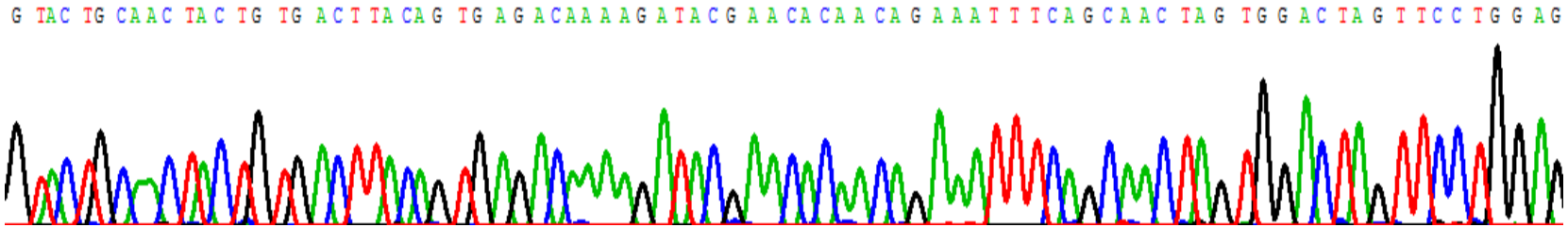

Exon 17 amplified with primer pair 18

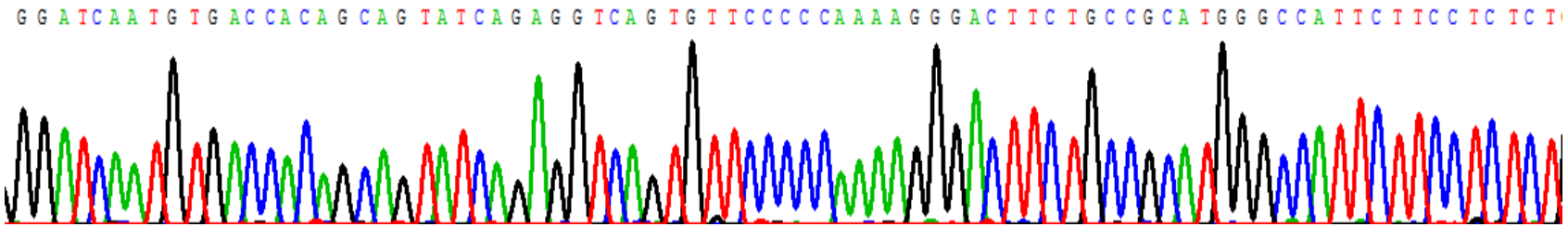

Exon 18 amplified with primer pair 19

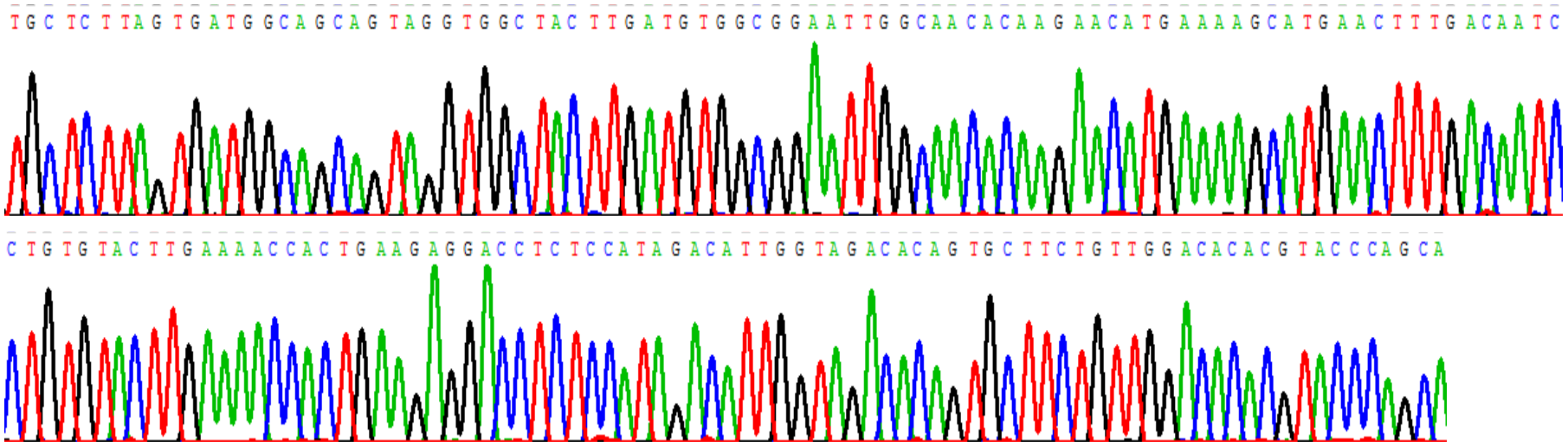

Exon 19 and 3’UTR amplified with primer pair 20

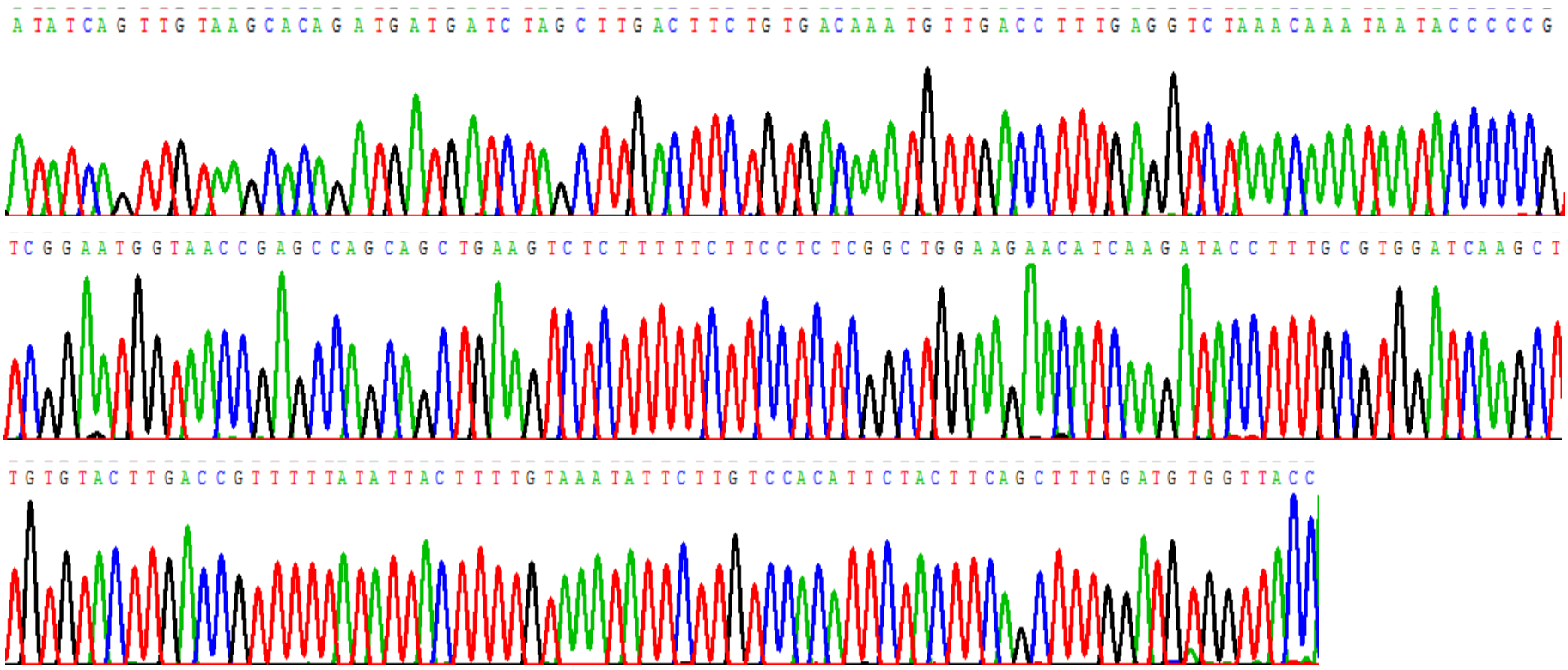

3’UTR amplified with primer pair 21

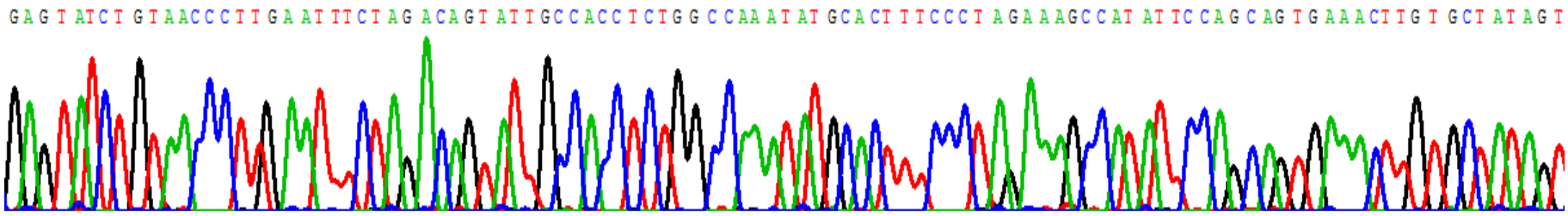

3’UTR amplified with primer pair 22

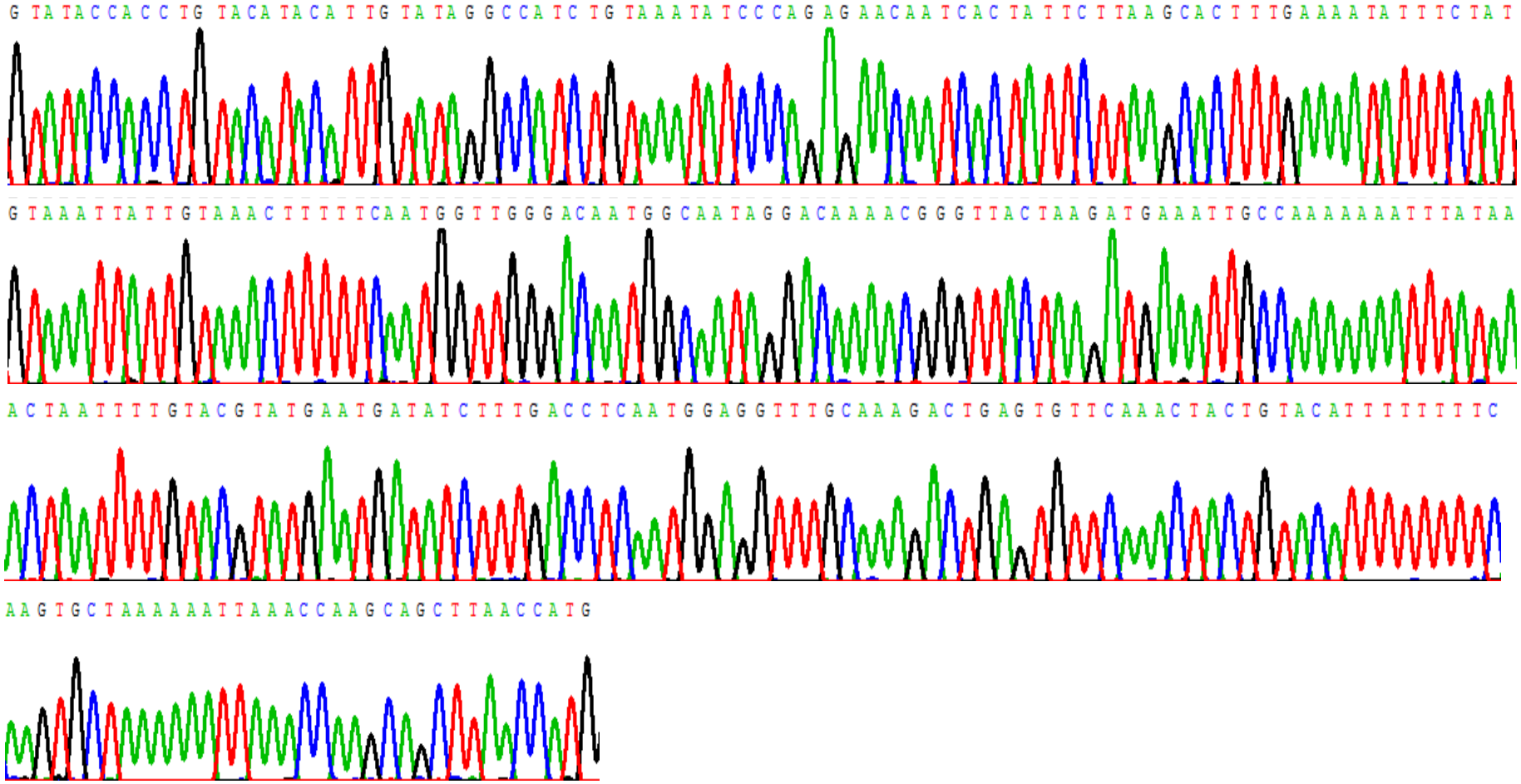

Affected Individual in Family C

5’UTR amplified with primer pair 1

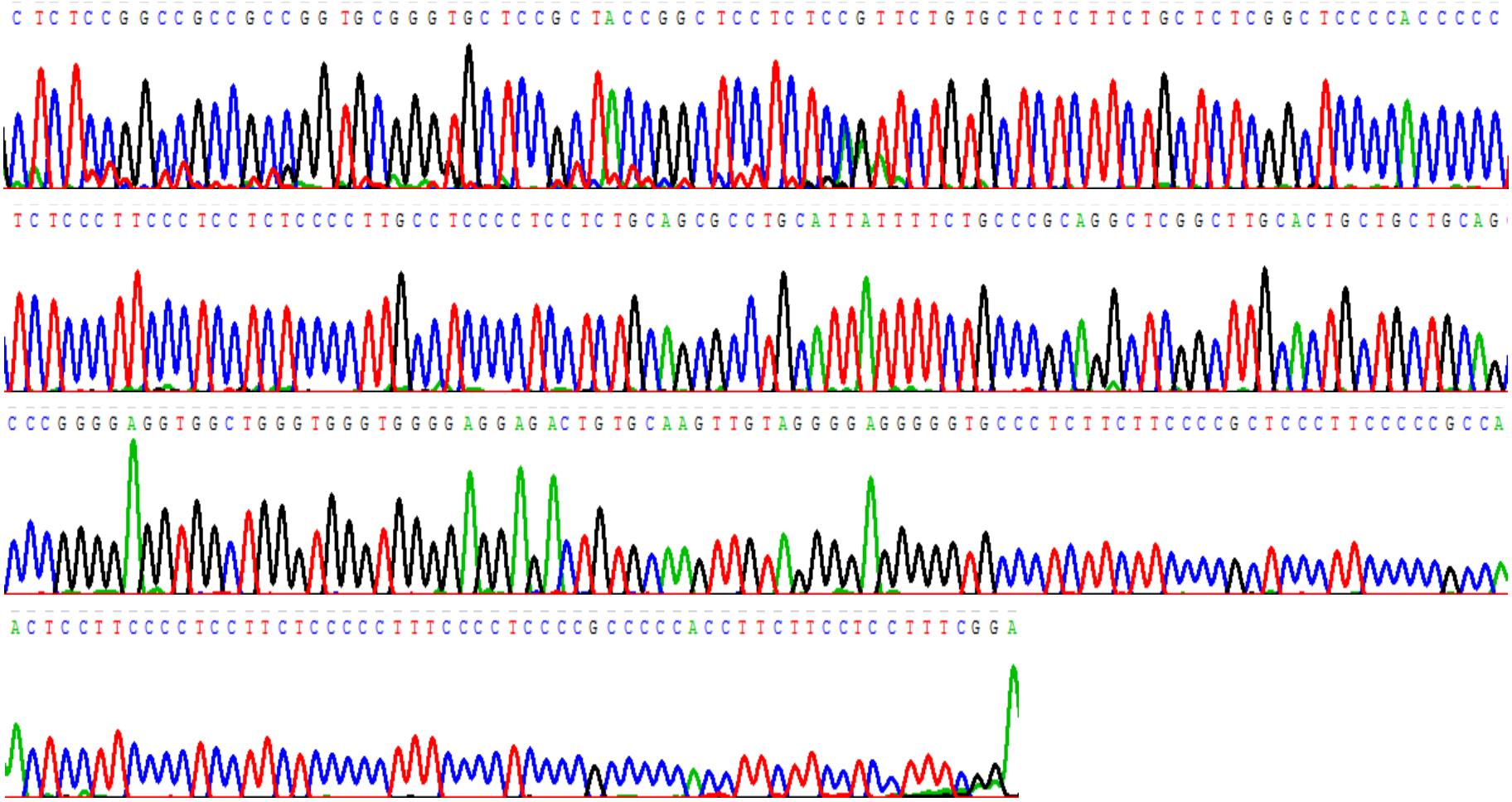

Exon 2 amplified with primer pair 3

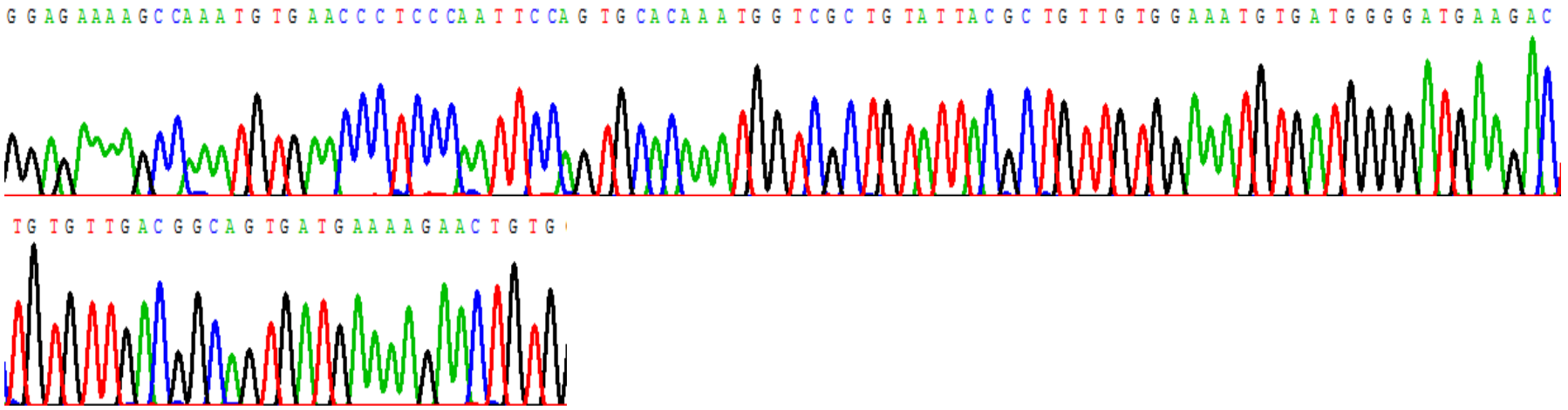

Exon 3 amplified with primer pair 4

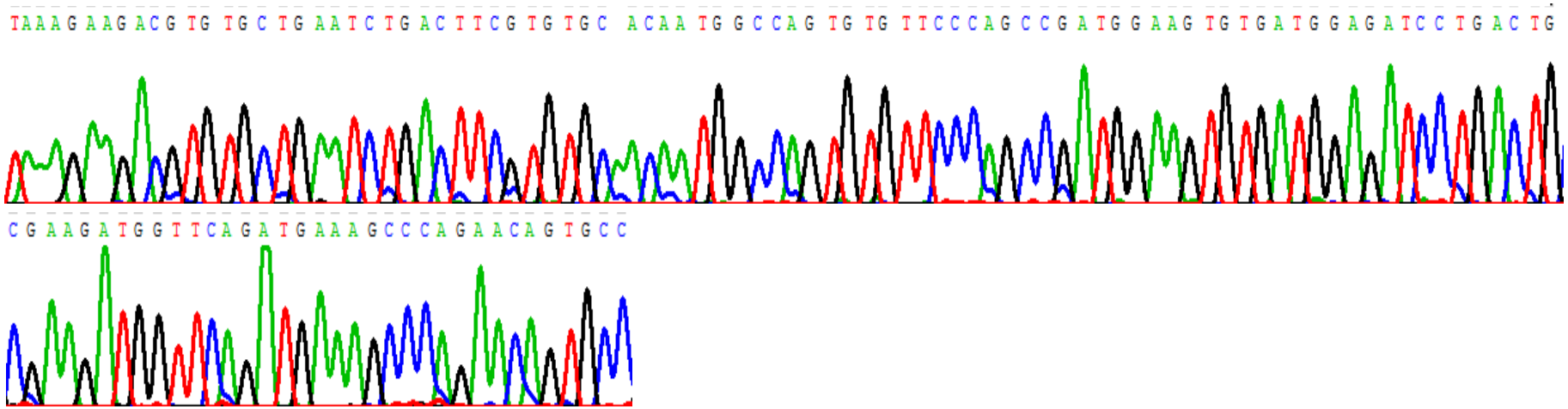

Exon 4 amplified with primer pair 5

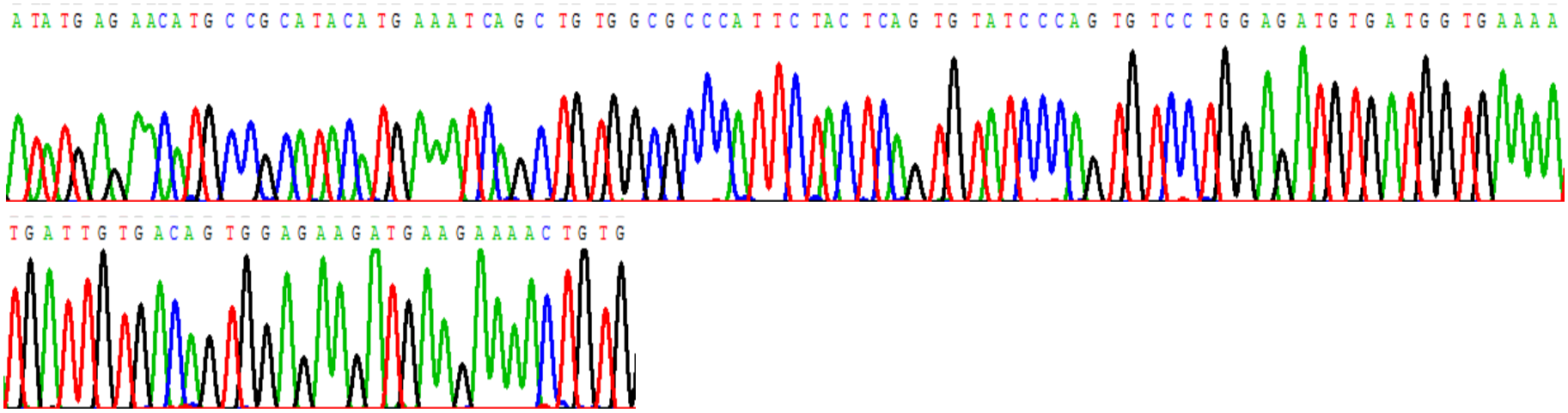

Exon 5 amplified with primer pair 6

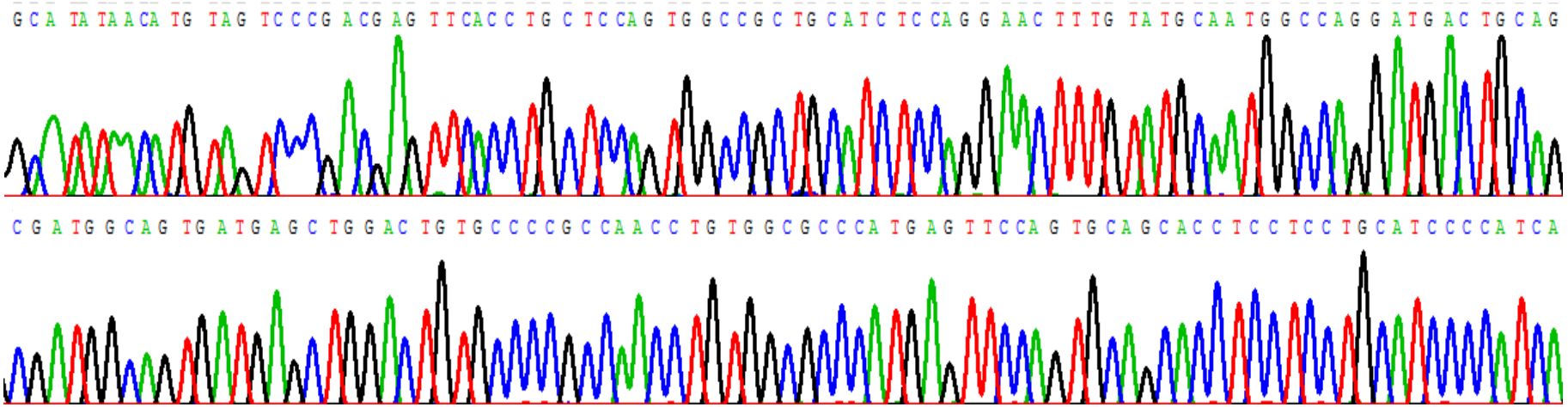

Exons 5 and 6 amplified with primer pair 7

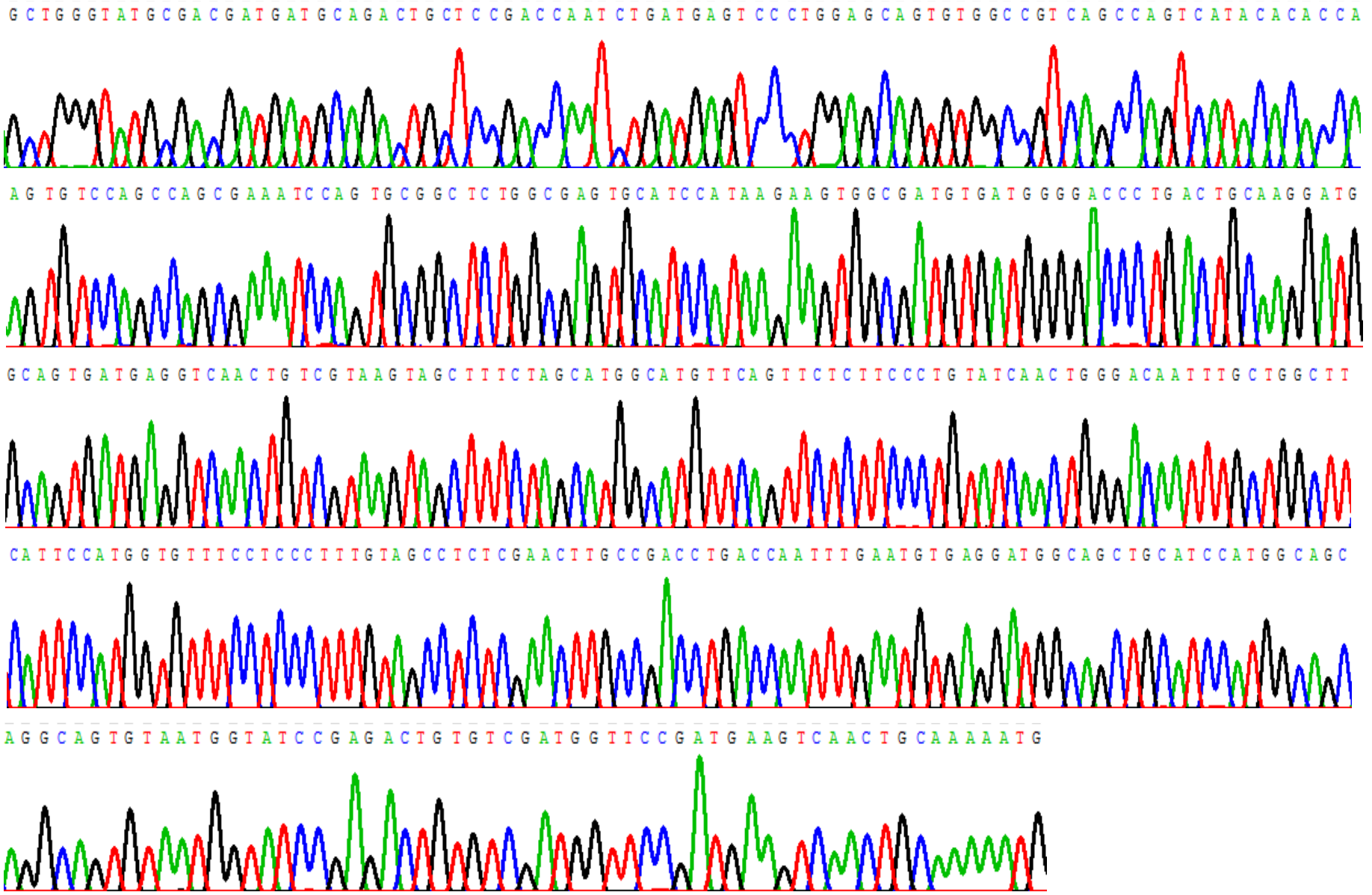

Exon 7 amplified with primer pair 8

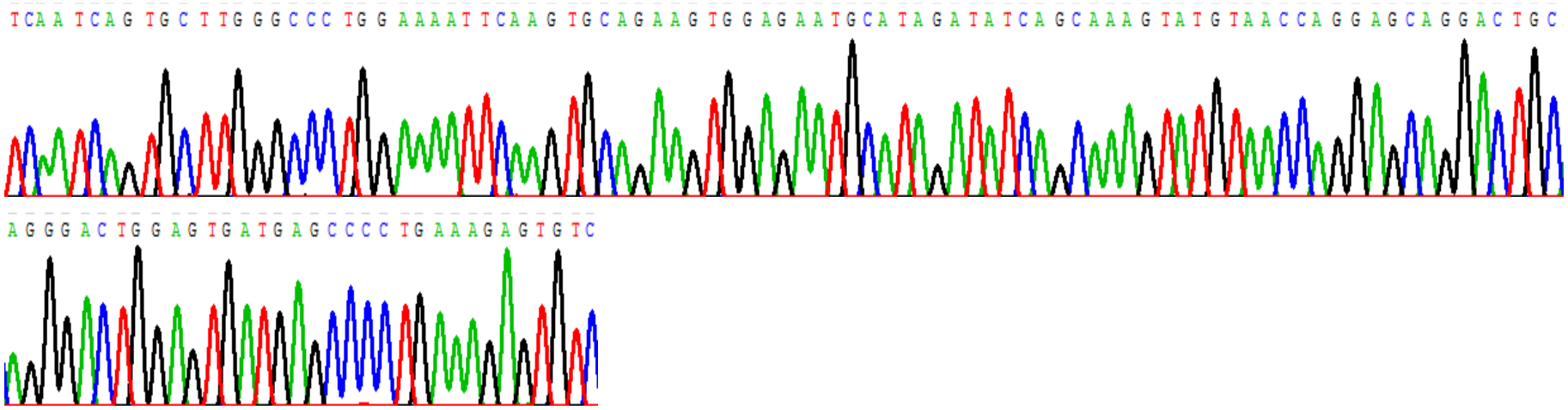

Exon 8 amplified with primer pair 9

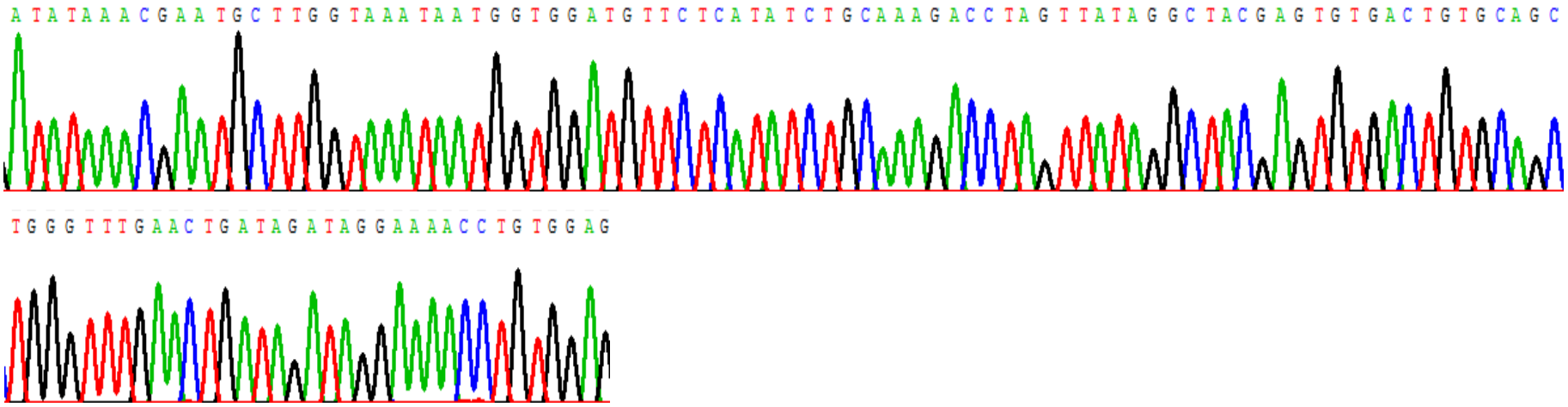

Exon 9 amplified with primer pair 10

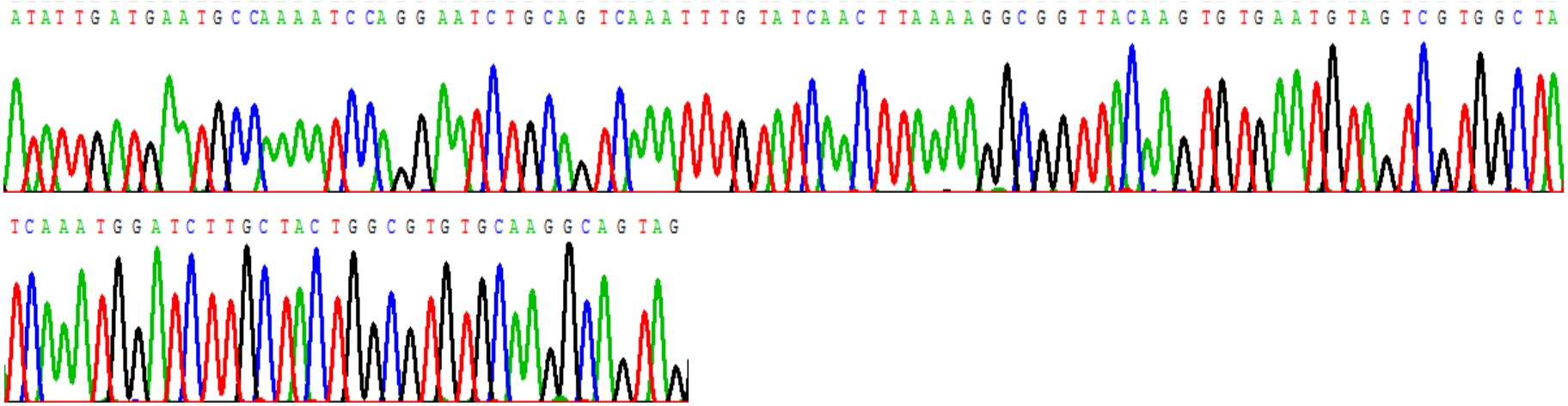

Exon 10 amplified with primer pair 11

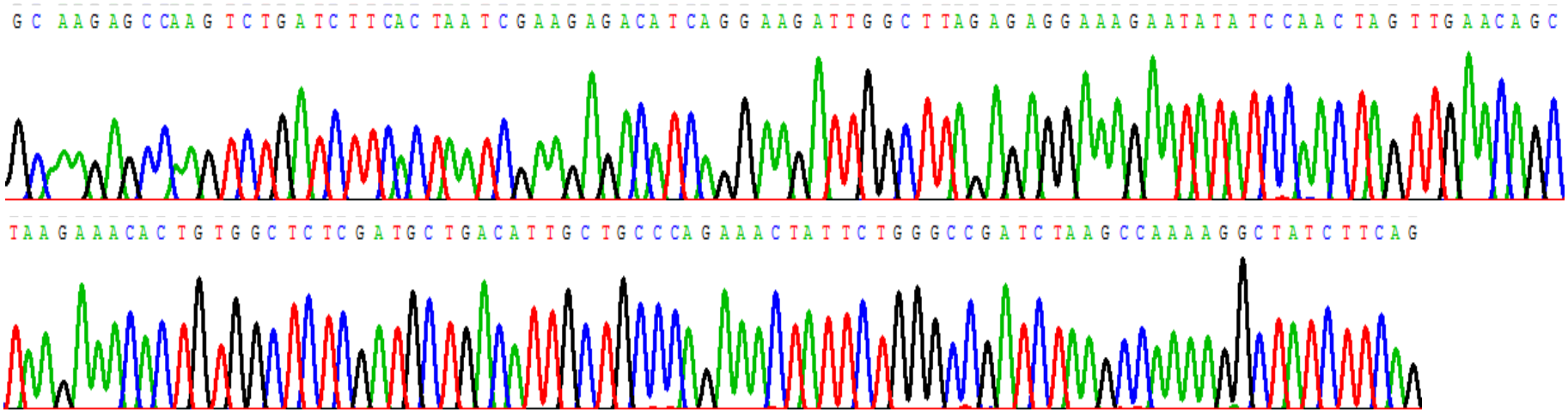

Exon 11 amplified with primer pair 12

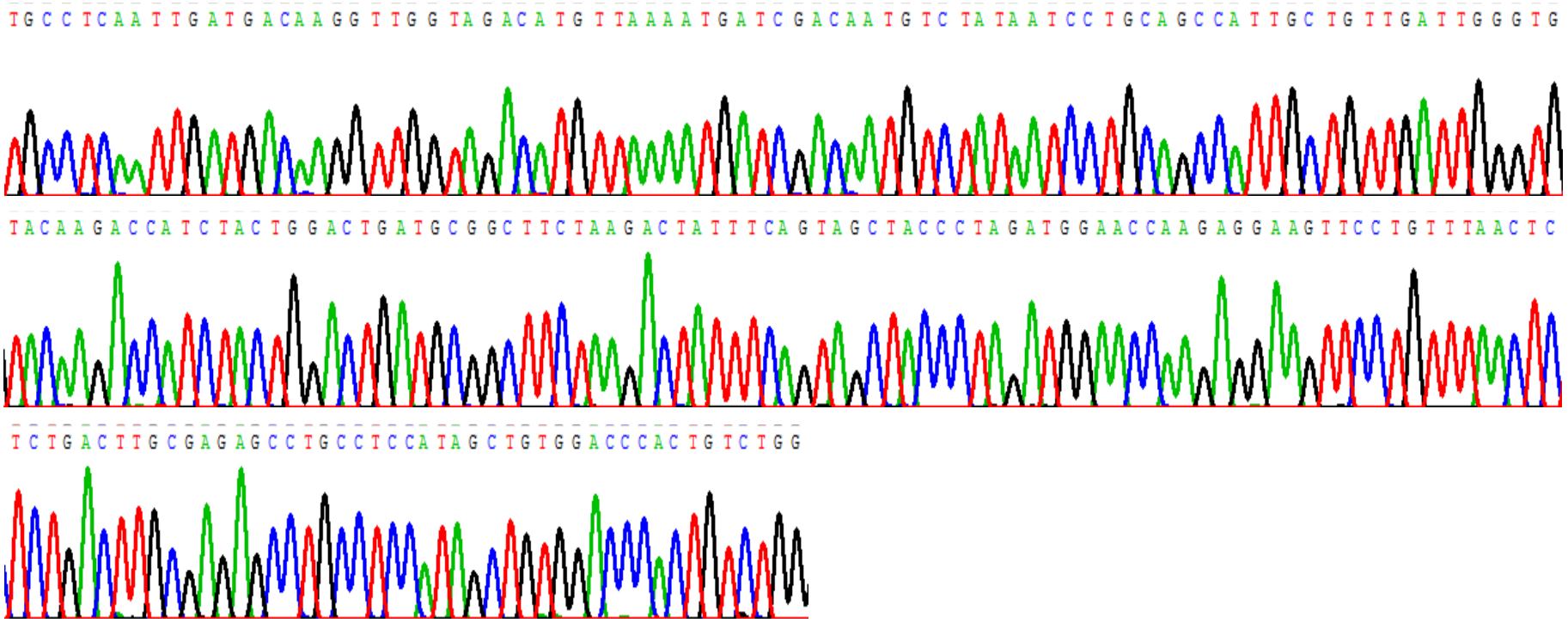

Exon 12 amplified with primer pair 13

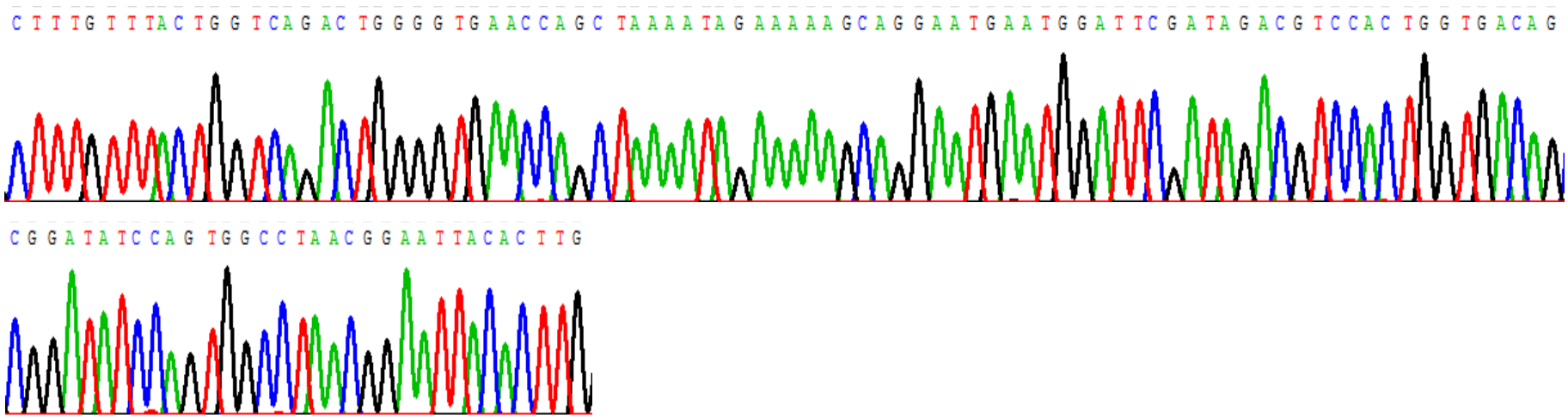

Exon 13 amplified with primer pair 14

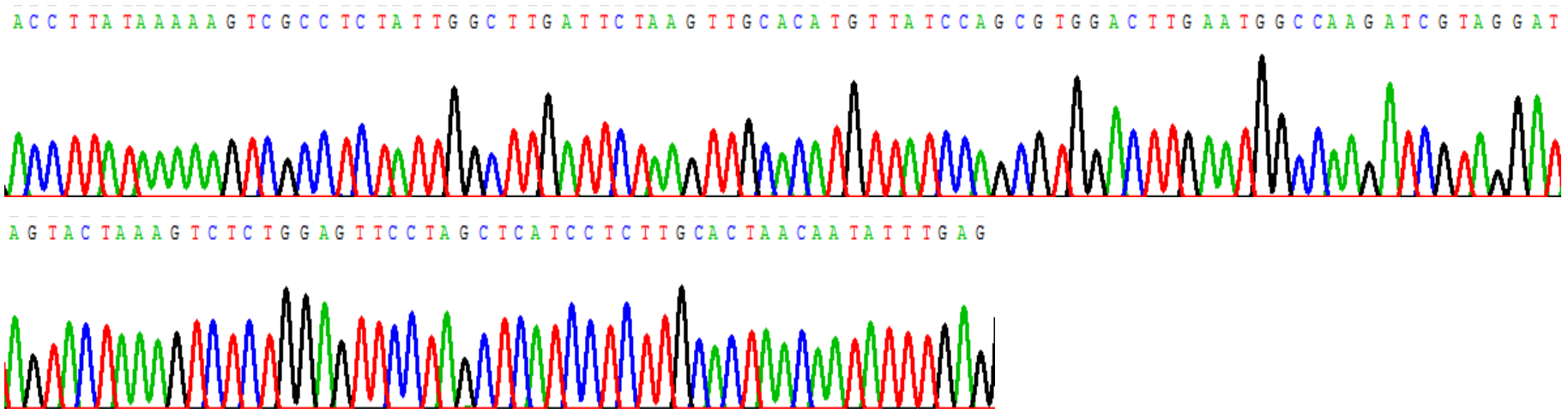

Exon 14 amplified with primer pair 15

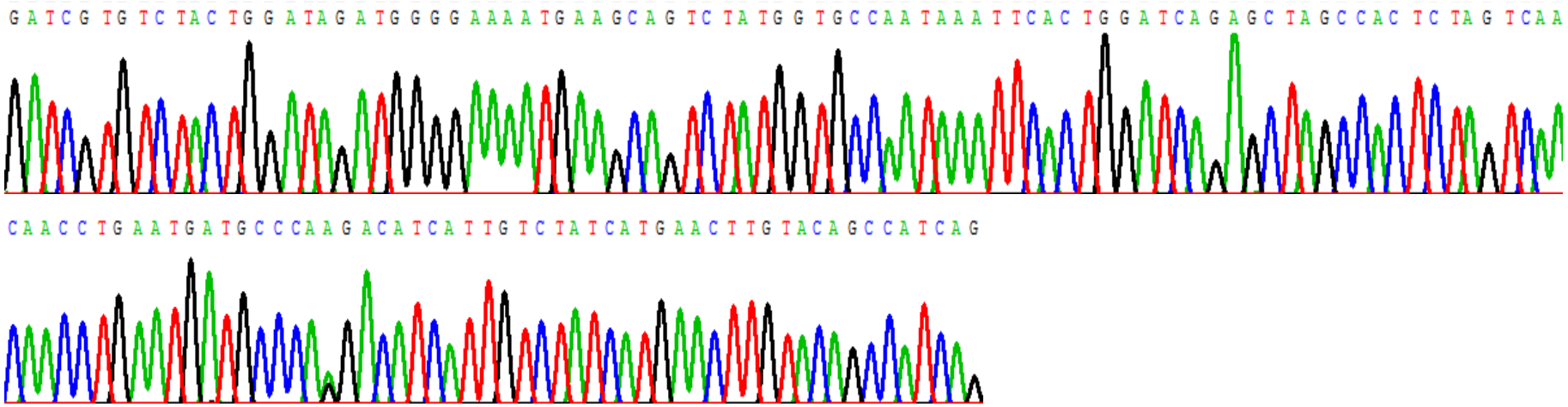

Exon 15 amplified with primer pair 16

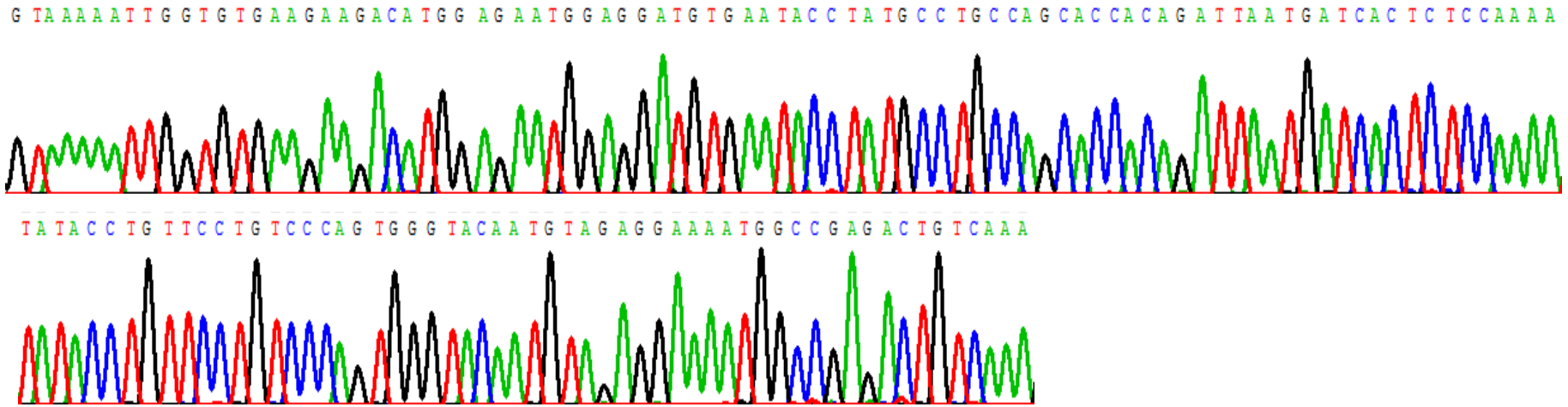

Exon 17 amplified with primer pair 18

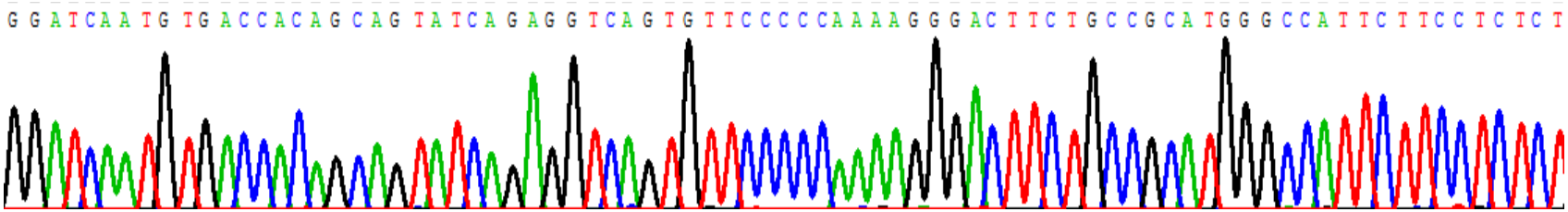

Exon 18 amplified with primer pair 19

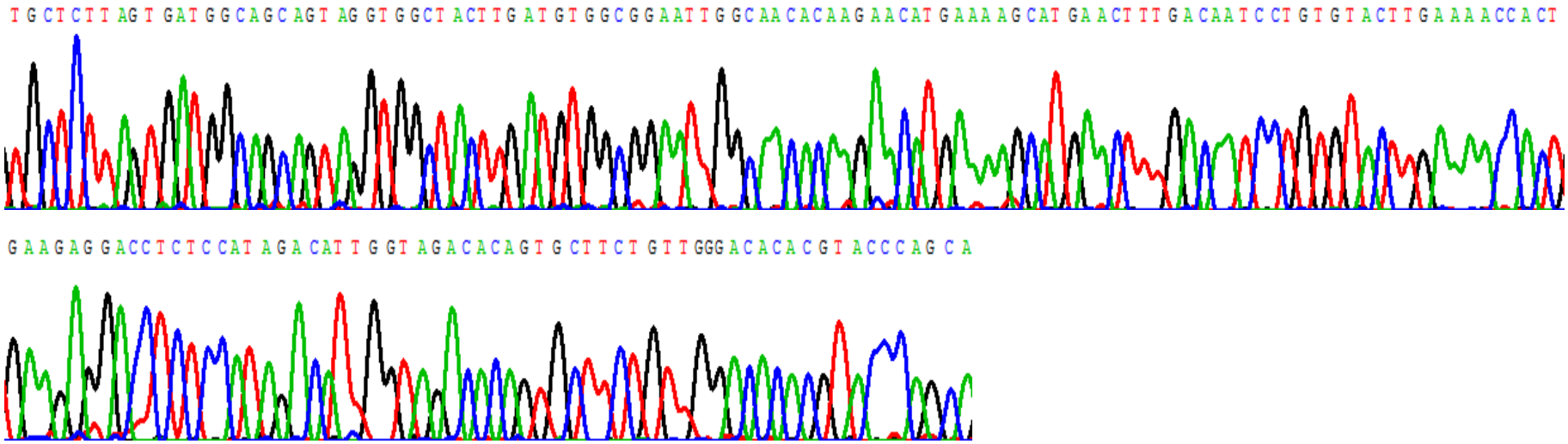

Exon 19 and 3’UTR amplified with primer pair 20

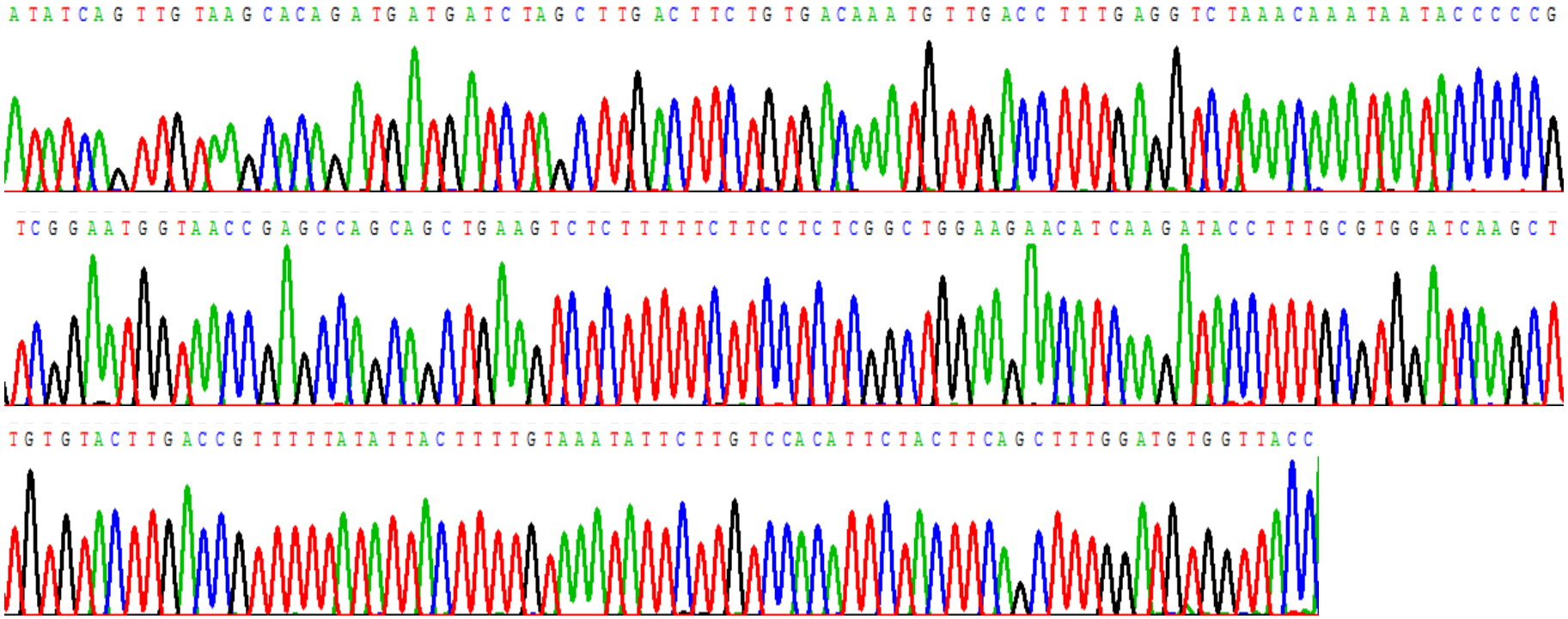

3’UTR amplified with primer pair 21

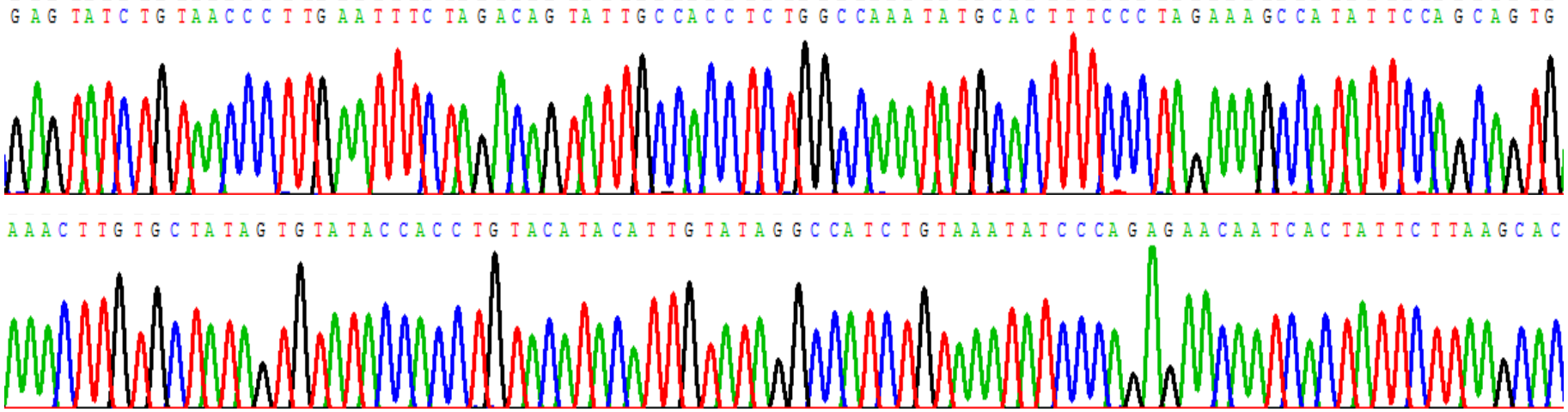

3’UTR amplified with primer pair 22

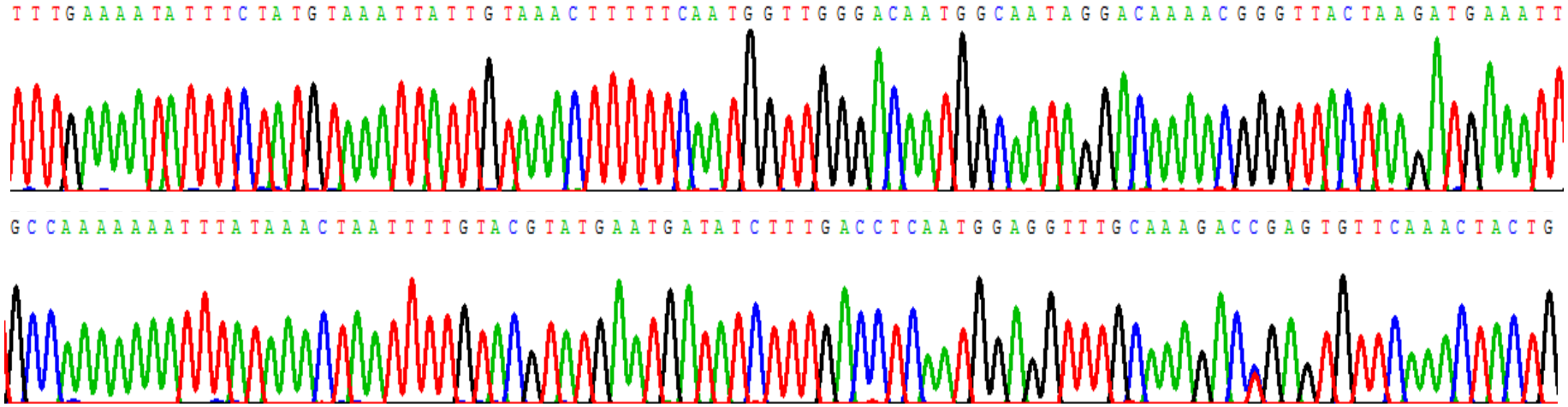

3’UTR amplified with primer pair 22

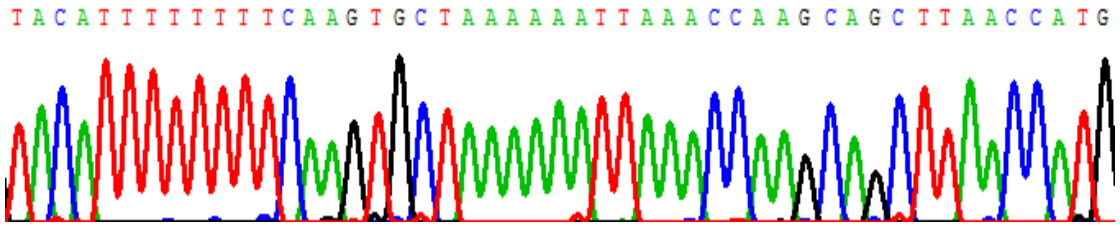

PUBLICATIONS

Mutations in the very low-density lipoprotein receptor *VLDLR* cause cerebellar hypoplasia and quadrupedal locomotion in humans

Tayfun Ozcelik*†‡, Nurten Akarsu§¶, Elif Uz*, Safak Caglayan*, Suleyman Gulsuner*, Onur Emre Onat*, Meliha Tan‖, and Uner Tan**

*Department of Molecular Biology and Genetics, Faculty of Science and ‡Institute of Materials Science and Nanotechnology, Bilkent University, Ankara 06800, Turkey; §Department of Medical Genetics and ¶Gene Mapping Laboratory, Department of Pediatrics, Pediatric Hematology Unit, Ihsan Dogramaci Children's Hospital, Hacettepe University Faculty of Medicine, Ankara 06100, Turkey; ‖Department of Neurology, Baskent University Medical School, Ankara 06490, Turkey; and **Faculty of Sciences, Cukurova University, Adana 01330, Turkey

Edited by Mary-Claire King, University of Washington, Seattle, WA, and approved January 16, 2008 (received for review October 22, 2007)

Quadrupedal gait in humans, also known as Unertan syndrome, is a rare phenotype associated with dysarthric speech, mental retardation, and varying degrees of cerebrocerebellar hypoplasia. Four large consanguineous kindreds from Turkey manifest this phenotype. In two families (A and D), shared homozygosity among affected relatives mapped the trait to a 1.3-Mb region of chromosome 9p24. This genomic region includes the *VLDLR* gene, which encodes the very low-density lipoprotein receptor, a component of the reelin signaling pathway involved in neuroblast migration in the cerebral cortex and cerebellum. Sequence analysis of *VLDLR* revealed nonsense mutation R257X in family A and single-nucleotide deletion c2339delT in family D. Both these mutations are predicted to lead to truncated proteins lacking transmembrane and signaling domains. In two other families (B and C), the phenotype is not linked to chromosome 9p. Our data indicate that mutations in *VLDLR* impair cerebrocerebellar function, conferring in these families a dramatic influence on gait, and that hereditary disorders associated with quadrupedal gait in humans are genetically heterogeneous.

genetics | Unertan syndrome

Obligatory bipedal locomotion and upright posture of modern humans are unique among living primates. Studies of fossil hominids have contributed significantly to modern understanding of the evolution of posture and locomotion (1–5), but little is known about the underlying molecular pathways for development of these traits. Evaluation of changes in brain activity during voluntary walking in normal subjects suggests that the cerebral cortices controlling motor functions, visual cortex, basal ganglia, and the cerebellum might be involved in bipedal locomotor activities (6). The cerebellum is particularly important for movement control and plays a critical role in balance and locomotion (7).

Neurodevelopmental disorders associated with cerebellar hypoplasias are rare and often accompanied by additional neuropathology. These clinical phenotypes vary from predominantly cerebellar syndromes to sensorimotor neuropathology, ophthalmological disturbances, involuntary movements, seizures, cognitive dysfunction, skeletal abnormalities, and cutaneous disorders, among others (8). Quadrupedal locomotion was first reported when Tan (9, 10) described a large consanguineous family exhibiting Unertan syndrome, an autosomal recessive neurodevelopmental condition with cerebellar and cortical hypoplasia accompanied by mental retardation, primitive and dysarthric speech, and, most notably, quadrupedal locomotion. Subsequent homozygosity mapping indicated that the phenotype of this family was linked to chromosome 17p (11). Thereafter, three additional families from Turkey (12–14) and another from Brazil (15) with similar phenotypes have been described, and video recordings illustrating the quadrupedal gait have been made (10–12). Here, we report that *VLDLR* is the gene responsible for the syndrome in two of these four Turkish families and report additional gene mapping studies that indicate the disorder to be highly genetically heterogeneous.

Fig. 1. Phenotypic (*A*) and cranial radiologic (*B*) presentation of quadrupedal gait in families A and D. (*A*) Affected brothers VI:20 and VI:18 and cousin VI:25 in family A (*Upper*) and the proband II:2 in family D (*Lower*) display palmigrate walking. This is different from quadrupedal knuckle-walking of the great apes (2). The hands make contact with the ground at the ulnar palm, and consequently this area is heavily callused as exemplified by VI:20. Strabismus was observed in all affected individuals. (*B*) Coronal and midsagittal MRI sections of VI:20, demonstrating vermial hypoplasia, with the inferior vermial portion being completely absent. Inferior cerebellar hypoplasia and a moderate simplification of the cerebral cortical gyri are noted. The brainstem and the pons are particularly small (*Left* and *Center*). Similar findings are observed for II:2 (*Right*).

Author contributions: T.O., N.A., and U.T. designed research; T.O., N.A., E.U., S.C., S.G., and O.E.O. performed research; T.O., N.A., E.U., S.C., S.G., and M.T. analyzed data; and T.O., N.A., and U.T. wrote the paper.

The authors declare no conflict of interest.

This article is a PNAS Direct Submission.

†To whom correspondence should be addressed. E-mail: tozcelik@fen.bilkent.edu.tr.

This article contains supporting information online at www.pnas.org/cgi/content/full/0710010105/DC1.

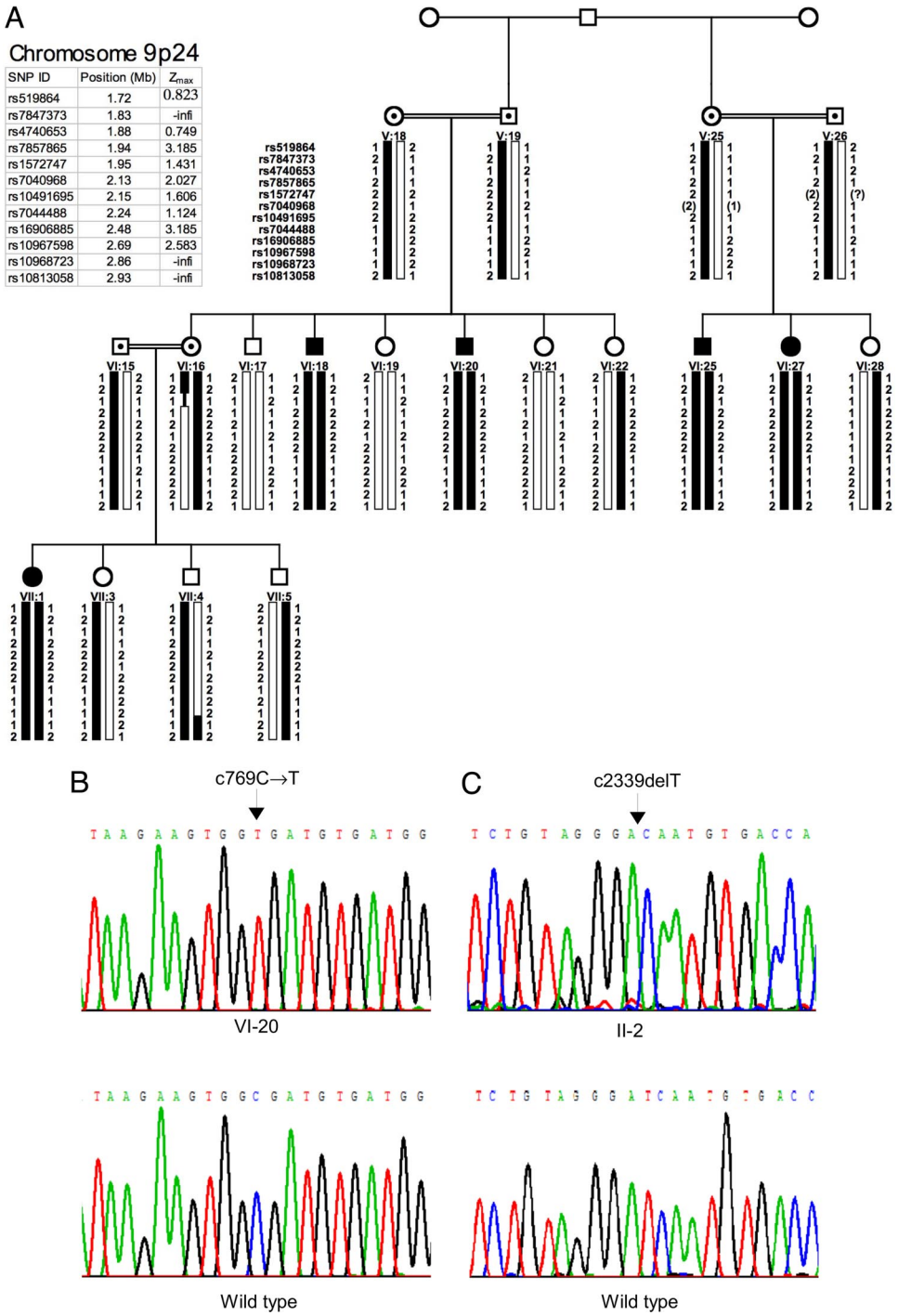

Fig. 2. Homozygosity mapping of cerebellar hypoplasia and quadrupedal locomotion to chromosome 9p24 (*A*) and identification of the *VLDLR* c769C → T mutation in family A (*B*) and of the *VLDLR* c2339delT mutation in family D (*C*). (*A*) Pedigree of family A; filled symbols represent the affected individuals. Squares indicate males, and circles indicate females. Black bars represent the haplotype coinherited with the quadrupedal phenotype in the family. Recombination events in individuals VI:16 (obligate carrier) and VII:4 (normal sibling) positioned the disease gene between markers rs7847373 and rs10968723. Physical positions and pairwise lod scores for each marker are shown on the upper left. Z_{max} represents the maximum lod score obtained at $\theta = 0.00$ cM. (*B* and *C*) Sequences of critical regions of *VLDLR* for wild-type and homozygous mutant genotypes.

Results

The proband of Family A (12) is a 37-year-old male with habitual quadrupedal gait (Fig. 1*A Upper Left* and Fig. 2*A*, VI:20). He did not make the transition to bipedality during his childhood despite the efforts of his healthy parents. He has dysarthric speech with a limited vocabulary, truncal ataxia, and profound mental retardation. He was not aware of place or of the year, month, or day. His MRI brain scan revealed inferior cerebellar and vermial hypoplasia, with the inferior vermial portion being completely absent. Whereas corpus callosum appeared normal, a moderate simplification of the cerebral cortical gyri accompanied by a particularly small brainstem and the pons was observed (Fig. 1 *B Left* and *Center*). Subsequently, we studied the proband's affected brother and cousin (Fig. 1*A Upper Center* and

Table 1. Physical, radiological, and genetic characteristics of the Turkish families in this study and of Hutterite family DES-H (27)

Characteristic	Family A	Family B	Family C	Family D	DES-H
Chromosomal location	9p24	17p	Not 9p or 17p	9p24	9p24
Gene and mutation	*VLDLR* (c769C → T)	Unknown	Unknown	*VLDLR* (c2339delT)	Deletion including *VLDLR* and *LOC401491*
Gait	Quadrupedal	Quadrupedal	Quadrupedal	Quadrupedal	Bipedal
Speech	Dysarthric	Dysarthric	Dysarthric	Dysarthric	Dysarthric
Hypotonia	Absent	Absent	Absent	Absent	Present
Barany caloric nystagmus	Normal	Cvs defect	Pvs defect	Not done	Not done
Mental retardation	Profound	Severe to profound	Profound	Profound	Moderate to profound
Ambulation	Delayed	Delayed	Delayed	Delayed	Delayed
Truncal ataxia	Severe	Severe	Severe	Severe	Severe
Lower leg reflexes	Hyperactive	Hyperactive	Hyperactive	Hyperactive	Hyperactive
Upper extremity reflexes	Vivid	Vivid	Vivid	Vivid	Vivid
Tremor	Very rare	Mild	Present	Absent	Present
Pes-planus	Present	Present	Present	Present	Present
Seizures	Very rare	Rare	Rare	Absent	Observed in 40% of cases
Strabismus	Present	Present	Present	Present	Present
Inferior cerebellum	Hypoplasia	Hypoplasia	Mild hypoplasia	Hypoplasia	Hypoplasia
Inferior vermis	Absent	Absent	Normal	Absent	Absent
Cortical gyri	Mild simplification	Mild simplification	Mild simplification	Mild simplification	Mild simplification
Corpus callosum	Normal	Reduced	Normal	Normal	Normal

Cvs, central vestibular system; Pvs, peripheral vestibular system.

Upper Right and Fig. 2*A*, VI:18 and VI:25) and other branches of the family living in nearby villages in southeastern Turkey. All affected individuals were offspring of consanguineous marriages (Fig. 2*A*). With the exception of one female (VII:1), who was an occasional biped with ataxic gait, all affected persons in family A had quadrupedal locomotion.

The proband of family D (14) is a 38-year-old male (Fig. 1*A Lower Left* and *Center*). Like all other quadrupedal individuals in these families, he did not make the transition to bipedality during his early childhood. He is profoundly retarded and exhibits dysarthric speech along with truncal ataxia. His MRI brain scan images are consistent with moderate cerebral cortical simplification and inferior cerebellar and vermial hypoplasia (Fig. 1*B Right*). The 65-year-old aunt and 63-year-old uncle of the proband are both mentally retarded and continue to walk on their wrists and feet despite their advanced ages. The family is consanguineous; all relatives were raised in neighboring villages on the western tip of the Anatolian peninsula.

All patients in these four families had significant developmental delay noted in infancy (Table 1). They sat unsupported between 9 and 18 months, and began to crawl on hands and knees or feet. Whereas normal infants make the transition to bipedal walking in a short period, the affected individuals continued to move on their palms and feet and never walked upright. All patients had severe truncal ataxia affecting their walking patterns. They can stand from a sitting position and maintain the upright position with flexed hips and knees. However, they virtually never initiate bipedal walking on their own and instead ambulate efficiently in a quadrupedal fashion. All patients had hyperactive lower leg and vivid upper extremity reflexes. Normal tone and power were observed in motor examination. All affected persons were mentally retarded to the degree that consciousness of place, time, or other experience appeared to be absent. However, no autistic features were expressed. The affected individuals all had good interpersonal skills, were friendly and curious to visitors, and followed very simple questions and commands. Additional clinical information on families A and D is provided in supporting information (SI) Table 2.

To identify the chromosomal locale of the gene or genes responsible for this phenotype, we carried out genome-wide linkage analysis and homozygosity mapping in families A–C (see *Materials and Methods* below). Although the families lived in isolated villages 200–300 km apart and reported no ancestral relationship, the rarity of the quadrupedal gait in humans led us to expect a single locus shared by affected individuals in all families. Instead, the trait mapped to three different chromosomal locales. In family A, linkage analysis and homozygosity mapping positioned the critical gene on chromosome 9p24 between rs7847373 and rs10968723 in a 1.032-Mb region (Fig. 2*A* and SI Fig. 4). In family B, the trait mapped to chromosome 17p13, confirming a previous study (11). In family C, highly negative logarithm of odds (lod) scores were obtained for both chromosomes 9p24 and 17p13 (SI Figs. 5 and 6); gene mapping in this family is ongoing. In family D, polymorphic markers from the critical intervals of chromosomes 9p24 and 17p13 were genotyped, and homozygosity was detected with markers on 9p24. Together, these results indicate that the syndrome including quadrupedal gait, dysarthric speech, mental retardation, and cerebrocerebellar hypoplasia is genetically heterogeneous.

The chromosome 9p24 region linked to the trait in families A and D includes *VLDLR*, the very low-density lipoprotein receptor. We hypothesized that a gene involved in neural development, cell positioning in brain, and cerebellar maturation could be involved in the pathogenesis of quadrupedal gait. In addition, cerebellar hypoplasia with cerebral gyral simplification was shown to be associated with a genomic deletion that includes *VLDLR* (16). We therefore considered *VLDLR* (17) to be a prime positional candidate for our phenotype and sequenced the gene in genomic DNA from probands of the four families (SI Table 3). The *VLDLR* sequence of affected members of family A was homozygous for a nonsense mutation in exon 5 (c769C → T; R257X) (Fig. 2*B*). The *VLDLR* sequence of the proband of family D was homozygous for a single-nucleotide deletion in exon 17 resulting in a stop codon (c2339delT; I780TfsX3) (Fig. 2*C*). *VLDLR* sequences excluded the possibility of compound heterozygosity in families B and C (SI Fig. 7). In families A and D, homozygosity for the *VLDLR* mutations was perfectly coinherited with quadrupedal gait (SI Figs. 8 and 9). Both mutations were absent from 100 unaffected individuals who live in the same local areas of southeastern and western Turkey as families A and D (SI Fig. 10).

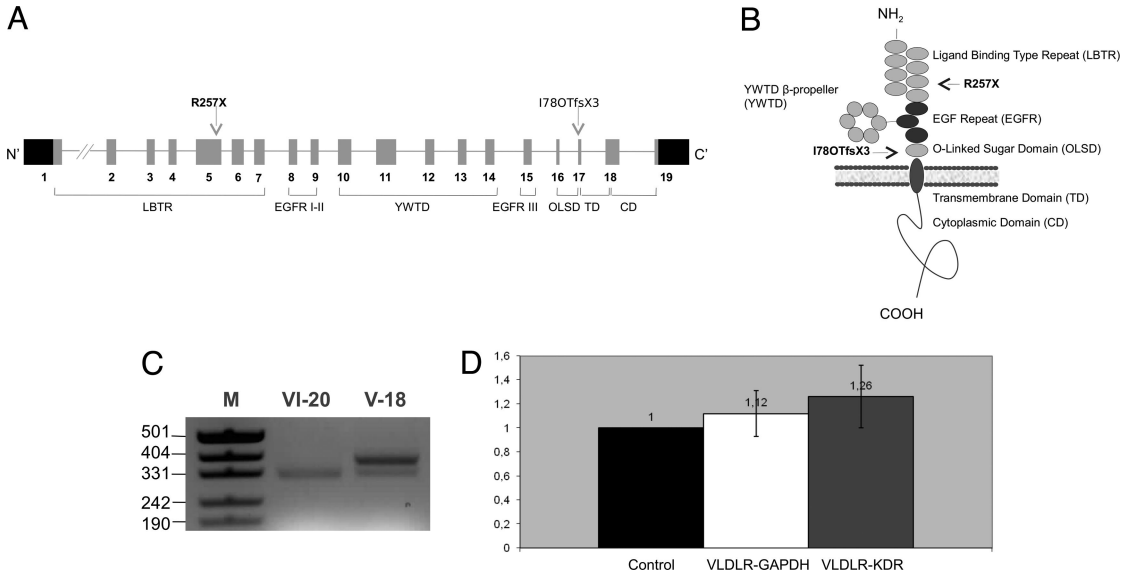

Fig. 3. Functional domains of *VLDLR* with positions of the mutations relative to the exons (*A*), domains (*B*), and the analysis of VLDLR transcript (*C* and *D*). (*A*) The gene consists of 19 exons. Arrows indicate the locations of the mutations. (*B*) VLDLR consists of ligand-binding type repeat (LBTR), epidermal growth factor repeat (EGFR) I–III, YWTD β-propeller (YWTD), *O*-linked sugar domain (OLSD), transmembrane domain (TD), and cytoplasmic domain (CD) (34) (www.expasy.org/uniprot/P98155). (*C*) Restriction-based analysis with HphI revealed the presence of only the mutant (347 bp) and both the mutant and wild type (396 and 347 bp; please note that the 49-bp fragment is not visible) VLDLR transcripts in patient VI:20 and carrier V:18 (both from family A), respectively. M is a DNA size marker. (*D*) Quantitative RT-PCR analysis of VLDLR transcript from peripheral blood samples of all probands in families A and D and controls was performed. Relative expression ratios were normalized according to the housekeeping gene *GAPDH* (glyceraldehyde-3-phosphate dehydrogenase) and the endothelial marker *KDR* (kinase insert domain receptor). ΔCt values were calculated from duplicate samples and were converted to linear scale (35). Control denotes ''VLDLR expression in controls,'' VLDLR-GAPDH denotes ''VLDLR expression in patients normalized to GAPDH,'' and finally VLDLR-KDR denotes ''VLDLR expression in patients normalized to KDR.''

VLDLR_R257X is in the ligand-binding domain, and *VLDLR_I780TfsX3* is in the *O*-linked sugar domain of the VLDLR protein (Fig. 3 *A* and *B*). Mutant VLDLR transcripts were expressed in endothelial cells from blood of affected individuals (Fig. 3*C*), and in these cells, levels of mutant and wild-type transcript expression appeared approximately equal (Fig. 3*D*; please also see *SI Text*). Because the stop codons of both mutations are located in the extracellular domain of VLDLR (Fig. 3*B*), the encoded mutant proteins could not be inserted into the membrane and could not function as receptors for reelin.

We propose *VLDLR*-associated Quadrupedal Locomotion (VLDLR-QL) or Unertan Syndrome Type 1 to describe the phenotype of families A and D.

Discussion

The identification of these *VLDLR* mutations provides molecular insight into the pathogenesis of neurodevelopmental movement disorders and expands the scope of diseases caused by mutations in components of the reelin pathway (18). Reelin is a secreted glycoprotein that regulates neuronal positioning in cortical brain structures and the migration of neurons along the radial glial fiber network by binding to lipoprotein receptors VLDLR and APOER2 and the adapter protein DAB1 (19). In the cerebellum, reelin regulates Purkinje cell alignment (20), which is necessary for the formation of a well defined cortical plate through which postmitotic granual cells migrate to form the internal granular layer (21). Homozygous mutations in the reelin gene (*RELN*) cause the Norman–Roberts type lissencephaly syndrome, associated with severe abnormalities of the cerebellum, hippocampus, and brainstem (OMIM 257320) (22). Mutation of *Reln* in the mouse results in the *reeler* phenotype and disrupts neuronal migration in several brain regions and gives rise to functional deficits such as ataxic gait and trembling (23). In contrast, mice deficient for *Vldlr* appear neurologically normal (24), but the cerebellae of these mice are small, with reduced foliation and heterotopic Purkinje cells (17).

In humans, homozygosity for either of two *VLDLR* truncating mutations leads to cerebrocerebellar hypoplasia, specifically vermial hypoplasia, accompanied by mental retardation, dysarthric speech, and quadrupedal gait. In the Hutterite population of North America, homozygosity for a 199-kb deletion encompassing the *VLDLR* gene leads to a form of Disequilibrium Syndrome (DES-H, OMIM 224050), characterized by nonprogressive cerebellar hypoplasia with moderate-to-profound mental retardation, cerebral gyral simplification, truncal ataxia, and delayed ambulation (16). The designation Disequilibrium Syndrome was originally given to cerebral palsy characterized by a variety of congenital abnormalities, including mental retardation, disturbed equilibrium, severely retarded motor development, muscular hypotonia, and perceptual abnormalities (25, 26). Neither DES-H nor other disequilibrium syndromes have been reported to include quadrupedal gait. The movement of most DES-H patients was so severely affected that independent walking was not possible. Those who could walk had a wide-based, nontandem gait (27).

The neurological phenotypes in the Turkish families and in the Hutterite families appear similar, with the most striking difference being the consistent adoption of efficient quadrupedal locomotion by the affected Turkish individuals (Table 1). In our view, the movement disorder described for the Hutterite patients may be a more profound deficit, with the patients perhaps lacking the motor skills for quadrupedal locomotion. The 199-kb deletion in DES-H encompasses the entire *VLDLR* gene and part of a hypothetical gene. *LOC401491*, the hypothetical gene, is an apparently noncoding RNA that shares a CpG island and likely promoter with *VLDLR*, and is represented by multiple alternative transcripts expressed in brain. It has been suggested that the DES-H phenotype could be the result of deletion of *VLDLR* or both *VLDLR* and the neighboring gene (16).

It has been suggested that in the Turkish families, lack of access to proper medical care exacerbated the effects of cerebellar hypoplasia, leading to quadrupedality. Although it may be true that family B lacked proper medical care, families A and D had consistent access to medical attention, and both families actively sought a correction of quadrupedal locomotion in their affected children. An unaffected individual in family A is a physician who was actively involved in the medical interventions. In family D, the proband's mother sought a definitive diagnosis and correction of the proband's quadrupedal locomotion from private medical practices and from two major academic medical centers. The parents in family A discouraged quadrupedal walking of their affected children, but without success. We conclude that social factors were highly unlikely to contribute to the quadrupedal locomotion of the affected individuals.

In conclusion, we suggest that *VLDLR*-deficiency in the brain at a key stage of development leads to abnormal formation of the neural structures that are critical for gait. Given the heterogeneity of causes of quadrupedal gait, identification of the genes in families B and C promises to offer insights into neurodevelopmental mechanisms mediating gait in humans.

Materials and Methods

Study Subjects. Parents of patients and other unaffected individuals gave consent to the study by signing the informed consent forms prepared according to the guidelines of the Ministry of Health in Turkey. The Ethics Committees of Baskent and Cukurova Universities approved the study (decision KA07/47, 02.04.2007 and 21/3, 08.11.2005, respectively).

Genome-Wide Linkage Analysis. Linkage analysis was performed by SNP genotyping with the commercial release of the GeneChip 250K (NspI digest) or 10K Affymetrix arrays as described (28). In addition, genotype data were analyzed by hand to identify regions of homozygosity. The parametric component of the Merlin package v1.01 was used for the multipoint linkage analysis assuming autosomal recessive mode of inheritance with full penetrance (29, 30). The analysis was carried out along a grid of locations equally spaced at 1 cM. Haplotype analysis was performed on chromosomal regions with positive lod scores (Fig. 2*A* and SI Figs. 4–6). Pairwise linkage was analyzed by using the MLINK component of the LINKAGE program (FASTLINK, version 3) (31–33). Markers D17S1298 (3.51 Mb) and D9S1779 (0.4 Mb), D9S1871 (3.7 Mb) were used to test for homozygosity to chromosomes 17p13 and 9p24, respectively.

Mutation Search. Sequencing primers were designed for each *VLDLR* exon by using Primer3, BLAST, and the sequence of NC_000009. DNA from all of the probands was sequenced in both directions by using standard methods. The mutations in exons 5 (c769C → T) and 17 (c2339delT) were detected in all affected (homozygous) and carrier (heterozygous) individuals of families A and D, respectively. The c769C → T mutation creates a restriction site for the enzyme HphI (5′-GGTGA(N)8 ↓ 3′), and the c2339delT mutation abolishes a restriction site for the enzyme MboI (5′-G↓ ATC-3′). Assays using these restriction enzymes were developed to test for the mutations in all four families and in 200 healthy controls from the Turkish population. Restriction based mutation and quantitative RT-PCR analyses of *VLDLR* transcript in patients and controls was also performed (please see *SI Text* relating to Fig. 3 *C* and *D*).

ACKNOWLEDGMENTS. We thank the patients and family members for their participation in this study, E. Tuncbilek and M. Alikasifoglu for providing the microarray facility at Hacettepe University, Iclal Ozcelik for help in writing the manuscript, and Mehmet Ozturk for support. This work was supported by the Scientific and Technological Research Council of Turkey Grant TUBITAK-SBAG 3334, International Centre for Genetic Engineering and Biotechnology Grant ICGEB-CRP/TUR04-01 (to T.O.), and by Baskent University Research Fund KA 07/47 and TUBITAK-SBAG-HD-230 (to M.T.).

1. Spoor F, Wood B, Zonneveld F (1994) *Nature* 369:645–648.
2. Richmond BG, Strait DS (2000) *Nature* 404:382–385.
3. Bramble DM, Lieberman DE (2004) *Nature* 432:345–352.
4. Alemseged Z, Spoor F, Kimbel WH, Bobe R, Geraads D, Reed D, Wynn JG (2006) *Nature* 443:296–301.
5. Wood B (2006) *Nature* 443:278–281.
6. Fukuyama H, Ouchi Y, Matsuzaki S, Nagahama Y, Yamauchi H, Ogawa M, Kimura J, Shibasaki H (1997) *Neurosci Lett* 228:183–186.
7. Morton SM, Bastian AJ (2007) *Cerebellum* 6:79–86.
8. Fogel BL, Perlman S (2007) *Lancet Neurol* 6:245–257.
9. Tan U (2005) *Neuroquantology* 4:250–255.
10. Tan U (2006) *Int J Neurosci* 116:361–369.
11. Turkmen S, Demirhan O, Hoffmann K, Diers A, Zimmer C, Sperling K, Mundlos S (2006) *J Med Genet* 43:461–464.
12. Tan U, Karaca S, Tan M, Yilmaz B, Bagci NK, Ozkur A, Pence S (2008) *Int J Neurosci* 118:1–25.
13. Tan U (2006) *Int J Neurosci* 116:763–774.
14. Tan U (2008) *In J Neurosci* 118:211–225.
15. Garcias GL, Roth MG (2007) *Int J Neurosci* 117:927–933.
16. Boycott KM, Flavelle S, Bureau A, Glass HC, Fujiwara TM, Wirrell E, Davey K, Chudley AE, Scott JN, McLeod DR, Parboosingh JS (2005) *Am J Hum Genet* 77:477–483.
17. Trommsdorff M, Gotthardt M, Hiesberger T, Shelton J, Stockinger W, Nimpf J, Hammer RE, Richardson JA, Herz J (1999) *Cell* 97:689–701.
18. Tissir F, Goffinet AM (2003) *Nat Rev Neurosci* 4:496–505.
19. Hiesberger T, Trommsdorff M, Howell BW, Goffinet A, Mumby MC, Cooper JA, Herz J (1999) *Neuron* 24:481–489.
20. Miyata T, Nakajima K, Mikoshiba K, Ogawa M (1997) *J Neurosci* 17:3599–3609.
21. Wechsler-Reya RJ, Scott MP (1999) *Neuron* 22:103–114.
22. Hong SE, Shugart YY, Huang DT, Shahwan SA, Grant PE, Hourihane JO, Martin ND, Walsh CA (2000) *Nat Genet* 26:93–96.
23. D'Arcangelo G, Miao GG, Chen SC, Soares HD, Morgan JI, Curran T (1995) *Nature* 374:719–723.
24. Frykman PK, Brown MS, Yamamoto T, Goldstein JL, Herz J (1995) *Proc Natl Acad Sci* 92:8453–8457.
25. Hagberg B, Sanner G, Steen M (1972) *Acta Paediat Scand* 61(Suppl. 226):1–63.
26. Sanner G (1973) *Neuropaediatrie* 4:403–413.
27. Glass HC, Boycott KM, Adams C, Barlow K, Scott JN, Chudley AE, Fujiwara TM, Morgan K, Wirrell E, McLeod DR (2005) *Dev Med Child Neurol* 47:691–695.
28. Matsuzaki H, Dong S, Loi H, Di X, Liu G, Hubbell E, Law J, Berntsen T, Chadha M, Hui H, *et al.* (2004) *Nat Methods* 1:109–111.
29. Abecasis GR, Cherny SS, Cookson WO, Cardon LR (2002) *Nat Genet* 30:97–101.
30. Abecasis GR, Wigginton JE (2005) *Am J Hum Genet* 77:754–767.
31. Lathrop GM, Lalouel JM (1984) *Am J Hum Genet* 36:460–465.
32. Cottingham RW, Jr, Idury RM, Schaffer AA (1993) *Am J Hum Genet* 53:252–263.
33. Schaffer AA, Gupta SK, Shriram K, Cottingham RW, Jr (1994) *Hum Hered* 44:225–237.
34. Herz J, Bock HH (2002) *Annu Rev Biochem* 71:405–434.
35. Pfaffi MW (2004) in *A-Z of Quantitative PCR*, ed Bustin S (International University Line, La Jolla, CA), pp 89–120.

LETTER

Reply to Herz *et al*. and Humphrey *et al*.: Genetic heterogeneity of cerebellar hypoplasia with quadrupedal locomotion

Mutations in the very low-density lipoprotein receptor VLDLR are responsible for cerebellar hypoplasia with quadrupedal gait (1). The most likely mechanism leading to this phenotype is that VLDLR deficiency in the brain at a key stage of development precludes the normal formation of neural structures critical for gait. Quadrupedal gait is an integral part of VLDLR-associated cerebellar hypoplasia syndrome in these families (1, 2). It is not necessary to invoke an "epiphenomenon" or "unfavorable environmental conditions" to explain the phenotype (3), but rather simply considering clinical heterogeneity in the context of genomic understanding of complex traits is sufficient.

Disequilibrium syndrome was first described by the Swedish neuropediatrician Bengt Hagberg and colleagues (4) as a form of cerebral palsy characterized by a variety of congenital abnormalities. Subsequently, Schurig *et al*. (5) described, in the North American Hutterite population, inherited cerebellar disorder with mental retardation, the genetic basis of which proved to be homozygous deletion of the VLDLR gene and the adjacent noncoding LOC401491 sequence (6). Based on the phenotypic similarities of the Swedish and Hutterite patients, the acronym DES-H [disequilibrium syndrome-Hutterites, Online Mendelian Inheritance in Man (OMIM) accession no. 224050] was adopted for this syndrome (6).

Our results (1) and those of others (7) extend these findings to different VLDLR mutations leading to cerebellar hypoplasia and related disequilibrium features, including in some families bipedal gait (5, 6), in other families quadrupedal gait (1, 8), and in another family "gait ataxia" (7). Additional kindreds with disequilibrium syndrome and quadrupedal gait have been described in Brazil (9) and Iraq (10). It will be interesting to know whether mutations responsible for the phenotype in these families lie in the VLDLR gene or in one of the other loci linked to this genetically heterogeneous phenotype (1).

The comments of Humphrey *et al*. (11) address three fundamental features of genomic analysis of human traits: allelic heterogeneity, genotype–phenotype correlations, and variable expression.

Allelic heterogeneity—the expression of the same phenotype due to different mutations in a gene—is characteristic of virtually all human genetic disease. For example, homozygosity for any of >300 different mutations in the LDL receptor leads to hypercholesterolemia. It was to be expected, therefore, that in different families different mutations in VLDLR would lead to a phenotype comprising cerebellar hypoplasia with quadrupedal gait. It would not be expected that quadrupedalism would be present only in the presence of one "specific mutation."

The converse observation, of a correlation between genotype and phenotype, is also characteristic of inherited human disease. Different mutations in the same gene frequently lead to different clinical phenotypes. Contrary to the statement of Humphrey *et al*. (11), the Hutterite families in North America and families A and D in Turkey do not carry "the same homozygous mutation." The Hutterite mutation is a complete genomic deletion of VLDLR; the mutations in Turkish families A and D are, respectively, a nonsense mutation and a single-base-pair deletion leading to a frame shift in VLDLR. It is not surprising, therefore, that features of the cerebellar hypoplasia syndrome, including presence or absence of quadrupedal walking, differ among families with different mutations in the gene.

Third, variable expression of a phenotype is frequently observed even among persons with the same mutation in a critical gene. Variable expression may be due to differences in genetic background of the individual, to differences in environmental exposures, or to chance. Among affected individuals in families A and D, none displays exclusively bipedal locomotion; two affected individuals can walk bipedally for short distances but prefer quadrupedal locomotion (1, 8).

Finally, the use of a walking frame to assist bipedalism in affected individuals (12) does not demonstrate that the cause of quadrupedalism was "local cultural environment." Wearing eyeglasses assists persons with myopia. Should we then conclude that near-sightedness is caused by "local cultural environment"?

Some descriptions by the press of Turkish families with cerebellar hypoplasia and quadrupedal gait have portrayed the affected individuals as doomed to quadrupedal gait by the religious beliefs of their parents (13). We hope that future descriptions of these families will conform to standards reflected in recent genomic analyses of their disorder.

Tayfun Ozcelik*[*†‡], Nurten Akarsu[§¶], Elif Uz*, Safak Caglayan*, Suleyman Gulsuner*, Onur Emre Onat*, Meliha Tan[‖], and Uner Tan*

**Department of Molecular Biology and Genetics, Faculty of Science, and †Institute of Materials Science and Nanotechnology, Bilkent University, Ankara 06800, Turkey; §Department of Medical Genetics and ¶Gene Mapping Laboratory, Department of Pediatrics, Pediatric Hematology Unit, Ihsan Dogramaci Children's Hospital, Hacettepe University Faculty of Medicine, Ankara 06100, Turkey; ‖Department of Neurology, Baskent University Medical School, Ankara 06490, Turkey; and **Faculty of Sciences, Cukurova University, Adana 01330, Turkey*

1. Ozcelik T, *et al.* (2008) Mutations in the very low-density lipoprotein receptor VLDLR cause cerebellar hypoplasia and quadrupedal locomotion in humans. *Proc Natl Acad Sci USA* 105:4232–4236.
2. Tan U (2005) A new theory on the evolution of human mind. Unertan syndrome: Quadrupedality, primitive language, and severe mental retardation. *NeuroQuantology* 4:250–255.
3. Herz J, Boycott KM, Parboosingh JS (2008) "Devolution" of bipedality. *Proc Natl Acad Sci USA* 105:E25.
4. Hagberg B, Scanner G, Steen M (1972) The dysequilibrium syndrome in cerebral palsy. Clinical aspects of treatment. *Acta Paediatr Scand* 61(Suppl 226):1–63.
5. Schurig V, Van Orman A, Bowen P (1981) Nonprogressive cerebellar disorder with mental retardation and autosomal recessive inheritance in Hutterites. *Am J Med Genet* 9:43–53.

www.pnas.org/cgi/doi/10.1073/pnas.0804078105

6. Boycott KM, *et al.* (2005) Homozygous deletion of the very low density lipoprotein receptor gene causes autosomal recessive cerebellar hypoplasia with cerebral gyral simplification. *Am J Hum Genet* 77:477–483.
7. Moheb LA, *et al.* (2008) Identification of a nonsense mutation in the very low-density lipoprotein receptor gene (VLDLR) in an Iranian family with dysequilibrium syndrome. *Eur J Hum Genet* 16:270–273.
8. Turkmen S, *et al.* (March 26, 2008) Cerebellar hypoplasia, with quadrupedal locomotion, caused by mutations in the very low-density lipoprotein receptor gene. *Eur J Hum Genet*, 10.1038/ejhg.2008.73.
9. Garcias GL, Roth MG (2007) A Brazilian family with quadrupedal gait, severe mental retardation, coarse facial characteristics, and hirsutism. *Int J Neurosci* 117: 927–933.
10. Fletcher M (October 17, 2007) Life on all fours. *Times Online*. Available at www.timesonline.co.uk/tol/life_and_style/health/article2671426.ece.
11. Humphrey N, Mundlos S, Turkmen S (2008) Genes and quadrupedal locomotion in humans. *Proc Natl Acad Sci USA* 105:E26.
12. Harrison J, Holt S (2006) *The Family That Walks on All Fours* (BBC, London).
13. Ahuja A (2007) We're all made with quadrupedal walking ability. *Times Online*. Available at http://women.timesonline.co.uk/tol/life_and_style/women/the_way_we_live/article2671044.ece.

Author contributions: T.O., N.A., E.U., S.C., S.G., O.E.O., M.T., and U.T. wrote the paper.

The authors declare no conflict of interest.

‡To whom correspondence should be addressed. E-mail: tozcelik@bilkent.edu.tr.